The Pathway of Electron Transfer within the Nitrogenase Complex

by

John W. Peters

Dissertation submitted to the faculty of the
Virginia Polytechnic Institute and State University
in partial fulfillment of the requirements for the degree of

DOCTOR OF PHILOSOPHY

in

Biochemistry and Anaerobic Microbiology

APPROVED:

D. R. Dean, Chairman

J. S. Chen

P. J. Kennelly

W. E. Newton

T. D. Wilkins

January, 1995

Blacksburg, VA

The Pathway of Electron Transfer within the Nitrogenase Complex

by

John W. Peters

Committee Chairman: Dennis R. Dean
Biochemistry and Anaerobic Microbiology

(ABSTRACT)

Site-directed mutagenesis and gene replacement were used to probe the pathway of electron transfer in nitrogenase by substituting single or groups of amino acid residues that, within the current view of component protein docking and nitrogenase catalysis, are likely to be involved in inter- or intra-molecular electron transfer. Intermolecular electron transfer was probed by substituting charged residues that, within the model for component protein docking proposed by Rees and Howard (Kim and Rees. 1992. *Nature* 360:553-60; Howard. 1993. In *Molybdenum Enzymes, Cofactors and Model Systems,* eds. EI Stiefel, D Coucouvanis, and WE Newton, pp.271-89. Washington DC: Am. Chem. Soc. 387 pp), are likely to be involved in electrostatic interactions that facilitate component protein association or dissociation. Intramolecular electron transfer was probed by substituting residues which are located in the polypeptide matrix that separates the P cluster and the iron-molybdenum cofactor based on the generally accepted view that the P cluster is an intermediate in electron transfer from the Fe protein to the iron-molybdenum cofactor at the substrate reduction site.

The results of the biochemical characterization of a hybrid *Azotobacter vinelandii-Clostridium pasteurianum* Fe protein indicate that the region of the *A. vinelandii* Fe protein defined by residues 59 through 67 is involved in Fe protein-MoFe protein interaction. The rationale for construction of this hybrid Fe protein was based partially on the observation that the Fe protein from *C. pasteurianum* forms a tight-binding inactive complex with the MoFe protein from *A. vinelandii*. Detailed studies involving NaCl sensitivity and component protein ratio titrations suggest that this region may have a

specific role in component protein dissociation. Further studies involving substitution of individual residues of the MoFe protein indicate that α-Asp^{161} is involved in component protein interaction.

MoFe protein intramolecular electron transfer was probed by placing amino acid substitutions at β-Tyr^{98}, which is located directly between the P cluster and the iron-molybdenum cofactor. The results of the biochemical characterization of an altered MoFe with β-Tyr^{98} substituted by His, support the generally accepted view that electron transfer from the Fe protein to the substrate reduction site involves the P cluster as an intermediate electron acceptor. It was also indicated that the P cluster may be able to accept more than one electron, which is consistent with the mechanism of P cluster reduction suggested by Rees (Rees DC, Chan MK, Kim J. 1993. *Adv. Inorg. Chem.* 40:89-119).

ACKNOWLEDGEMENTS

I give my sincere thanks to the following people who have made my education exciting and rewarding: my committee members: J. S. Chen, P. J. Kennelly, T. D. Wilkins, and W. E. Newton who took an interest in my research and encouraged me in my work, my advisor, Dennis Dean, who guided my intellectual development, my co-workers in the Dean and Newton labs, especially Valerie Cash for her assistance and friendship through my whole tenure in the lab, and Karl Fisher for his collaborative work and stimulating scientific discussions, Mary Wells and Steve Lowe who went above the call of duty to bail me out of countless administrational and equipment problems, and foremost my wife, Martha, for her patience, sense of humor, and love.

TABLE OF CONTENTS

ABSTRACT....ii
ACKNOWLEDGEMENTS....iv
TABLE OF CONTENTS....v
LIST OF ILLUSTRATIONS....vii
LIST OF TABLES....ix
ABBREVIATIONS....x
PURPOSE....1
LITERATURE REVIEW....3

Introduction....3
Overview....5
Gene Replacement....9
Assignment of MoFe Protein Metallocluster Domains....10
Fe Protein-Nucleotide Binding and Hydrolysis....16
Component Protein Interactions....23
P-Cluster Structure and Polypeptide Environment....31
FeMo-Cofactor Structure and Polypeptide Environment....37
Summary and Comments....46

CHAPTER I....50
Identification of a nitrogenase protein-protein interaction site defined by residues 59 through 67 within the *Azotobacter vinelandii* Fe protein.

Summary....50
Introduction....51
Experimental Procedures....56
Results and Discussion....59

CHAPTER II....77
Fe protein-MoFe protein interaction and intermolecular electron transfer: Role of the α-subunit aspartate-161 residue.

Summary....77
Introduction....78
Experimental Procedures....80
Results and Discussion....84

CHAPTER III.....97
Intramolecular electron transfer within the nitrognase MoFe protein: Role of the β-subunit tyrosine -98 residue.

Summary.....97
Introduction.....99
Experimental Procedures.....101
Results and Discussion.....108

DISCUSSION.....122

REFERENCES.....131

VITA.....150

LIST OF ILLUSTRATIONS

Figure 1. Ribbons diagrams of the *A. vinelandii* Fe protein and an αβ-unit of the MoFe protein poised to represent the proposed docking model....6

Figure 2. Gene replacement strategy....11

Figure 3. Ribbons diagram of the Fe protein....17

Figure 4. Coil diagram of the *A. vinelandii* Fe protein highlighting proposed component protein interaction sites....25

Figure 5. Coil diagram of an αβ-unit of the *A. vinelandii* MoFe protein highlighting proposed component interaction sites....29

Figure 6. Ball and stick models of the MoFe protein P cluster and organization of its coordinating cysteine residues....32

Figure 7. Ribbons diagram highlighting the location of the side chain of β-Tyr^{98} residue with respect to the P cluster and FeMo-cofactor in the MoFe protein....36

Figure 8. Ball and stick models of the FeMo-cofactor and selected residues contained within its polypeptide environment....38

Figure 9. Stereoscopic view of the Fe protein and an αβ-unit of the MoFe protein representing the component protein docking model....55

Figure 10. Coomassie-blue stained SDS-PAGE of purified Av2 and AvCp2....61

Figure 11. Determination of the maximum activity Av1 proton reduction specific activity that can be supported by titration with increasing amounts of Av2 or AvCp2....62.

Figure 12. Comparison of the effect of increasing NaCl concentration on the H_2 evolution activity of Av2-dependent and AvCp2-dependent reactions....64

Figure 13. Dependence of nitrogenase H_2 evolution and MgATP hydrolysis on the Av1:Av2 or AvCp2 molar ratio....66

Figure 14. Dependence of nitrogenase ethylene formation and MgATP hydrolysis on the Av1:Av2 or AvCp2 molar ratio....70

Figure 15. Percentage of total electron flux through nitrogenase diverted to H_2 formation under 10% acetylene as a function of Av1:Av2 or Av1:AvCp2 molar ratio....71

Figure 16. Effect of NaCl concentration on Av1-Av2, Av1(α-Asn^{161})-Av2, and Av1(α-Asn^{161})-AvCp2 dependent reactions....90

Figure 17. Dependence of nitrogenase H_2 evolution and MgATP hydrolysis on the Av1:Av2, Av1(α-Asn^{161}):Av2 or Av1(α-Asn^{161}):AvCp2 molar ratio....92

Figure 18. MgATP dependent electron transfer from the Fe protein to the MoFe protein and ensuing absorbance changes as steady-state is attained in Av1-Av2, Av1(α-Asn^{161})-Av2 or Av1(α-Asn^{161})-AvCp2 dependent reations....94

Figure 19. Ribbons diagram highlighting the location of the side chains of β-Tyr^{98} and α-Tyr^{91} residues with respect to the P cluster and FeMo-cofactor....102

Figure 20. Coomassie-blue stained SDS-PAGE of purified wild-type, β-His^{98}, β-Leu^{98}, and β-Phe^{98} MoFe proteins....105

Figure 21. The effect of component protein molar ratio on wild-type and β-His^{98} MoFe protein dependent H_2 evolution and acetylene reduction activities....114

Figure 22. MgATP dependent electron transfer from the Fe protein to the MoFe protein and ensuing absorbance changes as steady-state is attained in wild-type and β-His^{98} MoFe protein dependent reactions....115

Figure 23. Stopped-flow spectrophotometric traces of wild-type and β-His^{98} MoFe protein dependent flavodoxin oxidation....119

Scheme 1. Fe protein cycle highlighting two possible routes proposed to be responsible for the uncoupling of MgATP hydrolysis from substrate reduction....68

LIST OF TABLES

Table 1. Measured rate constants for primary electron transfer and apparent component protein dissociation of Av2 and AvCp2 dependent reactions.....73

Table 2. Construction of *A. vinelandii* mutant strains with amino acid substitutions at α-Asp^{161}, α-Asp^{162}, β-Asp^{160}, and β-Asp^{161} of theMoFe protein.....82

Table 3. Diazotrophic growth rates and crude extract activities of *A. vinelandii* mutant strains with amino acid substitutions at α-Asp^{161}, α-Asp^{162}, β-Asp^{160}, and β-Asp^{161}.....86

Table 4. Kinetics constants for Av1-Av2, Av1-AvCp2, Av1(α-Asn^{161})-Av2 or Av1(α-Asn^{161}-AvCp2) dependent reations.....88

Table 5. Construction and diazotrophic growth of *A. vinelandii* mutant strains with amino acid substitutions at α-Tyr^{91} and β-Tyr^{98} of the MoFe protein.....103

Table 6. Maximum specific activities and MgATP hydrolysis of altered MoFe proteins with amino acid substitutions at β-Tyr^{98} of the MoFe protein.....112

ABBREVIATIONS

The abbreviations and nomenclature used were as follows: MoFe protein is equivalent to component 1; Fe protein is equivalent to component 2. The abbreviations of these proteins, according to species are: Av1, Cp1 and Kp1, MoFe proteins from *Azotobacter vinelandii*, *Clostridium pasteurianum*, and *Klebsiella pneumoniae*, respectively; Av2, Cp2, and Kp2, Fe proteins from *A. vinelandii*, *C. pasteurianum*, and *K. pneumoniae*, respectively. AvCp2 indicates the hybrid Fe protein produced by strain DJ911. The oxidation state of the Fe protein, the identity of the bound nucleotide, and Fe protein–MoFe protein complexes are designated according to the convention described by Thorneley and Lowe, (1984). As examples, a complex of the MoFe protein and Fe protein from *A. vinelandii* is indicated as Av1–Av2; the oxidized, MgADP–bound form of the *A. vinelandii* Fe protein is indicated as $Av2_{ox}(MgADP)_2$; and the oxidized, MgADP–bound form of the Fe protein complexed to the MoFe protein is indicated as $Av2_{ox}(MgADP)_2$–Av1. Individual amino acids of either the Fe protein or MoFe protein are indicated by the three letter abbreviation for the amino acid followed by the residue number in superscript and in the case of the MoFe protein residues the subunit designation is used. For example, MoFe protein α-subunit residue aspartate-161 is indicated α-Asp^{161}. In the same manner, an amino acid substitution is indicated by replacing the original amino acid with the resulting amino acid. For example, the substitution α-Asp^{161} by Asn is represented as α-Asn^{161}. AvFldII is flavodoxin II from *A. vinelandii*; HQ, hydroquinone; SQ, semiquinone; HEPES, (N–[2–Hydroxyethyl] piperazine–N'–[2–ethanesulfonic acid]), SDS–PAGE, sodium dodecyl sulfate–polyacrylamide gel electrophoresis.

PURPOSE

Biological nitrogen fixation is catalyzed by the complex metalloenzyme nitrogenase, consisting of two separable components termed the Fe protein and the MoFe protein reflecting the metal content of their respective prosthetic groups. The Fe protein is a dimer of identical subunits (Mr ≈ 63,000) bridged by a single Fe_4S_4 cluster which serves as the unique electron donor to the MoFe protein. The MoFe protein is an $\alpha_2\beta_2$ tetramer (Mr ≈ 230,000) which contains two types of metalloclusters, P clusters (Fe_8S_8) and iron-molybdenum cofactors (Fe_7S_9Mo-homocitrate). Nitrogenase catalysis involves the sequential delivery of single electrons from the Fe protein to the MoFe protein, which contains the substrate binding and reduction site. Since the reduction of dinitrogen to ammonia requires a minimum of six electrons, there must be a mechanism by which multiple electrons can be accepted and stored within the MoFe protein while maintaining unidirectional electron flow.

Prior to the availability of x-ray crystallographic models for both component proteins, very little work had focused on probing the specific pathways of electron transfer in nitrogenase. As a result of the elucidation of the structure of both component proteins in 1992, a model for component protein docking was proposed that places the Fe_4S_4 cluster of the Fe protein in close proximity to the MoFe protein's P cluster (Kim and Rees, 1992b; Howard, 1993). This is consistent with the long accepted view that electrons are transferred from the Fe protein's Fe_4S_4 cluster to the MoFe protein's P cluster before their involvement in substrate reduction at the iron-molybdenum cofactor. In the discussion of the docking model, as well as the detailed description of the x-ray crystallographic structure, specific regions of the Fe protein and the MoFe protein were implicated as possibly having a role in component protein interaction. Similarly, regions of the MoFe protein were suggested as being involved in intramolecular electron transfer between the P cluster and the iron-molybdenum cofactor (Kim and Rees, 1992b; Howard, 1993; Kim and Rees, 1994).

In this study, the pathway of nitrogenase electron transfer was probed by using

site-directed mutagenesis to place either single or groups of amino acid substitutions within the regions proposed by Rees and Howard to be involved in either the component protein interaction that facilitates intermolecular electron transfer or the intramolecular electron transfer between the P cluster and the iron-molybdenum cofactor within the MoFe protein. The results of the detailed biochemical characterization of several of the altered nitrogenase component proteins constructed using this strategy are described and discussed in the context of an overall mechanism of electron transfer in nitrogenase.

LITERATURE REVIEW

This literature review was prepared by Dr. Dennis Dean, Dr. Karl Fisher and myself as a manuscript entitled "Nitrognease Structures: A biochemical-genetic perspective" which was submitted to be included in the 1995 Annual Review of Microbiology. Steve Muchmore and Jeff Bolin of Purdue University assisted in demonstration of the Molscript program used in generating most of the illustrations.

Introduction

Nitrogenase is a complex, two-component, metalloenzyme which catalyzes the MgATP dependent reduction of N_2 to yield two molecules of NH_3. This catalytic reduction of N_2 is called biological nitrogen fixation and the stoichiometry of the reaction is usually indicated as:

$$N_2 + 8e^- + 8H^+ + 16MgATP \rightarrow 2NH_3 + H_2 + 16MgADP + 16\ Pi$$

Nitrogen fixation, together with the processes of nitrification and denitrification, comprise the biogeochemical nitrogen cycle. There is considerable agronomic and ecologic relevance to biological nitrogen fixation research because the availability of a utilizable or "fixed" form of nitrogen frequently limits plant productivity. In agronomic situations where a fixed source of nitrogen is limiting, the application of industrially produced nitrogenous fertilizers is often used to increase productivity. Industrial formation of such nitrogenous fertilizers is expensive because the process necessitates the consumption of non-renewable fossil fuels. Furthermore, the run-off which occurs after application of industrially formed fertilizers represents a source of environmental pollution. Another aspect which concerns the agronomic significance of biological nitrogen fixation is that some nitrogen-fixing microorganisms, for example the rhizobia, are capable of establishing a symbiotic association with certain crop plants. In such a relationship the

microorganism benefits by catabolism of "fixed" carbon provided by plant photosynthesis and the plant benefits by utilization of nitrogen fixed by the microorganism. Within this framework of a symbiotic relationship, any improvement in the biochemical process of nitrogen fixation or any expansion in the ability of microorganisms to endow agronomically important plants with the ability to fix nitrogen by establishing novel symbiotic relationships could represent economically beneficial and ecologically sound avenues for increasing plant yield. In addition, plant–microbe interactions involving agronomically beneficial symbiotic relationships can be considered an example of controlled plant pathogenesis and, thus, studies on such processes provide a paradigm for understanding the nature of plant infection by microorganisms. Biological nitrogen fixation is also of general interest to microbiologists because the extreme oxygen lability of the biochemical process has restricted it to microorganisms, and to only those that are either capable of anaerobic metabolism or those that have developed mechanisms for protecting the catalytic system from oxygen inactivation. Finally, because nitrogenase catalysis involves familiar biochemical processes such as protein–protein interaction, signal transduction, and electron transfer reactions, studies on the enzymology of nitrogenase are of general relevance.

In 1992 a major advance in nitrogen fixation research was achieved when crystallographically determined three–dimensional models were proposed for both of the nitrogenase component proteins and their associated metalloclusters (Georgiadis *et al.*, 1992; Kim and Rees, 1992a; Kim and Rees, 1992b; Bolin *et al.*, 1993a; Bolin *et al.*, 1993b; Chan *et al.*, 1993; Rees *et al.*, 1993b). Since then several comprehensive reviews and brief overviews which describe various aspects of the structural features of the nitrogenase component proteins and their mechanistic implications have appeared (Dean *et al.*, 1993; Mortenson *et al.*, 1993; Rees *et al.*, 1993a; Eady and Leigh, 1994; Howard and Rees, 1994; Kim and Rees, 1994). Also, a number of reviews were published shortly before the availability of the three dimensional models (Burgess, 1990; Burris, 1991; Newton, 1992; Smith and Eady, 1992; Yates, 1992) and these provide excellent summaries of the biochemical and kinetic features of nitrogenase catalysis. In the present

chapter we have attempted to avoid extensive overlap with these other reviews by limiting our discussion to a description of several biochemical–genetic strategies that have been used to alter the nitrogenase component proteins as an approach to probe their structural and functional properties. The experimental rationale for certain of these experiments, formulated prior to the availability of structural information, are presented and are discussed in the context of the recently proposed crystallographic models for the nitrogenase component proteins.

Overview

The two component proteins of the nitrogenase complex, which can be separately isolated from each other, are often designated as the Fe protein and the MoFe protein. These terms reflect the metal compositions of the prosthetic groups contained within the respective component proteins. The Fe protein is a γ_2 homodimer (Mr $\approx$ 60,000; encoded by *nifH*) which contains 4 Fe atoms organized into a Fe_4S_4 cluster, and the MoFe protein is an $\alpha_2\ \beta_2$ heterotetramer (Mr $\approx$ 250,000; α encoded by *nifD*, and β encoded by *nifK*) which contains 30 Fe atoms and 2 Mo atoms organized into two pairs of metalloclusters, referred to as P clusters (Fe_8S_8) and FeMo–cofactors (Fe_7S_9Mo–Homocitrate). The structures and proposed functions of the nitrogenase metal clusters are described in detail in a later section. Figure 1 shows ribbon diagrams of two different views which represent the current model for the interaction of the *Azotobacter vinelandii* Fe protein with the MoFe protein that occurs during catalysis.

As a starting point for discussion of nitrogenase enzymology, a number of basic mechanistic features of the process, generally accepted for a number of years, but not necessarily experimentally proven for every case, are summarized as follows: 1. During catalysis electrons are delivered one at a time from the Fe protein to the MoFe protein. 2. The path of electron transfer occurs primarily towards substrate reduction. 3. Intermolecular electron transfer requires the association and dissociation of the component

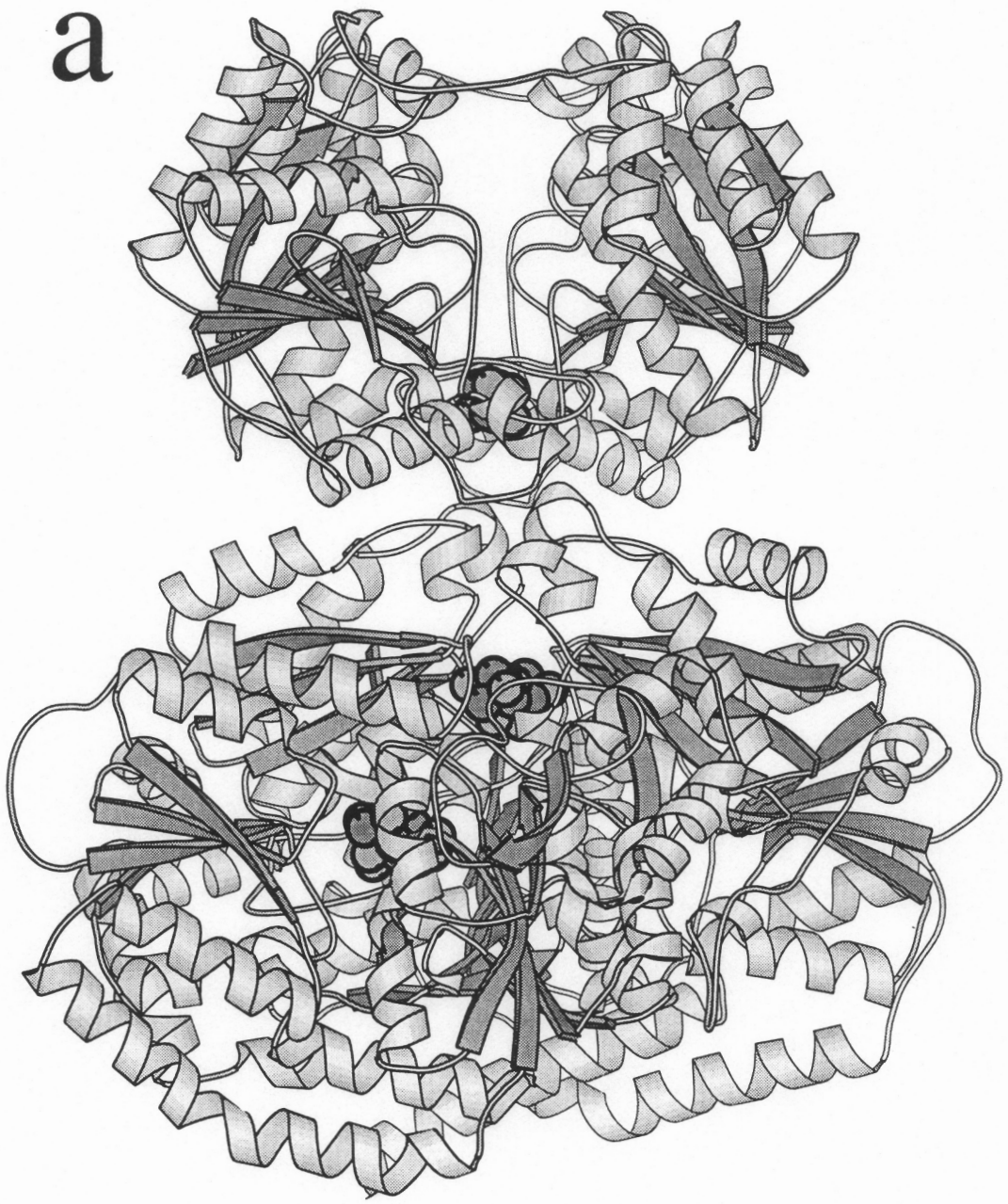

Figure 1. Ribbons diagrams (Kraulis, 1991) of the *A. vinelandii* Fe protein homodimer and an $\alpha\beta$-unit of the MoFe protein. The two different views, (a) and (b), represent 90 degree rotations about the y-axis. The associated metalloclusters are represented by space-filling models. The view in both (a) and (b) shows the Fe protein (top) poised for interaction with the MoFe protein (bottom) and is based on the docking model proposed by Rees and Howard (Kim and Rees, 1992b; Howard, 1993; Howard and Rees, 1994). It can be seen that upon docking the Fe protein's Fe_4S_4 cluster is positioned in the closest possible proximity to the MoFe protein's P cluster.

b

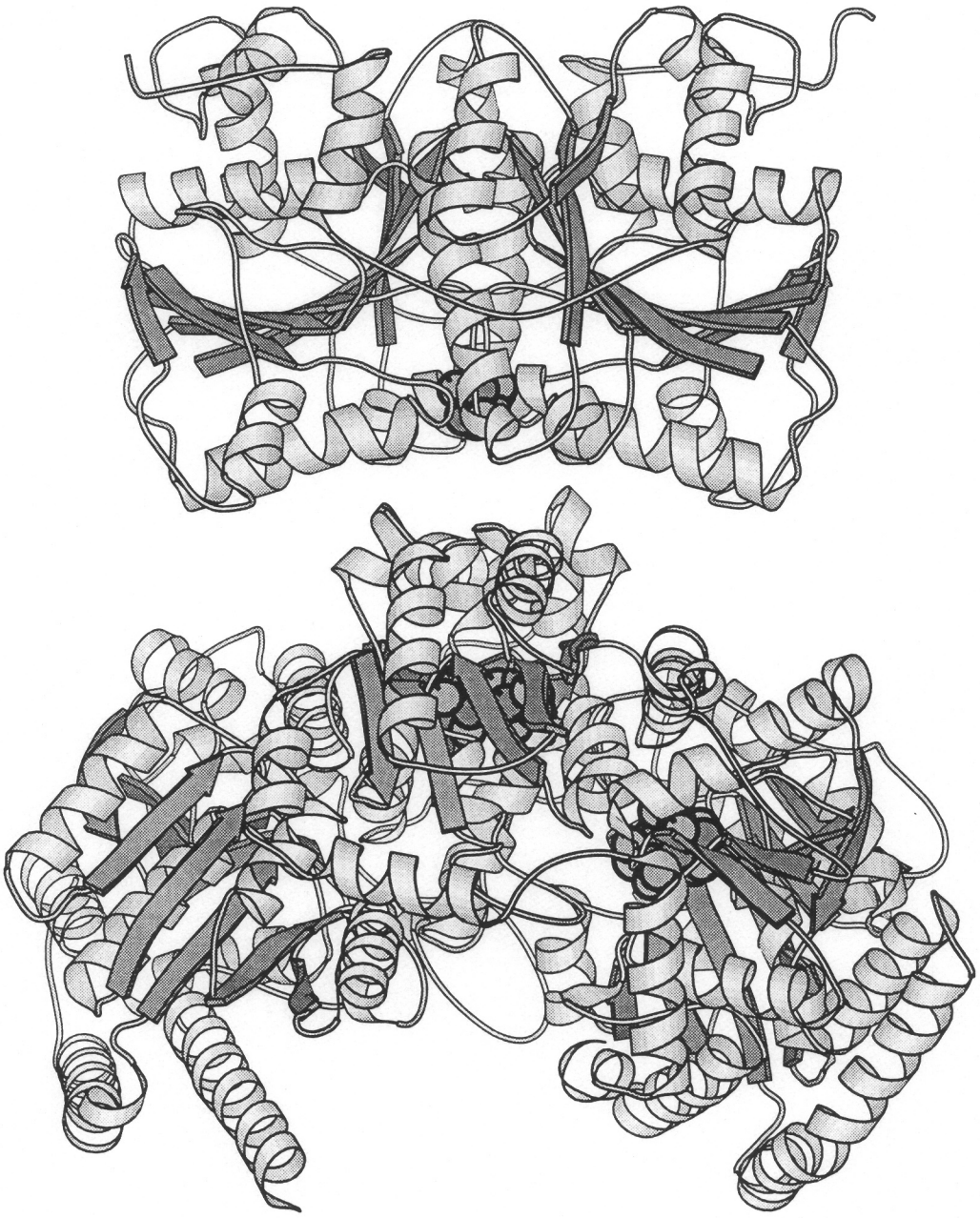

proteins and the hydrolysis of at least two molecules of MgATP for each electron transfered. 4. Dissociation of the component proteins following intermolecular electron transfer is rate limiting. 5. The MgATP binding sites are located within the Fe protein but no MgATP hydrolysis or intermolecular electron transfer occurs without formation of the Fe protein–MoFe protein complex. 6. The MgATP binding site and the Fe_4S_4 cluster are separately located within the Fe protein and they are unlikely to come within intimate contact with each other at any stage of catalysis. 7. Multiple rounds of intermolecular electron transfer must occur before any substrate is reduced. 8. The P cluster and FeMo–cofactor are separate entities that do not directly interact with each other. 9. The P cluster is the immediate acceptor in the intermolecular electron transfer event and probably brokers the intramolecular delivery of electrons to the FeMo–cofactor. 10. FeMo–cofactor provides the substrate reduction site. 11. The tetrameric MoFe protein contains two separate, but identical, substrate reduction sites, each contained within an individual $\alpha\beta$ unit of the MoFe protein. 12. Nitrogenase catalyzes evolution of one H_2 for every N_2 reduced. 13. Nitrogenase is able to reduce a variety of substrates other than N_2, most notably acetylene, which may be reduced by two electrons to yield ethylene. 14. In the absence of any other reducible substrate, nitrogenase catalyzes proton reduction to yield H_2. 15. All other conditions being equal, the total electron flux through the system is independent of the substrate reduced. Total flux refers to the sum of the rate of the total electrons distributed to all products under any particular condition. 16. N_2 is a competitive inhibitor of acetylene reduction but acetylene is a non–competitive inhibitor of N_2 reduction. 17. CO is not a nitrogenase substrate but is a non–competitive inhibitor of all substrates except protons. 18. No matter what the substrate, in the presence of CO, electron flux remains unchanged but is directed exclusively to proton reduction.

From these considerations it can be seen that the essential mechanistic issues associated with nitrogenase catalysis involve: (a) the role of MgATP in component protein interaction and electron transfer, (b) the nature of the interaction between the nitrogenase component proteins, (c) how the individual metalloclusters communicate with each other to accomplish their respective roles in mediating electron transfer, substrate binding, and

substrate reduction, (d) where and how multiple electrons are accumulated and stored within the MoFe protein prior to substrate binding and reduction, and (e) how and at what redox state(s) are various nitrogenase substrates and inhibitors bound to the active site. One powerful approach towards addressing these issues is to specifically alter the polypeptide environments (or structures) of the individual metalloclusters, or modify the MgATP binding site, and subsequently determine the spectroscopic, redox, and catalytic consequences that result from such alterations. This approach is now being vigorously pursued in several laboratories through alteration of the primary sequences of the nitrogenase component proteins by mutagenesis of the appropriate genes, and by structural alteration or elimination of the FeMo-cofactor by mutagenesis of genes involved in its assembly. In the following section we briefly summarize a gene replacement approach that has been used for site-directed mutagenesis of the nitrogenase structural genes from *A. vinelandii*. Subsequently we describe strategies that were used to target certain residues or regions for substitution without the benefit of structural models and, finally, the results of these "site-directed" amino acid substitution studies are discussed in the context of the structural models now available.

Gene Replacement

The genetic complexity of the nitrogenase system has denied the application of traditional molecular genetic strategies where altered proteins are hyperproduced in *Escherichia coli* using a heterologous expression system. The reason for this is that the primary translation products of the *nif* structural genes are not active, but require a consortium of other *nif*-specific gene products for their maturation (reviewed in Dean and Jacobson, 1992; Dean *et al.*, 1993). Also, the use of multicopy plasmids that are able to replicate in the native host are of little use because an elevation in the copy number of one *nif*-specific gene can unbalance the expression of other *nif*-specific genes by sequestering the available *nif*-specific activator molecules (Benyon *et al.*, 1983). This problem has been successfully circumvented by using a low-copy-number plasmid (Kent *et al.*, 1989),

but the approach is somewhat complicated because the recipient must have the corresponding chromosomal region inactivated without affecting expression of any of the other linked *nif*-specific genes. It was for these reasons that a gene replacement strategy was developed for genetic manipulation of the nitrogenase structural genes from *A. vinelandii* (Brigle *et al.*, 1987a). In this context gene replacement refers to the exchange of a gene that has been modified by in vitro techniques, for example by site-directed mutagenesis, for the corresponding chromosomally encoded gene. The major advantages of the gene replacement technique are that it avoids any deleterious effect that could arise indirectly through an unbalance of *nif*-specific gene expression and, providing they are not placed under severe selective pressure, the resulting mutant strains are stable. *A. vinelandii* is ideally suited for the gene replacement strategy because there is a highly efficient method for transformation (Page and von Tigerstrom, 1979) and high frequency of homologous recombination inherent to this organism. The technical aspects of the gene replacement procedure have been described in detail (Robinson *et al.*, 1986; Brigle *et al.*, 1987a) and a schematic representation is shown in Figure 2.

Assignment of MoFe Protein Metallocluster Domains

Once it became established that reasonably facile methods for site-directed mutagenesis and gene-replacement could be applied to the nitrogenase system, the next challenges became targeting specific amino acids for substitution and deciding which amino acids should be used as substituting residues. Because these studies were initiated without the benefit of structural models, it was necessary to use indirect methods to target individual residues and specific regions for modification. Although these indirect approaches have now been largely superseded by the availability of detailed structural information, there are several reasons why it remains worthwhile to summarize and comment on the logic employed in these initial studies. First, because the information and assumptions used to guide early amino acid substitution studies turned out to be essentially correct, the success of the approaches used in assigning functionally important

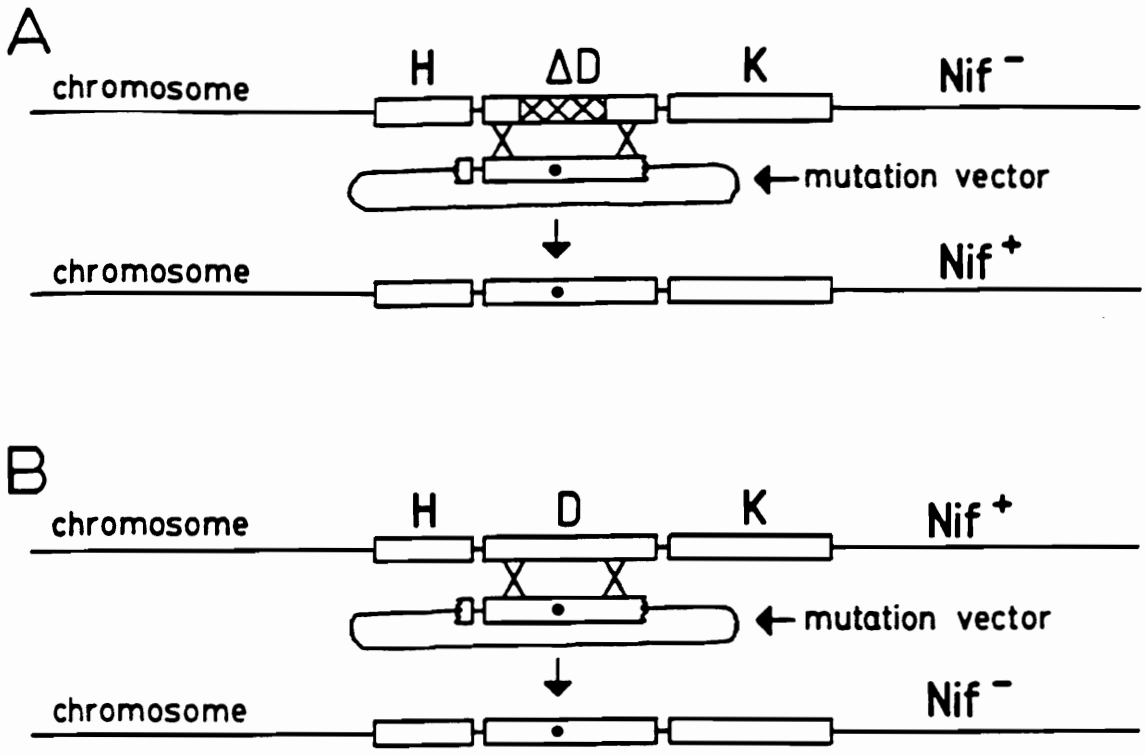

Figure 2. Gene replacement strategy. A specific mutation is first introduced into a hybrid plasmid which contains a portion of a nitrogenase structural gene using traditional in vitro site-directed mutagenesis techniques. The hybrid plasmid which carries the site-directed mutation is indicated as "mutation vector" in the figure and the mutation is indicated as a dot. During transformation with the mutation vector, DNA allelic exchange may occur by double reciprocal recombination events between homologous regions of the hybrid plasmid and the chromosome. In the figure, such reciprocal recombination events are indicated by crosses between the chromosome segments and the mutation vector. A silent or leaky mutation, i.e. one that does not result in a Nif⁻ phenotype, can be introduced into the *A. vinelandii* genome by transformation of a Nif⁻ strain that carries a defined deletion to prototrophy (A). A mutation that results in a Nif⁻ phenotype can be introduced into the genome by transforming the wild-type strain to the Nif⁻ character as indicated in (B). This is accomplished by congression using rifampicin as the selectable marker followed by scoring rifampicin resistant transformants for the Nif⁻ phenotype.

residues demonstrates the feasibility of designing informative amino acid substitution studies without necessarily having a structural model in-hand. Second, the fact that conclusions from amino acid substitution studies and the nitrogenase structural models are in substantial agreement justifies confidence that both techniques have arrived at a truly correct picture. The same point can be made equally well for spectroscopic studies, such as extended x-ray absorption fine structure, electron nuclear double resonance, and electron spin echo envelope modulation that were also successfully used to gain many structural insights concerning the nitrogenase associated metalloclusters and their respective polypeptide environments prior to the emergence of the crystallographically determined models (see discussions in Burgess, 1990; Newton, 1992; Chen *et al.*, 1993). Third, because of previous success, together with indications of the reliability of the information obtained by the various techniques, it can now be anticipated that a combination of sophisticated biophysical, kinetic, genetic, and structural approaches will provide a basis for gathering substantially more detailed mechanistic information about nitrogenase than now available. This situation underscores the importance of developing technologies in parallel rather than waiting for one or another technique to take the lead when attempting to understand complex biological processes. Below we describe criteria that were used to target potential metallocluster environments within the MoFe protein as an example of the logic involved in the development of amino acid substitution studies for analysis of the nitrogenase system. Results from experiments using both *K. pneumoniae* and *A. vinelandii* are discussed in this chapter but, for clarity and consistency, all numbers will refer only to the *A. vinelandii* primary sequences.

Site-directed mutagenesis programs for study of the nitrogenase MoFe protein were initiated both in Blacksburg (*A. vinelandii* model system) and in Sussex (*K. pneumoniae* model system) at about the same time, and at about the same time both groups proposed detailed assignments of the polypeptide environments for the metalloclusters contained within the MoFe protein to guide their respective amino acid substitution strategies (Brigle *et al.*, 1985; Kent *et al.*, 1989; Dean *et al.*, 1990a, Dean *et al.*, 1990b; Kent *et al.*, 1990; Scott *et al.*, 1990; May *et al.*, 1991; Scott *et al.*, 1992).

Although formulated independently, the common features of both models were essentially the same. The following information was used to target potential metallocluster polypeptide environments and to assign their spatial arrangements within the MoFe protein. 1. MoFe protein primary amino acid sequences from a variety of different organisms were compared. 2. The MoFe protein α– and β–subunit primary sequences were compared to each other. 3. The MoFe protein α– and β–subunit primary sequences were respectively compared to the primary sequences of the *nifE* and *nifN* gene products. 4. The requirements for chemical extrusion and the spectroscopic features of the metalloclusters were considered. 5. The chemical reactivities of the isolated clusters were taken into account. 6. Metallocluster binding motifs from other organisms were considered. 7. The results of amino acid substitution studies were taken into account as such data became available. Described below are salient features that emerged from these considerations and the experimental basis for making the assignments.

Assignment: Each 8–Fe–containing P cluster is coordinated to the MoFe protein through cysteine ligands provided by residues α–Cys^{62}, α–Cys^{88}, α–Cys^{154}, β–Cys^{70}, β–Cys^{95} and β–Cys^{153} and is solvent exposed or is located close to the polypeptide's surface. Rationale: (i) Fe–S clusters are typically bound to proteins through cysteine ligands and can be quantitatively extruded by unfolding the protein in an organic solvent in the presence of excess thiols (Orme-Johnson and Holm, 1978). Extrusion of P clusters by this method (Kurtz *et al.*, 1979), therefore, indicated cysteine ligands coordinate this cluster. (ii) These Cys residues are strictly conserved in all known MoFe protein sequences and are, therefore, likely to be functionally important (reviewed by Dean and Jacobson, 1992). (iii) Spatial and primary sequence conservations are observed when regions surrounding residues α–Cys^{62}, α–Cys^{88}, and α–Cys^{154} are compared to the corresponding regions surrounding residues β–Cys^{70}, β–Cys^{95} and β–Cys^{153} (Lammers and Haselkorn, 1983; Thöny *et al.*, 1985; Holland *et al.*, 1987). Such similarities in both spatial arrangement and primary sequence satisfy the requirement for four structurally similar domains within the MoFe protein that, on the basis of Mossbauer studies (Dunham *et al.*, 1985, McLean *et al.*, 1987), are needed to accommodate the P clusters. (iv)

Because the Fe protein's Fe_4S_4 cluster is bridged between identical subunits (Hausinger and Howard, 1983; Howard *et al.*, 1989) it was expected that during component protein interaction it would contact the MoFe protein at an interface that provides some aspect of two-fold symmetry. Although there are no repeated motifs within the primary sequences of either the α-subunit or the β-subunit, sequence conservation recognized between the subunits, which includes the proposed P cluster ligands, could accommodate such an arrangement. (v) A near surface location for P clusters is expected if they are primary acceptors during the intermolecular electron transfer event.

Assignment: The MoFe protein α-subunit Cys^{275} residue provides the only thiolate ligand to FeMo-cofactor and it is coordinated to an Fe atom within FeMo-cofactor. Rationale: (i) Thiols react with isolated FeMo-cofactor in a 1-to-1 stoichiometry indicating the presence of a single thiol ligand to FeMo-cofactor in its protein-bound form (Burgess *et al.*, 1980b; Conradson *et al.*, 1988). (ii) Nuclear magnetic resonance and extended x-ray absorption spectroscopies indicated that an Fe atom provides the thiol-reactive site on isolated FeMo-cofactor (reviewed in Burgess, 1990; Newton, 1992). (iii) The α-Cys^{275} residue is strictly conserved and it is contained in a region exhibiting high primary sequence conservation (Dean and Jacobson, 1992). (iv) Other cysteines were already assigned as potential P cluster ligands. (v) Residue α-Cys^{275} is the only cysteine residue flanked by residues having amide functions, which might be displaceable by N-methyl formamide, the chaotropic organic solvent commonly used to extract FeMo-cofactor from its polypeptide matrix (Shah and Brill, 1977). (vi) The MoFe protein α-Cys^{275} residue has an analogous residue conserved in the *nifE* gene product sequence, E-Cys^{250} (Dean and Jacobson, 1992). The *nifE* and *nifN* gene products bear significant primary sequence identity when compared to the MoFe protein α- and β-subunits, respectively, and they form a heterotetrameric complex that is proposed to provide a scaffold upon which FeMo-cofactor is assembled (Brigle *et al.*, 1987b; Paustian *et al.*, 1989 also, see below). (vii) In the native MoFe protein, residue α-Cys^{275} is refractive to alkylation but is hyper-reactive to alkylation in an apo-form of the MoFe protein which lacks FeMo-factor (J Howard, personal communication). In other words,

when bound to the MoFe protein, FeMo-cofactor protects residue α-Cys^{275} from alkylation. (viii) MoFe protein from a mutant strain that has α-Cys^{275} substituted by α-Ala^{275} has approximately the same electrophoretic mobility when electrophoresed under non-denaturing conditions as the apo-MoFe protein, but a different mobility when compared to the native MoFe protein (Kent *et al.*, 1990). This result indicated that a thiol group at the α-residue^{275} position is required to keep FeMo-cofactor attached to the MoFe protein. (ix) When residues that flank α-Cys^{275} are substituted by certain other residues there is a perturbation in the $S = 3/2$ EPR signal characteristic of protein-bound FeMo-cofactor (Dean *et al.*, 1990a).

Assignment: FeMo-cofactor is contained entirely within the MoFe protein α-subunit and interacts with domains which include residues α-Gln^{191} and α-His^{195}. Rationale: (i) Once FeMo-cofactor is assembled upon the *nifEN* products scaffold it must escape from the biosynthetic complex during maturation of the MoFe protein. It was therefore predicted that an FeMo-cofactor-binding domain located within the *nifEN* products complex is likely to be structurally similar but functionally inequivalent when compared to the corresponding domain contained within the MoFe protein (Brigle *et al.*, 1987b; Scott *et al.*, 1990). Namely, certain functional groups contained within the MoFe protein that serve to keep FeMo-cofactor attached to the MoFe protein might not be duplicated in the biosynthetic scaffold. In this way comparison of the MoFe protein α-subunit and the *nifE* gene product primary sequences identified the MoFe protein residues α-Gln^{191} and α-His^{195} as likely being located within an FeMo-cofactor-binding domain (Scott *et al.*, 1990). (ii) The α-Gln^{191} residue was targeted as interacting with the homocitrate moiety because substitution by α-Lys^{191} results in a biochemical phenotype similar to one where homocitrate has been replaced by citrate (Hawkes *et al.*, 1984; Scott *et al.*, 1992). (iii) Electron spin echo envelope modulation (ESEEM) spectroscopic comparison of isolated and MoFe protein-bound FeMo-cofactor revealed an N-coordination to the FeMo-cofactor present only in the protein-associated species. This modulation was assigned as arising from a deprotonated N-ligand provided by a histidine residue (Thomann *et al.*, 1987). Because substitution of α-His^{195} by α-Asn^{195}

eliminated the characteristic ESEEM signal, it was suggested that FeMo-cofactor is either covalently bound to the MoFe protein through α-His^{195} or that α-His^{195} is necessary for N-coordination by some other residue (Thomann *et al.*, 1991). (iv) It was not considered likely that the MoFe protein β-subunit participated directly in FeMo-cofactor binding because comparison of the primary sequences of the *A. vinelandii* MoFe protein β-subunit and the *nifN* gene product revealed relatively lower sequence identity than did comparison of the MoFe protein α-subunit and the *nifE* gene product (Brigle *et al.*, 1987b).

Fe Protein-Nucleotide Binding and Hydrolysis

A ribbons diagram of the Fe protein structural model is shown in figure 3. The key function of the Fe protein is coordination of MgATP binding and hydrolysis with electron transfer between its Fe_4S_4 cluster and the MoFe protein's P cluster. Upon binding of MgATP the Fe protein undergoes a conformational change that is manifested by a lowering of the redox potential of its Fe_4S_4 cluster, changes in the line shape of its characteristic electron paramagnetic resonance (EPR) spectrum , and an increased susceptibility of its Fe_4S_4 cluster to specific Fe chelators (reviewed in Mortenson *et al.*, 1993). It is likely that such changes reflect a repositioning of the Fe_4S_4 cluster so that it becomes poised for the electron transfer event which is coupled to MgATP hydrolysis, which, in turn, is triggered by Fe protein-MoFe protein complex formation. Concerning the mechanism of nucleotide binding and hydrolysis, and their role in catalysis, there are three important issues to be considered. First, because the nucleotide binding site and the Fe_4S_4 cluster are separated by about 20 Å (Georgiadis *et al.*, 1992; figure 3), there must be a mechanism for communication between these two sites. Second, because formation of the Fe protein-MoFe protein complex is an absolute requirement for nucleotide hydrolysis, there must be reciprocal interactions between the two protein partners which ultimately leads to MgATP hydrolysis, electron transfer, and dissociation of the ternary complex. Third, there must be a mechanism that ensures the direction of electron flow

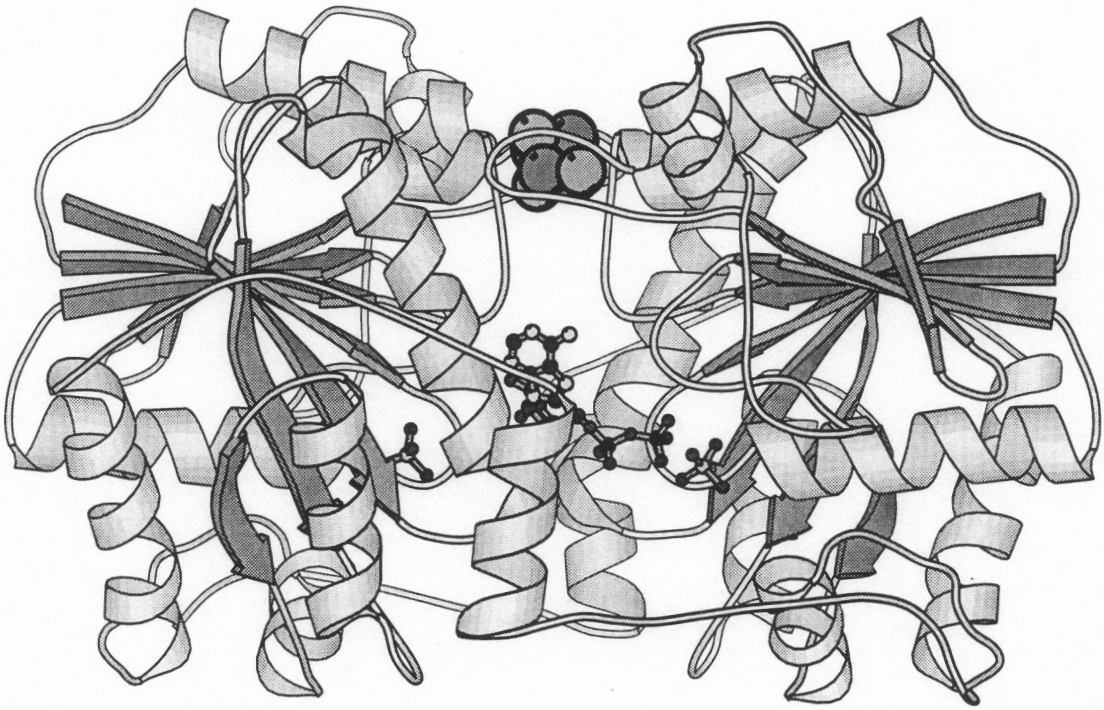

Figure 3. Ribbons diagram (Kraulis, 1991) of the *A. vinelandii* Fe protein homodimer. A space-filling model of the Fe_4S_4 cluster which bridges the identical subunits is located at the top of the structure. One ball-and-stick ADP molecule is shown bound in the intersubunit configuration. Ball-and-stick molybdate ions also indicate where residues which comprise the two Walker A nucleotide binding motifs, one per each subunit, are located.

occurs mainly towards the substrate reduction site. This latter issue is a critical one because electrons are delivered from the Fe protein to the MoFe protein in one-electron steps, yet the reduction of N_2 requires, at a minimum, six electrons for product formation. Thus, the MoFe protein must be able to accumulate multiple electrons without transferring them back to the oxidized Fe protein.

Much of what is suspected concerning communication between the Fe protein's MgATP binding site and its Fe_4S_4 cluster has come from the comparison of primary sequence (Seefeldt *et al.*, 1992; Robson, 1984) and structural features (Geogiadis *et al.*, 1992; Howard and Rees, 1994; Kim and Rees, 1994) that are common to both the Fe protein and a functionally diverse class of other nucleotide-binding proteins. The salient functional feature shared among this group of proteins is a nucleotide binding and/or hydrolysis event that is coupled to a protein conformational change. Close inspection of the structural model, described in detail elsewhere (Georgiadis *et al.*, 1992; Wolle *et al.*, 1992a; Howard and Rees, 1994), reveals that in the absence of MgATP, residue Lys^{15} (located within a Walker A-type nucleotide binding motif; Robson, 1984) probably forms a salt bridge with residue Asp^{125} (located within a Walker B-type nucleotide binding motif; Seefeldt *et al.*, 1992; Wolle *et al.*, 1992a). By comparison to other nucleotide binding proteins, it is expected that, in the MgATP bound form, residue Lys^{15} probably interacts with the β and γ phosphate groups of the nucleotide, whereas residue Asp^{125} indirectly interacts with Mg^{++} through a water molecule. This situation immediately suggests the rudiments of a signal transduction mechanism where, upon nucleotide binding, disruption of the salt bridge between Lys^{15} and Asp^{125} might trigger a cascade of structural rearrangements within the Fe protein ultimately leading to the observed changes in the Fe_4S_4 cluster environment. In this context it may be significant that residue Asp^{125} potentially provides a direct path for communication to the cluster because it is connected by a short helix to the cluster coordinating residue, Cys^{132}. The potential roles for both residue Lys^{15} and residue Asp^{125} in the signal transduction mechanism have been examined by substituting these residues by other amino acids.

Substitution of Lys^{15} by Gln^{15} results in an altered Fe protein that is unable to

undergo the MgATP induced conformational change (Seefeldt *et al.*, 1992). This property is evidenced by an inability of MgATP to cause either a perturbation in the EPR spectrum of the altered Fe protein, or to increase the susceptibility of its Fe_4S_4 cluster to chelation. However, in the absence of any added nucleotide, the EPR spectrum of the altered Gln^{15} Fe protein is identical to the normal Lys^{15} Fe protein, indicating that the Gln^{15} substitution does not cause a direct rearrangement of the polypeptide environment immediately surrounding the Fe_4S_4 cluster but probably exerts its effect by compromising the signal transduction pathway. The Gln^{15} Fe protein binds MgADP at the normal level, but binds MgATP at a somewhat reduced level when compared to the unaltered Lys^{15} Fe protein. Thus, the observation that Lys^{15} is needed to stabilize the MgATP complex, but apparently not the MgADP complex, can be interpreted to indicate that, in the MgATP bound form, Lys^{15} is normally coordinated to the terminal phosphate group of the nucleotide. This conclusion is in line with what is expected on the basis of comparison of the Fe protein structure to other nucleotide binding proteins. Nevertheless, it is somewhat surprising that, although the altered Gln^{15} Fe protein retains an ability to bind MgATP, there is not even a hint of a nucleotide induced conformational change, nor is there any detectable MgATP hydrolytic activity when the complete system is assayed under the appropriate catalytic conditions. These observations, and the fact that the Gln^{15} Fe protein is unable to compete with the Lys^{15} Fe protein for interaction with the MoFe protein, suggest that coordination of the terminal phosphate of MgATP by residue Lys^{15} is needed for at least two purposes. First, it might serve to anchor the bound nucleotide in an appropriate position to elicit the nucleotide induced conformational change necessary for complex formation between the Fe protein and the MoFe protein and, second, it might also facilitate MgATP hydrolysis once the complex is formed. It is obvious from analysis of the altered Gln^{15} Fe protein that the Lys^{15} residue plays a critical role in effecting the nucleotide induced conformational shift. Nevertheless, the signal transduction mechanism cannot be explained by a simple breaking of a salt bridge between Lys^{15} and Asp^{125} because substitution of the Lys^{15} residue by Gln^{15}, which cannot participate in forming such a salt bridge, does not render the altered protein's Fe_4S_4 cluster susceptible to

chelation. Perhaps a more reasonable scenario is that once the putative salt bridge is eliminated by nucleotide binding, and the MgATP becomes locked into the appropriate position through interaction of its terminal phosphate with the Lys^{15} residue, Asp^{125} becomes forced to adopt a new position within the nucleotide binding pocket which triggers a conformational change in the polypeptide backbone that is propagated down the short loop connecting Asp^{125} and the cluster coordinating Cys^{132} residue. By analogy to ras p21, the reorientation of Asp^{125} within the nucleotide binding pocket could be induced by indirect coordination of its carboxyl group to Mg^{++} through an intervening water molecule (Wolle *et al.*, 1992a). Thus, in this model the biochemical phenotype of the Gln^{15} Fe protein can be explained by its inability to lock MgATP into the appropriate position so that either the bound nucleotide remains too remote to interact with Asp^{125}, or the bound MgATP remains flexible enough to interact with Asp^{125} without demanding a significant reorientation of Asp^{125} within the nucleotide binding pocket.

The participation of Asp^{125} in the signal transduction mechanism has been probed through substitution of this residue by Glu^{125} (Wolle *et al.*, 1992a). The inactive Glu^{125} Fe protein shares some similarities with the Gln^{15} Fe protein because, in the absence of nucleotide, neither substitution appears to directly alter the Fe_4S_4 cluster environment. Also, like the Gln^{15} Fe protein, the Glu^{125} Fe protein is ineffective in electron transfer and is unable to catalyze MgATP hydrolysis. The distinguishing feature of the Glu^{125} Fe protein is that, unlike the Gln^{15} Fe protein, it retains the ability to undergo a conformational shift upon binding MgATP. Moreover, either MgADP or MgATP binding can effect a conformational change upon their interaction with the Glu^{125} Fe protein and the requirement for Mg^{++} has been eliminated as well. The observation that MgADP binding induces a conformational change in the Glu^{125} Fe protein was anticipated from the original design of the experiment because the goal was to test whether or not the addition of an extra methylene group might extend the primary signalling event to interaction with MgADP in addition to, or rather than, MgATP. Nevertheless, the elimination of the Mg^{++} requirement was not expected and a convincing explanation for this effect is not yet available.

A fascinating aspect of nitrogenase catalyzed MgATP binding and hydrolysis is that there appears to be a series of reciprocal signalling events which are transmitted back and forth among the nucleotide binding site, the Fe_4S_4 cluster, and the Fe protein–MoFe protein interaction site(s). In the initial event, a reduced form of the Fe protein binds probably two molecules of MgATP thereby inducing a conformational change which makes the Fe protein competent for productive complex formation with the MoFe protein. As discussed above, amino acid substitution studies, interpreted in light of the structural model, provide compelling evidence that both Lys^{15} and Glu^{125} are key players in triggering the initial events in the signal transduction mechanism. Upon complex formation, a signal must then be sent back to the nucleotide binding site with the information that it is now time to hydrolyze MgATP and transfer the electron. Because Fe protein cannot hydrolyze MgATP without interaction with the MoFe protein, it is clear that the docking event must result in a conformational change within the nucleotide binding pocket so that the residues needed to effect MgATP hydrolysis become appropriately positioned for that purpose. Next, a gating mechanism must occur so that the electron delivered to the MoFe protein is not simply donated back to the Fe protein, and finally, there must be some mechanism which results in the dissociation of the ternary complex.

What are the residues specifically involved in MgATP hydrolysis? Once again, comparison to other systems leads to speculation that either or both Asp^{39} and Asp^{129} (Georgiadis *et al.*, 1992; Howard, 1993) are involved. Asp^{129} is a particularly attractive candidate because it is located between Asp^{125} and Cys^{132} and, therefore, conformational changes propagated back and forth between Asp^{125} and Cys^{132} caused by nucleotide binding or component protein docking could be reflected by dynamic changes in the orientation of Asp^{129}. Evidence supporting this possibility has come from characterization of an altered Fe protein where Asp^{129} has been substituted by Glu^{129} (W Lanzilotta, M Ryle and L Seefeldt, personal communication). The Glu^{129} Fe protein is able to bind nucleotides with normal affinity, and undergoes the MgATP induced conformational shift, but is unable to hydrolyze MgATP or transfer electrons to the MoFe protein.

Characterization of an altered Fe protein having the Ser^{16} residue, located within the Walker A nucleotide binding motif, substituted by Thr^{16} indicates that this residue also has an important role in nucleotide hydrolysis (Seefeldt and Mortenson, 1993). The altered Thr^{16} Fe protein exhibits a higher affinity for MgATP and is dramatically impaired in its ability to utilize an alternative form of ATP, MnATP, during catalysis when compared to the same properties of the wild-type Fe protein. These results have been interpreted to indicate that during MgATP hydrolysis the γ-OH group of Ser^{16} facilitates the transition of Mg^{++} from its coordination to the γ- and β-phosphates of MgATP to coordination of the β- and α-phosphates of MgADP. This interpretation is in agreement with structural and spectroscopic evidence which indicate that the equivalent Ser residue in ras p 21 interacts with Mg^{++} of MgGTP (discussed in Seefeldt and Mortenson, 1993) and has this function as well. Although, the altered Thr^{16} Fe protein is the only Fe protein having a substitution at this position that has been characterized at the biochemical level, other substitutions have been placed at this position (Ala^{16}, Asp^{16}, Gly^{16} and Cys^{16}) and these substitutions all lead to inactivation of Fe protein catalytic activity (Seefeldt and Mortenson, 1993). These data provide further evidence for the importance of this residue. In contrast, altered Fe proteins having one of the three threonine residues located immediately following Ser^{16} substituted by serine or alanine remain active, indicating they are probably not as functionally important as Ser^{16}.

Although a reasonably clear picture of the signal transduction mechanism leading to MgATP hydrolysis is beginning to emerge, there is less direct mechanistic information concerning how the gate might close following intermolecular electron transfer. Some insight has been gained by inspection of the structural model. In the "as solved" structure only one of the two available nucleotide binding sites is occupied (Georgiadis *et al.*, 1992). This site, which is only partially occupied by MgADP, is not bound in the typical ras mode but rather spans a cleft between the subunits as shown in figure 3. Assuming this binding mode is mechanistically relevant, it leads to speculation that nucleotide bound to the Fe protein can assume two configurations (Wolle *et al.*, 1992a). For example, upon docking with the MoFe protein, MgATP bound in the ras-like mode might be hydrolyzed

leading to a transition state where intermolecular electron transfer can be achieved. Following hydrolysis, the nucleotide, now in the form of MgADP, might adopt the intersubunit binding configuration which could stabilize a conformation of the Fe protein that is incompetent to accept an electron from the MoFe protein. In this way the nucleotide can be considered to act as a swinging gate which participates in controlling the direction of electron flow. The biochemical properties of the altered Gln^{15} protein have been interpreted in view of this model (Wolle *et al.*, 1992a) where the Gln^{15} protein is suggested to only bind nucleotide in the intersubunit configuration so that no nucleotide induced movement of the cluster can be effected. This model explains the relatively lower level of MgATP binding to the Gln^{15} Fe protein but normal binding of MgADP. Conversely, for the Glu^{125} Fe protein, the ras-like binding mode could be available to both ADP and ATP such that either nucleotide can induce a conformational change, yet, neither nucleotide can be hydrolyzed to achieve electron transfer. It appears that, following the MgATP induced conformational change, the Glu^{125} Fe protein is unable to transmit the nucleotide hydrolysis signal that normally results from the component protein docking event, perhaps by preventing Asp^{129} from adopting the correct position for the postulated water-assisted attack on the terminal phosphate of MgATP or MgADP.

Component Protein Interactions

How do the Fe protein and MoFe protein interact to couple nucleotide hydrolysis to intermolecular electron transfer? A docking model based on the crystal structures of the separate components, and which takes into account chemical cross-linking studies and amino acid substitution studies has been proposed (Kim and Rees, 1992b; Howard, 1993; Howard and Rees, 1994). This model pairs the 2-fold symmetric surface of the Fe protein homodimer with the exposed surface of a MoFe protein pseudosymmetric $\alpha\beta$-unit interface. Two different views of this docking model are shown in figure 1. In this arrangement the Fe protein's Fe_4S_4 cluster is positioned in the closest possible proximity to the MoFe protein's P cluster, which accommodates the view that the primary electron

transfer event involves transient delivery of an electron from the Fe_4S_4 cluster of the Fe protein to a MoFe protein P cluster. It also places a number of charged groups located on the respective surfaces of the Fe protein and MoFe protein in an arrangement which could permit reciprocal ionic interactions between the component proteins. Studies on the salt sensitivity of nitrogenase catalytic activity indicate that such ionic interactions are critical to productive complex formation (Deits and Howard, 1990; Wolle *et al.*, 1992b; Peters *et al.*, 1994).

Inspection of the Fe protein structural model reveals a crown of positively charged residues (Arg^{100}, Arg^{140}, and Lys^{143}), located within the proposed docking interface, and which surround the Fe protein's Fe_4S_4 cluster (figure 4, Lys^{143} is not shown). One of these residues, Arg^{100}, corresponds to the reversible ADP–ribosylation site involved in the regulation of Fe protein activity in *Rhodospirrilum rubrum* (Pope *et al.*, 1985). ADP–ribosylation exerts its regulatory effect by preventing intermolecular electron transfer. Altered Fe proteins having Arg^{100} substituted by His^{100} (Lowery *et al.*, 1989; Wolle *et al.*, 1992b), Arg^{140} substituted by Gln^{140} (Seefeldt, 1994), or Lys^{143} substituted by Gln^{143} (Seefeldt, 1994), all share similar biochemical phenotypes exhibiting various levels of increased salt sensitivity and various levels of uncoupling of MgATP hydrolysis from intermolecular electron transfer. The increased salt sensitivity and substantial reduction in catalytic activity of these altered Fe proteins indicate that residues Arg^{100}, Arg^{140} and Lys^{143} normally provide dominant ionic interactions with the MoFe protein during complex formation. Namely, it appears that elimination of any of these ionic interactions renders other ionic interaction sites more susceptible to disruption by salt. Also, the fact that these residues are in close proximity to the Fe_4S_4 cluster is compatible with a model where reciprocal ionic interactions are involved in bringing the Fe protein's Fe_4S_4 cluster and a complementary site on the MoFe protein in the proper juxtaposition to effect electron transfer. Nevertheless, the functional role of these residues cannot be assigned simply to ionic interactions, because certain substitutions which eliminate the potential for the contribution of a specific ionic interaction, for example, substitution of Arg^{100} by Tyr^{100}, has only a modest effect on catalytic activity and MgATP hydrolysis remains effectively

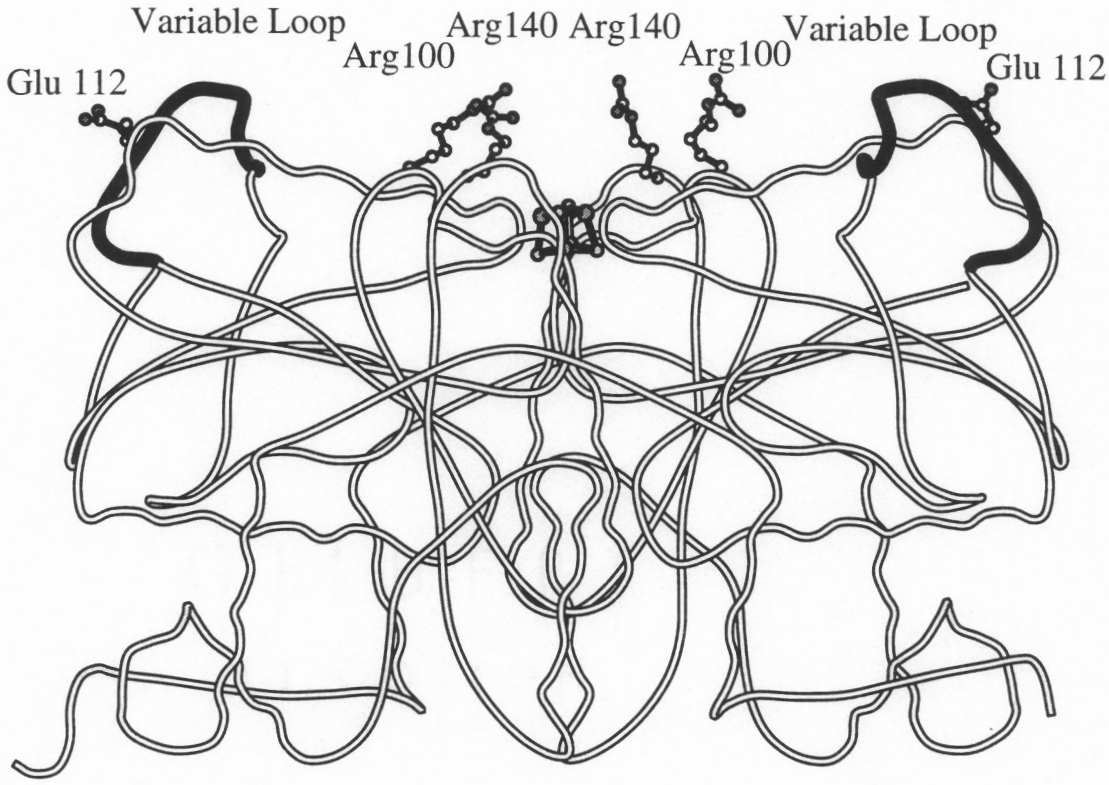

Figure 4. Coil diagram (Kraulis, 1991) of the *A. vinelandii* Fe protein homodimer which highlights the proposed component protein interaction sites. The variable loop discussed in the text is shown in bold. The view of the Fe protein is the same as in figure 1(b) except that it has been rotated by 180 degrees about the z axis.

coupled to electron transfer. It should also be noted that, because MgATP hydrolysis becomes substantially uncoupled from intermolecular electron transfer in certain of the altered Fe proteins (for example, His^{100}, in Lowery *et al.*, 1989; Wolle *et al.*, 1992b and Gln^{143}, in Seefeldt, 1994), these residues are not necessarily directly involved in the primary signalling process that leads to MgATP hydrolysis. In other words, if MgATP hydrolysis and electron transfer are obligately coupled to exactly the same signal provided by component protein interaction, they should be equally affected by any perturbation in the pathway.

Inspection of the component docking model shows that there is a loop (designated the "variable loop" in figure 4, see Howard, 1993), contained within residues 61 through 75, which is likely to interact with the MoFe protein during component protein interaction. The potential role for this region in component protein interaction was tested by construction of an *A. vinelandii* strain which produces a "hybrid" Fe protein for which a portion of this loop was replaced by the corresponding residues from the Fe protein of *Clostridium pasteurianum* (Peters *et al.*, 1994). The experimental rationale for the construction was based on the observation that a heterologous mixture of Fe protein from *C. pasteurianum* and MoFe protein from *A. vinelandii* is not catalytically active, but rather forms a tight complex (Emerich *et al.*, 1978). Thus, it was anticipated that replacement of this region of the *A. vinelandii* Fe protein primary sequence by the corresponding *C. pasteurianum* Fe protein sequence might result in duplication of the phenomenon of inactive complex formation between the resulting hybrid protein and the MoFe protein.

The hybrid Fe protein constructed in this way exhibits half the maximum specific activity of the normal Fe protein when compared to the unaltered Fe protein and its activity is insensitive to inhibition by low levels of salt. Also, the hybrid Fe protein activity is hypersensitive to a molar excess of MoFe protein, which also results in the uncoupling of MgATP hydrolysis from substrate reduction. These results can be explained if it is considered that the hybrid Fe protein forms a relatively tighter complex with the MoFe protein, which is consistent with the original experimental rationale and is also in agreement with the docking model. Direct evidence for this conclusion was provided by

stopped-flow spectrophotometric experiments which showed that the hybrid Fe protein dissociates from the MoFe protein at only half the normal rate (Peters *et al.*, 1994). In these experiments it was also shown that the apparent dissociation rate of the wild-type complex was slowed by moderate salt concentration but dissociation of the complex involving the hybrid Fe protein was unaffected under the same conditions. One interpretation of these results is that an ionic interaction involving an electrostatic repulsion which facilitates component protein dissociation has been eliminated in the hybrid Fe protein. A more detailed description of the results and conclusions of the biochemical characterization of this hybrid Fe protein can be found in Chapter I. A similar series of experiments, where the carboxyl terminus of the *A. vinelandii* Fe protein was substituted by the corresponding region from the *C. pasteurianum* Fe protein, led to the conclusion that this region does not play a significant role in component protein interaction (Jacobson *et al.*, 1990). This conclusion is also in line with the docking model which places the carboxyl region of the Fe protein on the opposite side from the proposed docking interface (figures 1 and 3).

Experiments involving the use of the chemical crosslinking reagent carbodiimide have shown that the Fe protein Glu^{112} residue and the MoFe protein β−subunit Lys^{400} come within close contact during some stage of component protein interaction (Willing and Howard, 1990). Such crosslinking is sensitive to high concentrations of salt (Willing *et al.*, 1989). Residue Glu^{112} is located on the same face of the Fe protein but at the opposite end of a helix which extends to the Arg^{100} residue and is, therefore, appropriately positioned for interaction with the MoFe protein. This helix and the variable loop discussed above comprise ridges of an anionic cleft which, in the docking model, are likely to come within contact with the MoFe protein. It is notable that Glu^{112} and the adjacent Glu^{111} from the *A. vinelandii* primary sequence are respectively replaced by leucine and glutamine in the corresponding *C. pasteurianum* primary sequence. Thus, it will be of future interest to substitute Glu^{112} by Leu^{112} and Glu^{111} by Gln^{111}, both separately and in combination, to determine if these differences in interspecific primary sequence also contribute to the phenomenon of inactive complex formation observed in heterologous

mixtures of *C. pasteurianum* Fe protein and *A. vinelandii* MoFe protein.

Although the docking model places the Fe protein's Fe_4S_4 cluster in the closest possible proximity to the MoFe protein's P cluster there is still a distance of about 15 Å which separates the clusters because the P cluster is located below the polypeptide surface (see figures 1, 3 and 5). This means that either (i) the MoFe protein polypeptide itself provides an adequate path for cluster–to–cluster electron transfer or, (ii) the MoFe protein undergoes a conformational change when it interacts with the Fe protein such that its cluster becomes more accessible to the Fe protein's cluster or, (iii) the Fe protein is able to approach the P cluster by squeezing through a cleft that is apparent at the pseudosymmetric $\alpha\beta$–interface of the MoFe protein. Note that, although mentioned individually, possibilities (ii) and (iii) are conceptually the same. The possibility that, upon association and dissociation with the Fe protein, the MoFe protein might undergo sequential conformational changes that effects movement of the P cluster towards and away from the polypeptide surface is attractive because movement of the P cluster towards the polypeptide surface could permit a direct cluster–to–cluster electron jump and the subsequent sequestering of the P cluster below the polypeptide surface could contribute to the unidirectionality of the electron transfer pathway. It has also been noted that conformational changes within the MoFe protein induced by docking and MgATP hydrolysis could lead to a rearrangement in the P cluster structure so as to alter its ability to accept or donate an electron (Howard and Rees, 1994; Rees *et al.*, 1993a).

What MoFe protein residues might be involved in transducing such conformational changes? The view of the MoFe protein structure in figure 5 shows that residues α–Asp^{161}, α–Asp^{162}, and α–Phe^{125} and the corresponding residues β–Asp^{160}, β–Asp^{161}, and β–Phe^{125} are located at or near the mouth of the pseudosymmetric cleft leading to the P cluster. The side chains of α–Asp^{162} and β–Asp^{161} are solvent exposed and appear to be appropriately positioned to interact with one of the positively charged residues which form the crown surrounding the Fe protein's Fe_4S_4 cluster. Thus, it can be imagined that ionic interactions between positively charged sidechains located on the surface of the Fe protein near its Fe_4S_4 cluster and the negatively charged aspartates could result in coordinate

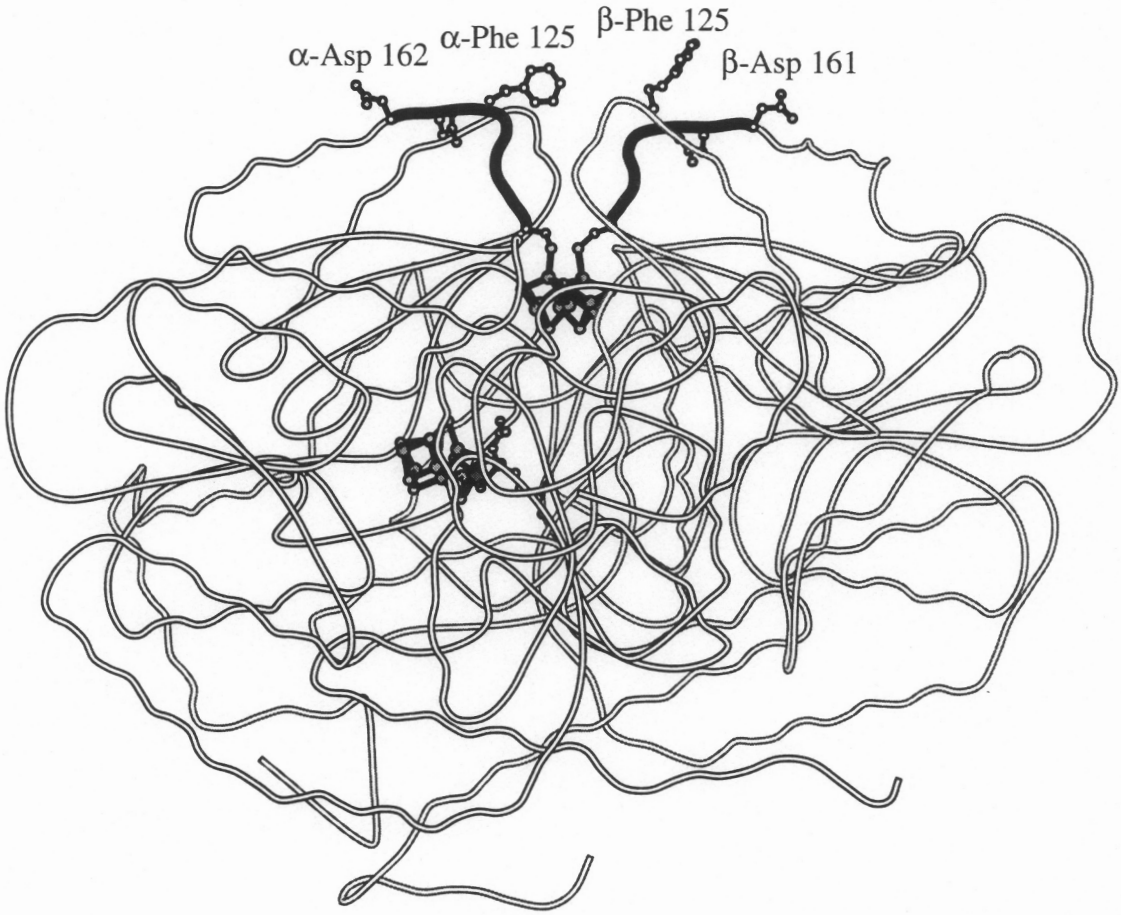

Figure 5. Coil diagram (Kraulis, 1991) of an $\alpha\beta$–unit of the *A. vinelandii* MoFe protein which highlights the proposed component protein interaction sites. The P cluster is located at the pseudosymmetric $\alpha\beta$–interface. Pathways from the surface of the molecule to the P cluster coordinating residues α–Cys^{154} and the β–Cys^{153} are indicated in bold.

transmission of signals down short helices connecting α-Asp^{162}-α-Asp^{161} and β-Asp^{161}-β-Asp^{160} to the P cluster coordinating ligands α-Cys^{154} and β-Cys^{153}, respectively. The parallel α- and β-subunit pathways from the MoFe protein surface to the respective cluster coordinating ligands are shown as dark lines in figure 5. Although not shown in the figure, another interesting feature is that the carboxylate group of α-Asp^{161} appears to be hydrogen-bonded to α-His^{83} and α-Gly^{127} and the analogous carboxylate group of β-Asp^{160} appears to be hydrogen-bonded to β-His^{90} and β-Gly^{127}. This network of hydrogen bonding allows potential communication between other surface residues, for example α-Phe^{125} and β-Phe^{125}, and the residues that provide the ligands which bridge the P cluster subcluster fragments, α-Cys^{88} and β-Cys^{95}.

Biochemical evidence that the β-Phe^{125} residue is located at the polypeptide surface was provided by the fact that this residue is located at a site that, in the *K. pneumoniae* MoFe protein, is uniquely accessible to cleavage by chymotrypsin (Fisher *et al.*, 1993). The involvement of β-Phe^{125} in component protein interaction was subsequently confirmed by kinetic analysis of an altered β-Ile^{125} MoFe protein which exhibits an approximately 70% reduction in the rate of primary electron transfer from the Fe protein to the MoFe protein (Thorneley *et al.*, 1993). These results indicate that hydrophobic interactions, as well as ionic interactions, are important in the component protein docking process. On the other hand, substitution of either α-Asp^{162} or β-Asp^{161} by asparagine residues, singly or in combination have very little effect on catalytic activity (Kim *et al.*, 1993). In contrast, substitution of the α-Asp^{161} residue by asparagine leads to a biochemical phenotype almost identical to the altered Arg^{100} Fe protein. Namely, productive complex formation becomes hypersensitive to elevated salt concentrations and MgATP hydrolysis becomes substantially uncoupled from electron transfer. The interesting aspect of the biochemical phenotype of the α-Asn^{161} MoFe protein is that the α-Asp^{161} residue is not exposed to the surface in the structural model. Thus, it seems plausible that during component protein interaction the hydrogen bonding pattern mentioned above might indeed be disrupted to effect a conformational change within the MoFe protein which could ultimately result in an ionic interaction between α-Asp^{161} and a

positively charged residue located on the Fe protein. Importantly, such a conformational change, if it does occur, could also cause a perturbation in the P cluster polypeptide environment. A curious observation is that the analogous substitution within the β−subunit, substitution of β−Asp^{160} by β−Asn^{160}, has very little effect on catalytic activity. Thus, although there is an apparent conservation in structure between these pseudosymmetric regions located at the α− and β−subunit interface, there is not a stringent conservation in functionality. The results and conclusions from the biochemical characterization of the α-Asn^{161} MoFe protein are included in Chapter II.

P-Cluster Structure and Polypeptide Environment

Each P cluster contains eight Fe atoms constructed from two, linked, cuboidal Fe_4S_4 subcluster fragments. Four cysteines, two from the α−subunit (α−Cys^{62} and a−Cys^{154}) and two from the β−subunit (β−Cys^{70} and β−Cys^{153}), coordinate individual Fe atoms within the P cluster as typical cysteinyl thiolate ligands (Chan *et al.*, 1993). In addition, two cysteines (α−Cys^{88} and β−Cys^{95}) link the subclusters by binding two Fe atoms, one from each subcluster. There is also evidence that a corner−to−corner disulfide bond links the subcluster fragments and this disulfide bridge has been proposed to be the entity which permits redox reactions to occur within the all ferrous P cluster (Rees *et al.*, 1993a; Howard and Rees, 1994). In addition to the cysteine ligands which coordinate the P cluster, the *A. vinelandii* MoFe protein structural model indicates that β−Ser^{188} also appears to coordinate the same iron as β−Cys^{153}. Two different views of the P cluster model and the organization of its coordinating ligands are shown in figure 6.

Although the apparent structural symmetry between the corresponding polypeptide environments of the individual P cluster subfragments is rather striking, amino acid substitution studies have revealed that counterpart ligands from the two subunits are not necessarily functionally identical (Kent *et al.*, 1989; Dean *et al.*, 1990b; Kent *et al.*, 1990; May *et al.*, 1991). Substitution of α−Cys^{62}, α−Cys^{154}, β−Cys^{70}, or β−Cys^{95} by serine or alanine inactivates MoFe protein activity. In many cases the loss of enzymatic activity

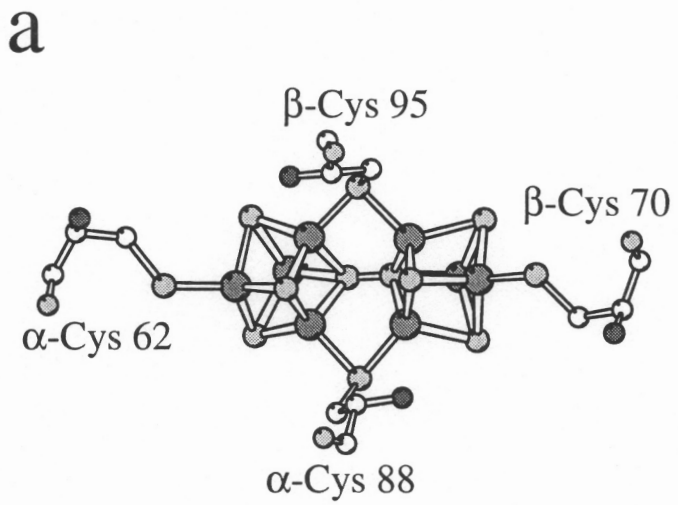

Figure 6. Ball–and–stick models (Kraulis, 1991) of the P cluster and the organization of its coordinating cysteine ligands. Each P cluster is coordinated by residues α–Cys^{62}, α–Cys^{88}, α–Cys^{154}, β–Cys^{70}, β–Cys^{95}, and β–Cys^{153}. For the sake of clarity all of the cluster coordinating ligands are not shown in each view but the location of residues not shown can be ascertained by consideration that each view is separated by an approximately 90 degree rotation about the x–axis.

b

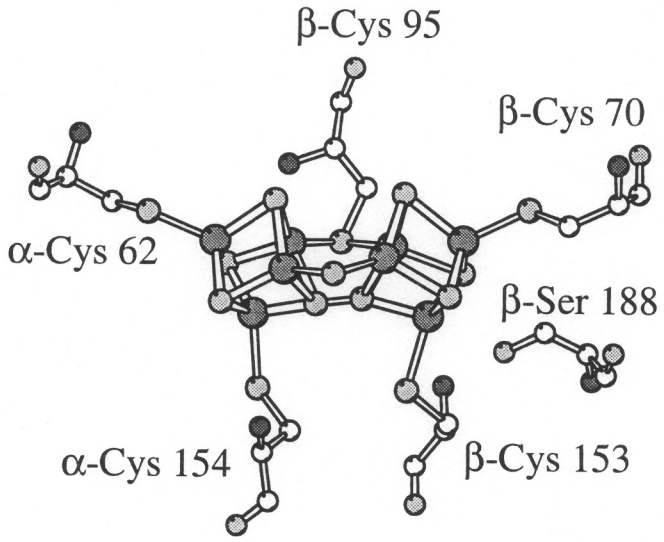

associated with these substitutions, and certain other substitutions located in the P cluster environment, is accompanied by failure to form the tetramer (Govezensky and Zamir, 1989; Kent *et al.*, 1990), indicating that the P clusters are necessary for proper assembly of the MoFe protein. In contrast to the P cluster cysteine ligands mentioned above, certain substitutions can be tolerated for the α-Cys^{88} and β-Cys^{153} residues. Why substitutions can be tolerated at these positions, but apparently not for other P cluster ligands is not yet known. It has also been shown that substitution of alanine for either α-Cys^{88} or β-Cys^{95} inactivates the MoFe protein, but some activity is recovered when both residues are substituted by alanine (Kent *et al.*, 1990). In a similar type of experiment it was shown that individual substitution of asparagine for α-His^{83} or the analogous β-His^{90} residue does not appreciably affect MoFe protein activity but a combination of both substitutions eliminates MoFe protein activity (Dean *et al.*, 1990b). It was these results and the effect of certain substitutions on the assembly of the MoFe tetramer that originally led to the hypothesis that P clusters are located at the $\alpha\beta$-interface, but again, the mechanistic implications of these findings are not understood.

It is a generally accepted working hypothesis that the catalytic role for the P cluster involves the acceptance and storage of electrons from the Fe protein and their ultimate delivery to the substrate reduction site provided by FeMo-cofactor. The spectroscopic and kinetic evidence along these lines has been recently reviewed (Lowe *et al.*, 1993). Although biochemical-genetic studies have not yet contributed towards the development of a mechanistic role for the P cluster in nitrogenase catalysis, they have provided some evidence that the P cluster does indeed broker intermolecular and intramolecular electron transfer events (May *et al.*, 1991). Substitution of the known P cluster ligand β-Cys^{153} by β-Ser^{153} results in an altered MoFe protein that supports only 50% of the maximum activity under conditions of high flux. Such a decrease in activity can be explained by (i) an alteration in the substrate reduction site, (ii) a disruption in the specific component protein interactions, or (iii) an alteration in the intramolecular delivery of electrons to the substrate reduction site. Possibility (i) was ruled out by demonstration that the catalytic and spectroscopic features of the substrate reduction site remained unchanged in the

β−Ser^{153} MoFe protein. Possibilities (ii) and (iii) were distinguished by comparison of the specific activities of the β−Ser^{153} MoFe protein and wild-type β−Cys^{153} MoFe protein under conditions of both high and low flux. It was found that under low flux conditions both proteins have approximately the same specific activity but under high flux conditions the β−Ser^{153} exhibits only 50% of the maximum specific activity when compared to the wild-type protein. The interpretation of this result is that, under conditions of high electron flux, the maximum specific activity of the β−Ser^{153} MoFe protein must be limited by the intramolecular delivery of electrons to the substrate−reduction site. On the other hand, if the β−Ser^{153} MoFe protein was defective in its ability to interact with the Fe protein, it was expected that it would exhibit a lower specific activity relative to the wild-type MoFe protein under conditions of both low flux and high flux, which was not observed. More recently, similar results have been obtained for an altered MoFe protein where the β−Ser^{188} P cluster coordinating residue was substituted by glycine. Spectroscopic studies on both the altered β−Ser^{153} and β−Gly^{188} MoFe proteins from *A. vinelandii* reveal marked differences in their MCD spectra when compared to wild-type MoFe protein (K. Fisher, W. Newton, M. Johnson, unpublished data). These results indicate substantial changes in the electronic properties of the P clusters contained within the altered β−Ser^{153} and β−Gly^{188} MoFe proteins as might be expected from their altered catalytic properties. In contrast, MCD studies on the β−Ser^{152} MoFe protein from *Klebsiella pneumoniae*, analogous to the β−Ser^{153} MoFe protein from *A. vinelandii*, indicate that it has similar properties when compared to the wild-type MoFe protein (Smith *et al.*, 1993).

The high resolution MoFe protein structural model has now also provided the opportunity to investigate the route of intramolecular electron transfer within the MoFe protein. Four helices that are aligned in parallel between the P cluster and FeMo−cofactor have been recognized to have the potential to participate in electron transfer between these entities (Kim and Rees, 1992b). Inspection of the crystal structure reveals that the β−Tyr^{98} residue, which is located on one of these helices, is a good candidate to be involved in the pathway of electron transfer between the P cluster and FeMo−cofactor

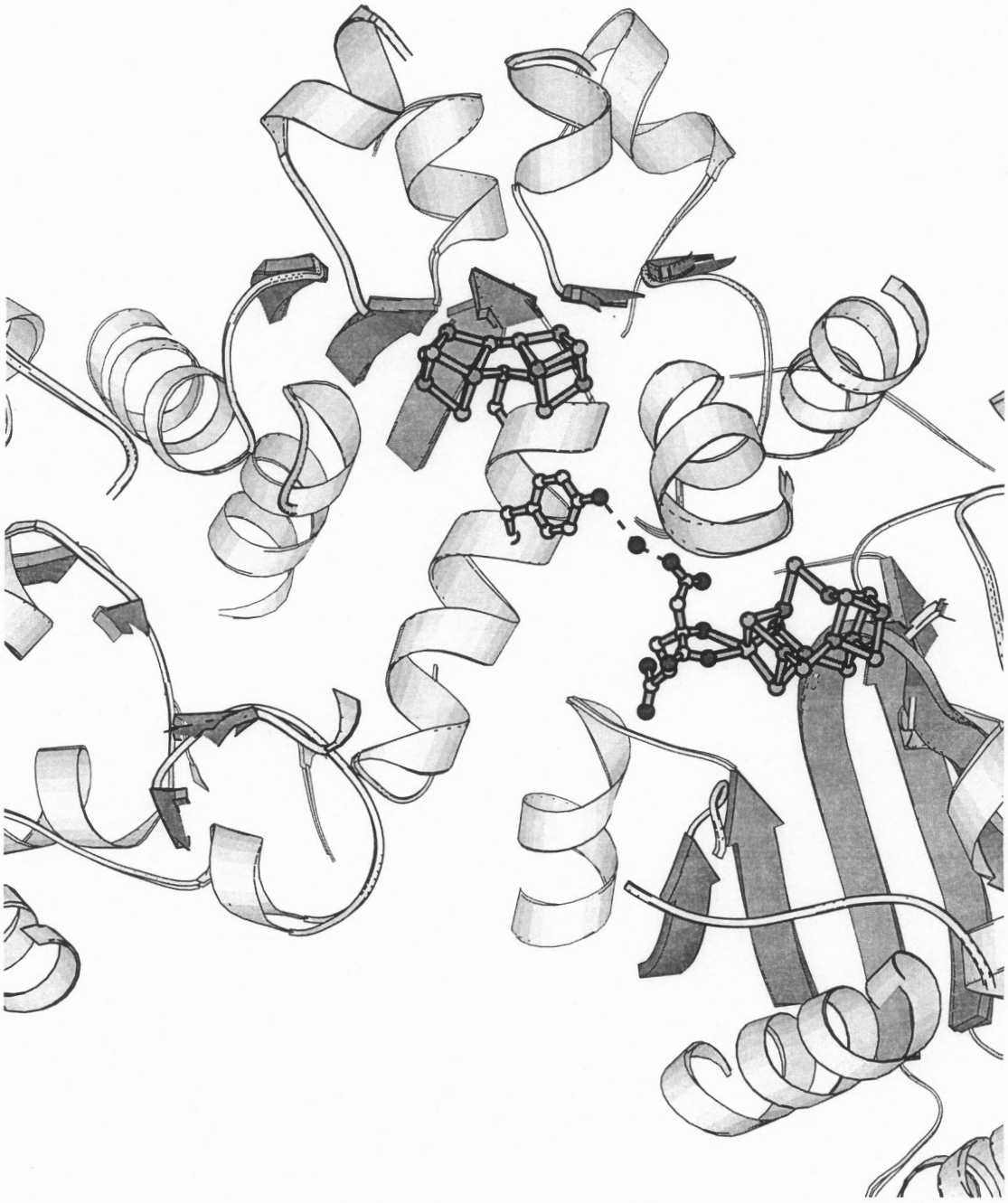

Figure 7. A ribbons diagram (Kraulis, 1991) highlighting the side chain of the β−Tyr^{98} residue which might participate in the intramolecular pathway of electron transfer between the P cluster and FeMo−cofactor. A water molecule that is hydrogen−bonded between the hydroxyl group of β−Tyr^{98} and the terminal carboxylate of homocitrate is also shown.

(figure 7). This residue is strictly conserved in all known MoFe protein primary sequences and is located in a direct line with the shortest apparent route between the P cluster and FeMo-cofactor. The potential participation of β-Tyr^{98} in mediating intramolecular electron transfer has been investigated by amino acid substitution studies (J. Peters, K. Fisher, M. Johnson, W. Newton and D. Dean, unpublished data). Substitution of β-Tyr^{98} by either β-Leu^{98} or β-Phe^{98} results in altered MoFe proteins having activities comparable to the wild-type. However, substitution of β-Tyr^{98} by β-His^{98} has a more dramatic effect. Biochemical characterization of the β-His^{98} MoFe protein reveals that maximum specific activity occurs at a lower Fe protein-to-MoFe protein ratio than observed with the wild-type MoFe protein. Also, a substantial reduction in the rate of protein turnover, as determined by stopped-flow experiments, is observed after a brief initial period at the normal rate. These results suggest a backup in the transfer of electrons from the P cluster to the FeMo-cofactor occurs in the β-His^{98} MoFe protein. Spectroscopic analyses of the β-His^{98} MoFe protein revealed no indication of any alteration in the respective polypeptide environments of either the P cluster or FeMo-cofactor. All of these results are consistent with a model where the direction of intramolecular electron flow occurs from the P cluster to the FeMo-cofactor, which is also in agreement with the docking model where the P cluster is positioned in a path between the Fe protein's Fe_4S_4 cluster and the MoFe protein's FeMo-cofactor. However, the results do not necessarily indicate that β-Tyr^{98} is directly involved in mediating intramolecular electron transfer. A more detailed discussion of the biochemical characterization of the β-His^{98} MoFe protein is included in Chapter III.

FeMo-Cofactor Structure and Polypeptide Environment

FeMo-cofactor contains a metal-sulfide core (Fe_7S_9Mo) and one molecule of (R)-homocitrate (figure 8). The metal-sulfide core is constructed from two partial cubes, one each of $MoFe_3S_3$ and Fe_4S_3 subcluster fragments, that are joined by a ring of three sulfide bridges that connect pairs of opposing Fe atoms. The organic constituent,

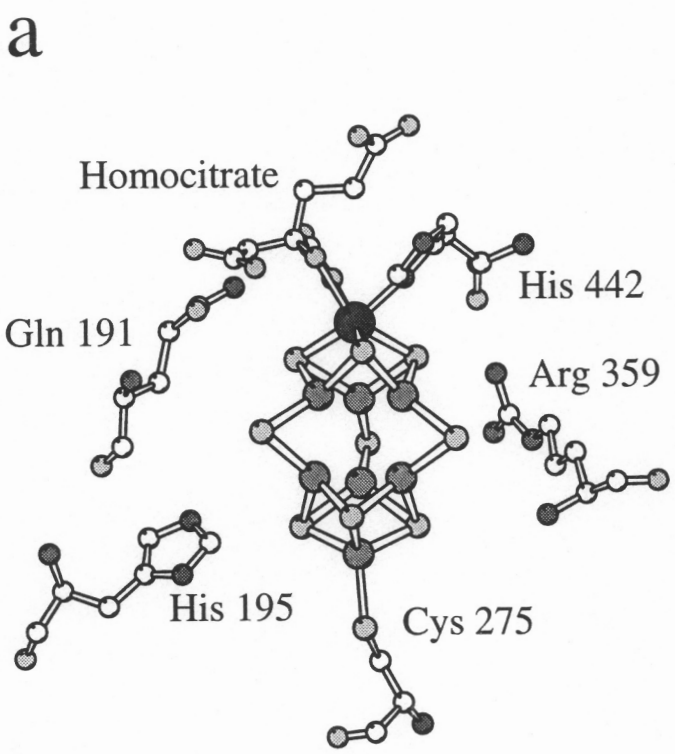

Figure 8. Ball-and-stick models (Kraulis, 1991) of FeMo-cofactor and selected residues contained within its polypeptide environment. The views shown in panels (a), (b), and (c) are related by rotations about the y-axis. groups.

b

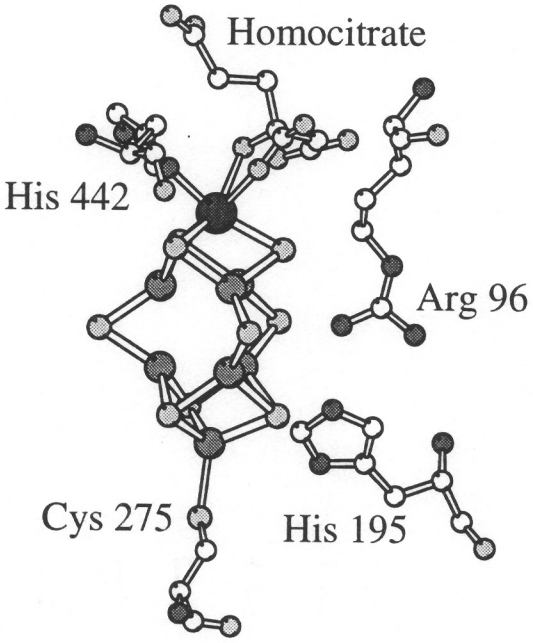

C

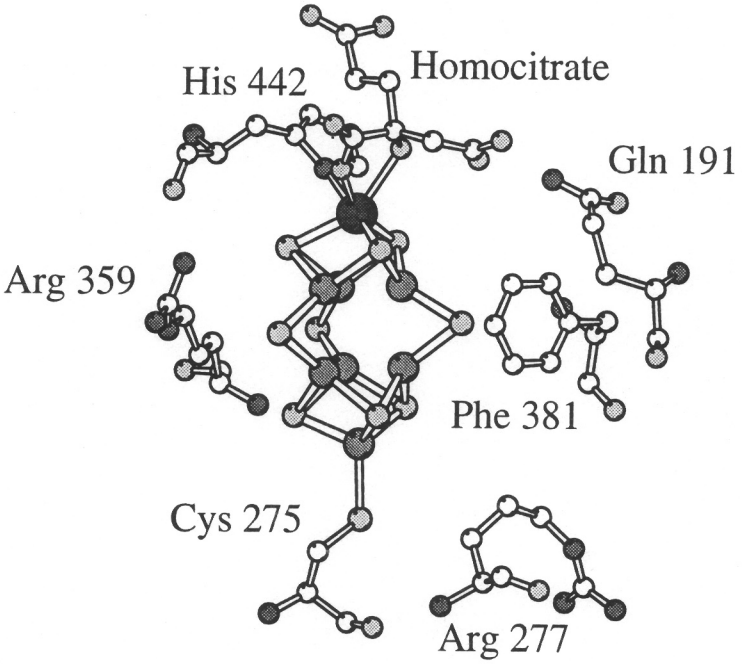

homocitrate, is coordinated to the Mo atom through its 2-hydroxy and 2-carboxyl FeMo-cofactor is covalently attached to the α-subunit through a thiolate ligand provided by α-Cys^{275} to an Fe atom at one end of the molecule and by the side-chain nitrogen atom of α-His^{442} to the Mo atom at the opposite end. Although FeMo-cofactor is completely contained within the α-subunit, some β-subunit residues, for example β-Tyr^{98}, approach the homocitrate and are indirectly linked to it by water molecules. No amino acids other than α-Cys^{275} and α-His^{442} are covalently attached to the FeMo-cofactor, although several other residues appear to interact with it through hydrogen bonding. The structure of FeMo-cofactor and three different views of its polypeptide environment are shown in figure 8.

The logic used to assign certain residues, for example, α-Gln^{191}, α-His^{195}, and α-Cys^{275}, as being located within the FeMo-cofactor-binding pocket was outlined in an earlier section. Other than the structural information, biochemical-genetic evidence that α-Cys^{275} and α-His^{442} both participate in anchoring FeMo-cofactor within the binding pocket was obtained by non-denaturing electrophoretic studies of altered MoFe proteins having substitutions for or near these residues. For example, substitution of α-Cys^{275} by α-Ala^{275} (Kent *et al.*, 1990) or α-His^{442} by α-Asn^{442} (Govezensky and Zamir, personal communication) results in altered MoFe proteins exhibiting native electrophoretic mobilities characteristic of the apo-MoFe protein. It was also shown that the pool of available FeMo-cofactor is increased in extracts of the altered α-Ala^{275} MoFe protein (Kent *et al.*, 1989). Although such substitution studies were useful in the original assignment of potential FeMo-cofactor ligands and are in agreement with the structural models, they are of little use in mechanistic studies because all substitutions placed at either the α-Cys^{275} or α-His^{442} position tested so far lead to the complete loss of all MoFe protein activities. In contrast, substitutions for α-Gln^{191} and α-His^{195} residues contained within the binding pocket but not covalently attached to FeMo-cofactor, do not necessarily result in a loss of all activities and certain of these altered MoFe proteins have been studied in detail.

Substitution of the α-Gln^{191} residue by α-Lys^{191} results in an altered MoFe protein

that is not able to reduce N_2 but retains its ability to reduce both protons and acetylene, although at lower levels (Scott *et al.*, 1992). The α-Lys^{191} MoFe protein is also distinguished from the wild-type MoFe protein in that it exhibits proton reduction that is 50% sensitive to CO. This latter feature is a characteristic of MoFe protein produced by *nifV* mutant strains (Hawkes *et al.*, 1984), which raised the possibility that an alteration in FeMo-cofactor's polypeptide environment might also lead to an alteration in the structure of the bound FeMo-cofactor. Inactivation of the *nifV* gene from *K. pneumoniae* is known to result in formation of an altered FeMo-cofactor that contains citrate rather than homocitrate (Hoover *et al.*, 1988a; Hoover *et al.*, 1988b; Hoover *et al.*, 1989; Liang *et al.*, 1990). The possibility that the α-Lys^{191} MoFe protein results in a structural rearrangement in FeMo-cofactor was addressed by using FeMo-cofactor isolated from the α-Lys^{191} MoFe protein to reconstitute an apo-form of an otherwise wild-type α-Gln^{191} MoFe protein (Scott *et al.*, 1992). Apo-MoFe protein reconstituted in this way exhibits proton reduction that is insensitive to CO inhibition, the wild-type phenotype. In the reverse experiment it was shown that when FeMo-cofactor isolated from the wild-type MoFe protein is used to reconstitute an apo-form of the α-Lys^{191} MoFe protein, the reconstituted protein does exhibit CO sensitive proton reduction. Thus, the CO-sensitive phenotype of the α-Lys^{191} MoFe protein is only a consequence of altering the polypeptide environment of FeMo-cofactor rather than causing a structural alteration in FeMo-cofactor itself. The similar biochemical consequences of either substituting homocitrate by citrate or substituting α-Gln^{191} by α-Lys^{191} can now be understood in light of the structural model because α-Gln^{191} is normally hydrogen bonded to a terminal carboxylate of homocitrate (figure 8). The fact that either an alteration in the organic acid attached to the Mo atom or substitution of an amino acid which coordinates the organic acid leads to CO sensitive proton reduction indicates that at least a portion of hydrogen evolution catalyzed by the MoFe protein must occur at the FeMo-cofactor site and that homocitrate is likely to play an integral role in the mechanism of hydrogen evolution. Although the chemical basis for substrate binding and reduction is beyond the scope of this review, we draw the attention of the reader to several recent articles on this subject (Deng

and Hoffman, 1993; Schrauzer *et al.*, 1993; Dance, 1994; Eady and Leigh, 1994; Hughes *et al.*, 1994).

Another interesting feature of the α-Lys^{191} MoFe protein is its ability to catalyze the reduction of acetylene by both two and four electrons to give either ethylene or ethane (Scott *et al.*, 1990; Scott *et al.*, 1992), whereas the wild-type MoFe protein is only able to catalyze the two electron reduction of acetylene to give ethylene (Dilworth, 1966). Reduction of acetylene to both ethylene and ethane is also a property of the vanadium-dependent nitrogenase (Dilworth *et al.*, 1987). The V-dependent nitrogenase is structurally and functionally similar to the Mo-dependent nitrogenase except that its cofactor contains V rather than Mo (reviewed in Smith and Eady, 1992; note, the V-containing nitrogenase should not be confused with the NifV$^-$ phenotype). Reconstitution of an apo-form of the Mo-dependent nitrogenase with the V-containing cofactor results in a species that can reduce acetylene to both ethylene and ethane (Smith *et al.*, 1988). Thus, the ability of the V-dependent nitrogenase to reduce acetylene by two and four electrons can be attributed to the nature of the metal composition of its cofactor rather than the polypeptide environment of the cofactor. This conclusion is supported by the results of the converse experiment where it was shown that replacement of the V-containing cofactor from the V-dependent nitrogenase by FeMo-cofactor results in a hybrid species that is able to reduce acetylene to ethylene but does not catalyze ethane formation. Nevertheless, the FeMo-cofactor-containing "V-dependent" nitrogenase is unable to reduce N_2, which suggests there must be specific differences in the polypeptide interactions between the different cofactor types and their respective proteins (Smith *et al.*, 1988). Ethane production catalyzed by the α-Lys^{191} MoFe protein probably occurs by a different mechanism than ethane formation catalyzed by the V-dependent enzyme because the α-Lys^{191} MoFe protein: (i) does not exhibit a lag before ethane production, (ii) exhibits an increased sensitivity to inhibition by CO, (iii) does not show a temperature dependence on ethylene or ethane formation, and, (iv) catalyzes ethane and ethylene formation in a ratio that does not change with a variation in electron flux (Scott *et al.*, 1992). Since these observations were reported, it has been found that MoFe protein from

a *nifV* mutant of *Rhodobacter capsulatus* is also able to catalyze the reduction of acetylene by two and four electrons to give ethylene and ethane (Masepohl *et al.*, 1993) and this phenotype has also been observed for the MoFe protein isolated from a *nifV*-deficient strain of *A. vinelandii* (L. Comerrata and D. Dean, unpublished observations). The observations that either substitution of Mo by V, an alteration in the organic acid attached to Mo, or substitution of a residue which is coordinated to homocitrate all lead to profound changes in the catalytic properties of the MoFe protein again point to an important role for homocitrate in the catalytic mechanism. Whether or not this role is a structural one that serves to properly orient FeMo-cofactor within the polypeptide pocket or a functional one that involves the direct participation of homocitrate in substrate binding and reduction is not yet known. Another approach, involving the use of various homocitrate analogs to probe the functional role of this organic acid in nitrogenase catalysis has been discussed in detail (Ludden *et al.*, 1993).

The MoFe protein α-His^{195} residue was originally targeted for amino acid substitution studies because primary amino acid sequence comparisons indicated that this residue might be located within an FeMo-cofactor binding domain (Scott *et al.*, 1990) and a pulsed EPR technique (ESEEM) suggested that a histidine residue might be covalently coordinated to one of FeMo-cofactor's metal atoms (Thomann *et al.*, 1987). In order to test this possibility the α-His^{195} residue was substituted by α-Asn^{195}, which indeed resulted in the disappearance of the ESEEM signal characteristic of the N-coordination to FeMo-cofactor and a concomitant loss of N_2 reduction activity (Thomann *et al.*, 1991). In contrast, substitutions for certain other histidine residues, for example α-His^{83}, α-His^{196}, α-His^{274}, or β-His^{90}, did not eliminate either the ESEEM signature or the ability to reduce N_2. Although the most logical interpretation of this data was that α-His^{195} is directly coordinated to one of FeMo-cofactor's metal atoms, the structural model revealed that α-His^{442}, rather than α-His^{195}, is covalently attached to the Mo atom of FeMo-cofactor (see figure 8). In retrospect it would not have been possible to identify α-His^{442} as providing a coordinating ligand to FeMo-cofactor by ESEEM studies because substitutions at this position lead to accumulation of an apo-MoFe protein which does not

exhibit any EPR spectrum (J. Peters, W. Newton, D. Dean, unpublished data). It is pointed out, however, that one research group did, in fact, propose that α-His^{442} was a candidate to provide N-coordination to FeMo-cofactor and this prediction was based on the native electrophoretic mobility of an altered MoFe protein having a substitution located near α-His^{442} (Govensky and Zamir, 1989). Once the x-ray crystallographic data revealed that α-His^{195} is not covalently attached to a metal atom of FeMo-cofactor but is within hydrogen bonding distance of one of the bridging sulfides the ESEEM analysis of altered MoFe proteins having substitutions at this position were revisited (DeRose *et al.*, 1995). Although the dramatic decrease in the intensity of the ESEEM signal resulting from the α-Asn^{195} substitution was confirmed, it was found that substitution by α-Gln^{195} caused no detectable change in the modulation. These results indicate that the observed nitrogen modulation is not directly associated with the hydrogen-bond provided by α-His^{195}, but rather with the nitrogen moiety of a different residue whose proximity to the FeMo-cofactor is sensitive to certain substitutions at the α-His^{195} position. Thus, it appears that the NH-S hydrogen bond normally provided by α-His^{195} might be important in positioning FeMo-cofactor within the polypeptide pocket.

Characterization and comparison of the catalytic features of the altered α-Asn^{195} and α-Gln^{195} MoFe proteins has provided some insight concerning the nature of the interaction of different substrates with the nitrogenase substrate-reduction site (Kim *et al.*, 1995). Although N_2 is not reduced by the α-Gln^{195} MoFe protein it is an effective competitive inhibitor of both acetylene reduction and proton reduction. In contrast, acetylene and proton reduction catalyzed by the α-Asn^{195} protein is not inhibited by N_2. The most reasonable interpretation of these results is that the α-Gln^{195} MoFe protein, but not the α-Asn^{195} protein, retains the ability to bind N_2. In this context it is interesting that there appears to be a correlation between the ability of N_2 to bind altered MoFe proteins and the presence or absence of the ESEEM signal. The observation that N_2 is not reduced by the α-Gln^{195} MoFe protein but effectively inhibits both proton reduction and acetylene reduction suggests that N_2 is able to compete with both acetylene and protons for active site occupancy. Although these results do not address the question of whether or not

different substrates bind to the active site in different ways or bind at different subsites within the active site, or bind at different redox states, it appears that different substrates cannot bind and be reduced at the active site at the same time.

The other important feature of the α-Gln^{195} MoFe protein is that, although N_2 slows the overall rate of proton reduction, it does not slow the overall rate of MgATP hydrolysis. In other words, in the presence of N_2, MgATP hydrolysis catalyzed by the α-Gln^{195} MoFe protein becomes uncoupled from proton reduction. One explanation for this result is that because N_2 is able to occupy the substrate-reduction site, but cannot be reduced, electrons accumulated within the α-Gln195 MoFe protein are ultimately back-donated to the Fe protein (Orme-Johnson and Davis, 1977). A related possibility is that, once the altered MoFe protein becomes saturated with electrons that cannot be captured by substrate reduction, the Fe protein and MoFe protein retain their ability to associate and effect MgATP hydrolysis but are no longer able to achieve intermolecular electron transfer. This possibility is supported by evidence that nucleotide hydrolysis precedes intermolecular electron transfer (Thorneley *et al.*, 1989), although MgATP-dependent proton release appears to be slower than electron transfer (Mensink *et al.*, 1992). The observation that N_2 uncouples MgATP hydrolysis from proton reduction catalyzed by the α-Gln^{195} MoFe protein, but does so without substantially lowering the overall rate of MgATP hydrolysis, indicates that, in the unaltered system, the flow of electrons from the Fe protein to the MoFe protein must be controlled, in part, by the substrate acting as an effective electron sink.

Summary and Comments

Prior to the availability of the three-dimensional structures of the nitrogenase component proteins and their associated metal clusters there was already a considerable amount of data accumulated from biochemical characterization of nitrogenases altered by site-directed mutagenesis. As its experimental basis much of this work involved the attempted identification of the metal cluster ligands within the MoFe protein and probing

the importance of individual amino acids identified within the nucleotide binding motifs of the Fe protein. When the nitrogenase three-dimensional structures became available in 1992 the majority of the predictions made using biochemical, biophysical, and genetic probes turned out to be correct, although incomplete. Thus, both the validity and limitations of using a biochemical–genetic approach to probe functional aspects of the nitrogenase complex have become evident. Perhaps the more profound contribution of the biochemical–genetic approach, at its current stage, is that it has established the feasibility of altering individual features of nitrogenase catalysis by amino–acid substitution without necessarily compromising other aspects of the process. Moreover, it has been shown that altered nitrogenase components obtained by site–directed mutagenesis are amenable to purification and biochemical characterization. With detailed structural information now in–hand the biochemical–genetic analysis of nitrogenase will move away from descriptive issues such as the identification and organization of the major players involved in the catalytic process to the analysis of more mechanistic issues. Namely, now that it has been established that certain residues are involved in catalysis the challenge is to elucidate the molecular mechanisms or structural features associated with their participation in catalysis.

The potential importance of biological nitrogen fixation research and, more specifically, the study of nitrogenase catalysis with the goal of increasing plant productivity is well documented. With the availability of structural models, however, nitrogenase research has become of broader significance because the system has emerged as a model for more general biochemical processes, such as signal transduction, protein–protein interaction, inter– and intra–molecular electron transfer reactions and metal center mediated enzyme catalysis. In this regard, the complexity of the nitrogenase system might be viewed as a drawback for its use as a model for examination of these general biochemical processes. However, from our perspective, it is the very complexity of nitrogenase, together with the numerous biochemical and biophysical probes that can be used to characterize specific aspects of the catalytic process, that make it an ideal model system. This complexity also gives researchers the opportunity to ascertain how these

general processes act in concert. For example, how MgATP binding and hydrolysis and signal transduction are linked to effect electron transfer from the Fe protein to the MoFe protein in a manner which greatly favors a unidirectional electron flow to substrate reduction remains an intriguing and fundamental biological question. A better understanding of how these aspects of nitrogenase catalysis are intimately linked is clearly relevant to other related processes which also utilize conformational changes induced by nucleotide binding and hydrolysis to drive biochemical reactions.

The most striking feature of nitrogenase catalysis is the dynamics of the process. Namely, two proteins associate and dissociate in a MgATP dependent manner that leads to electron transfer. In our view another major challenge of future biochemical–genetic analyses will be to dissect the molecular details involved in this dynamic interaction. Of particular interest will be to construct altered forms of the nitrogenase components which are trapped in intermediate stages of catalysis. In this regard it is emphasized that our current structural view of the nitrogenase component proteins is in their resting states. Amino acid substitution studies to date provide a good indication that such efforts will be successful. For example, altered forms of the Fe protein which are able to bind MgATP but either can or cannot undergo the nucleotide induced conformational change are already available. Thus, comparison of the structural features of these altered Fe proteins by x–ray crystallographic techniques should be very informative. Another approach that we believe will be of considerable value is the isolation of altered component proteins which are able to associate but fail to dissociate. Again the feasibility of this approach is already indicated by heterologous mixing experiments and amino acid substitution studies. The obvious value of obtaining a stable Fe protein–MoFe protein complex is that structural analysis of the complex should provide detailed information concerning the nature of component protein interaction and could also provide mechanistic insight by revealing whether or not there is a significant structural rearrangement around any of the nitrogenase associated metalloclusters during complex formation. Clearly this information will provide new targets for amino acid substitution. Also, the availability of a mutant strain which produces an inactive complex caused by alteration of one component protein

could then be used in genetic experiments to search for suppressor mutations that lead to an alteration in the other component protein. In this way it should be possible to identify residues involved in various aspects of the dynamic reciprocal interactions that must occur between the component proteins during catalysis but are not necessarily obvious from the available structural models. Finally, the structural and functional analysis of altered component proteins having a combination of different amino acid substitutions could prove extremely valuable. For example, once an altered Fe protein that forms a tight inactive complex with the MoFe protein is obtained, it would be most interesting to determine the biochemical and structural consequences of placing this construct in combination with an alteration in the ability of the complex to bind or hydrolyze MgATP.

CHAPTER I.

Identification of a nitrogenase protein-protein interaction site defined by residues 59 through 67 within the *Azotobacter vinelandii* Fe protein

This chapter was written by the combined efforts of myself, Karl Fisher, and Dennis Dean and was published in the *Journal of Biological Chemistry* (Peters *et al.*, 1994). Karl Fisher was responsible for all pre-steady state stopped-flow experiments. Valerie Cash was involved in generating the original plasmid construct and Steve Muchmore was responsible for the preparation of figure 9.

Summary

During nitrogenase catalysis the Fe protein and the MoFe protein associate and dissociate in a MgATP-dependent process involving electron transfer from the Fe protein to the MoFe protein. A docking model, based primarily on the crystal structures of the separate components from *Azotobacter vinelandii,* was previously proposed in which the two-fold symmetric surface of the homodimeric Fe protein interacts with the exposed surface of a MoFe protein pseudo-symmetric $\alpha\beta$-unit interface. In this model, a loop, which is included within residues 59 through 67 of the Fe protein primary sequence, is likely to interact with the MoFe protein during component protein docking. In the present study, evidence supporting the component protein docking model was obtained by construction of an *A. vinelandii* strain that produces a hybrid Fe protein for which residues 59 through 67 have been replaced by the corresponding residues from the Fe protein of *Clostridium pasteurianum*. Biochemical analyses of the hybrid Fe protein revealed the following features when compared to the unaltered Fe protein. First, the hybrid Fe protein exhibited half the maximum specific activity of the normal Fe protein and was insensitive to inhibition by low levels of NaCl. Second, the hybrid Fe protein activity was hypersensitive to a molar excess of MoFe protein, which also resulted in the uncoupling of MgATP hydrolysis from substrate reduction. Third, stopped-flow spectrophotometry

experiments showed that during catalysis the hybrid Fe protein dissociates from the MoFe protein at only half the normal rate of Fe protein–MoFe protein dissociation. Thus, the salient feature of the hybrid Fe protein is that it appears to form a relatively tighter complex with the MoFe protein. This property is in line with previous biochemical reconstitution experiments where it was shown that a heterologous mixture of Fe protein from *C. pasteurianum* and MoFe protein from *A. vinelandii* form a tight, inactive complex and supports the proposal that a region defined by residues 59 through 67 within the Fe protein is involved in component protein interaction.

Introduction

Biological reduction of dinitrogen is catalyzed by nitrogenase, an enzyme composed of two metalloproteins called the Fe protein and the MoFe protein (recently reviewed by and Dean *et al.* 1993; Kim and Rees, 1994). The overall reaction is usually indicated as follows:

$$N_2 + 8H^+ + 8e^- + 16MgATP \rightarrow 2NH_3 + H_2 + 16MgADP + 16Pi$$

During catalysis, electrons are delivered one at a time from the Fe protein to the MoFe protein in a process involving component protein association and dissociation and hydrolysis of at least two MgATP for each electron transfer. The MgATP binding sites are located on the Fe protein and the substrate reduction site(s) is contained entirely within the MoFe protein, yet, neither MgATP hydrolysis nor substrate reduction catalyzed by nitrogenase can be achieved without the participation of both protein partners. Because multiple electrons are required for substrate reduction, the association and dissociation of the nitrogenase component proteins must be coordinated with MgATP hydrolysis so that electron flux is directed toward substrate reduction. Consequently, the molecular mechanism by which the two component proteins interact such that MgATP hydrolysis is effectively coupled to electron transfer is an important aspect of nitrogenase catalysis.

The Fe protein is a γ_2 homodimer ($M_r \approx 60,000$) which contains 4 Fe atoms organized into a single Fe_4S_4 cluster, whereas the MoFe protein is an $\alpha_2\beta_2$ heterotetramer ($M_r \approx 250,000$) which contains 30 Fe atoms and 2 Mo atoms organized into two pairs of metalloclusters, called P clusters and FeMo-cofactors. The P cluster is believed to be involved in the acceptance, storage, and ultimate transfer of electrons to FeMo-cofactor, which is the active site for substrate reduction. A stereoview of the α-carbon backbone of the Fe protein homodimer and an $\alpha\beta$ unit of the MoFe protein, together with the spatial organization of their associated metalloclusters, is shown in figure 9.

That nitrogenases from phylogenetically diverse organisms are similar in structure and mechanism was first indicated in experiments where complementary nitrogenase components isolated from different organisms were mixed to form heterologous, catalytically competent, enzymes (see, for example, Emerich and Burris, 1976). A phylogenetic conservation in the structure and function of the nitrogenase component proteins indicated by such biochemical complementation studies was later confirmed by extensive DNA sequence data (reviewed by Dean and Jacobson, 1992) and crystallographic analyses of the nitrogenase component protein structures (Kim and Rees, 1992b; Georgiadis *et al.*, 1992).

Because heterologous-component protein-mixing experiments are frequently used in nitrogenase research, a nomenclature that distinguishes not only a particular component protein but also the source of that protein is commonly used. According to convention (Eady *et al.*, 1972), the first letters of the genus and species designations are combined to indicate the component protein source, followed by 1 or 2 to indicate the MoFe protein or the Fe protein, respectively. For example the Fe protein from *A. vinelandii* is indicated by Av2. Also, because: (a) the Fe protein is able to bind either MgADP or MgATP, (b) the component proteins can exist in different redox forms, and (c) the component proteins are able to complex with each other; a shorthand is commonly used to designate these various species (see, Thorneley and Lowe, 1984b). For example, the oxidized MgADP-bound form of the *A. vinelandii* Fe protein complexed with the MoFe protein from *A. vinelandii* is designated as $Av2_{ox}(MgADP)_2$-Av1. Other examples of this nomenclature are

described in the Abbreviations section.

Although many heterologous Fe protein and MoFe protein mixtures exhibit catalytic activity, a reconstituted mixture of purified Fe protein from *Clostridium pasteurianum* (Cp2) and purified MoFe protein from *Azotobacter vinelandii* (Av1) is ineffective in substrate reduction. Instead, this heterologous mixture results in formation of a catalytically inactive Cp2–Av1 complex (Emerich and Burris, 1976; Emerich *et al.*, 1978). We have previously described a biochemical–genetic strategy aimed at exploiting inactive Cp2–Av1 complex formation to test for the contribution of specific polypeptide regions within the Fe protein to aspects of component protein interaction (Jacobson *et al.*, 1990). The rationale involves using site–directed mutagenesis and gene–replacement techniques to construct mutant strains of *A. vinelandii* that produce hybrid Fe proteins where specific polypeptide primary sequences within Av2 are replaced by the corresponding primary sequences from Cp2. For example, we previously constructed and characterized a hybrid Fe protein for which the carboxyl end of Av2 was replaced by the corresponding Cp2 sequence. Results from biochemical analysis of the hybrid Fe protein constructed in this way revealed that formation of the inactive Cp2–Av1 complex cannot be accounted for only by differences in the primary sequences of Av2 and Cp2 located at their respective carboxyl ends (Jacobson *et al.*, 1990).

Our conclusion that the carboxyl terminus of the Fe protein is unlikely to play a dominant role in component protein interaction was recently confirmed by reports on the three dimensional structures for both Av1 (Kim and Rees, 1992b) and Av2 (Georgiadis *et al.*,1992). A docking model (Kim and Rees, 1992b; Howard, 1993), based primarily on the crystal structures of the separate components, but also on results from amino acid substitution studies (Wolle, *et al*, 1992b) and chemical cross–linking experiments (Willing and Howard, 1990), has now been formulated (see figure 9). Hereafter, this model will be referred to as the Rees–Howard model. There are several important features of the Rees–Howard model. First, the model pairs the two–fold symmetric surface of the Fe protein homodimer with the exposed surface of a MoFe protein pseudo-symmetric $\alpha\beta$-unit interface. Second, upon docking, the Fe protein's Fe_4S_4 cluster is positioned in

the closest possible proximity to the MoFe protein's P cluster. This arrangement accommodates the current view that the primary electron transfer event (i.e., the initial intermolecular transfer of an electron from the Fe protein to the MoFe protein) involves transient delivery of an electron from the Fe_4S_4 cluster of the Fe protein to a MoFe protein P cluster (reviewed by Kim and Rees, 1994). Third, it places a number of charged groups located on the respective surfaces of the Fe protein and MoFe protein in an arrangement which could permit reciprocal ionic interactions between the two component proteins. Studies on the salt sensitivity of nitrogenase catalytic activity have been interpreted to indicate that such ionic interactions are critical to productive complex formation (Deits and Howard, 1990; Wolle *et al.*, 1992b).

Inspection of the Rees–Howard model (figure 9) reveals a potential component protein interaction site, residues 60 through 68 in the Av2 primary sequence, that is located on the surface of the Fe protein and which forms a "loop" that contains several anionic residues. Certain of these exposed residues appear to be among those that could interact with the MoFe protein at an early stage in complex formation. There are two notable differences in primary sequence when this region of Av2 is compared to Cp2. First, Av2 residues Thr^{66} and Val^{67} are deleted and, second, Ala^{62} is substituted by Arg, in the corresponding Cp2 primary sequence (figure 9). Consequently, the distribution of charged groups and the specific orientation of individual residues contained within the loop must be different in the respective Cp2 and Av2 structures (Howard, 1993). Such differences could contribute to formation of the inactive Av1–Cp2 complex formed when these heterologous component proteins are mixed in biochemical complementation experiments. In the present study, we constructed a mutant strain of *A. vinelandii* that produces a hybrid Fe protein where residues 59 through 67 within the Av2 primary sequence were substituted by the corresponding residues of the Cp2 sequence. The hybrid Fe protein produced by this strain was purified and its catalytic properties characterized.

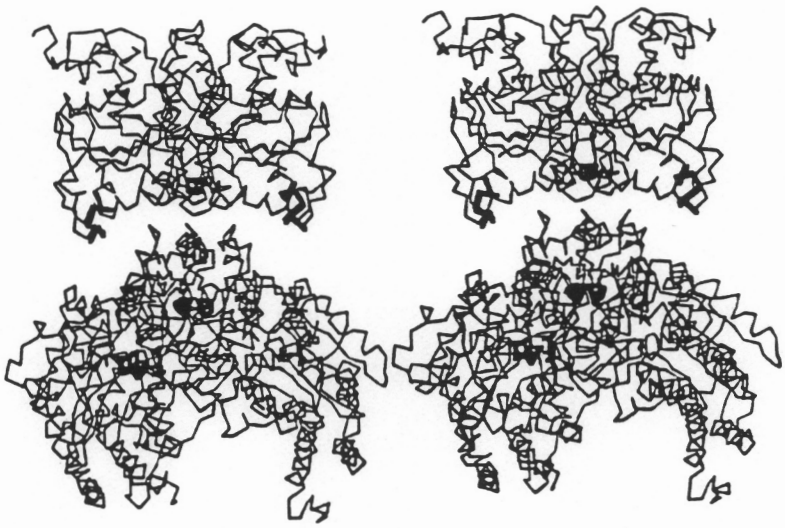

	60					65					70	
Av	Met	Glu	Met	Ala	Ala	Glu	Ala	Gly	Thr	Val	Glu	Asp	Leu	Glu
Cp	Leu	Asp	Thr	Leu	Arg	Glu	Glu	Gly	---	---	Glu	Asp	Val	Glu
Av/Cp	Met	Asp	Thr	Leu	Arg	Glu	Glu	Gly	---	---	Glu	Asp	Leu	Glu

Figure 9. Stereoscopic view adapted from the Rees–Howard component–protein docking model. The model shows the α–carbon backbone trace for the Av2 homodimer (top) and an αβ unit of Av1 (bottom) poised at the proposed site of interaction. The portions of the polypeptide backbone shown in bold correspond to the region of amino acid residues of the Av2 homodimer that were replaced with the analogous residues from the Cp2. The spatial organization of the associated metalloclusters are also shown in bold. A comparison of Av2, Cp2, and AvCp2 primary sequences in the region relevant to the present study is shown below the stereoscopic view. Numbering corresponds to the Av2 sequence.

Experimental Procedures

The *Escherichia coli* strain 71-18 (Δ(*lac-proAB*) *thi supE* (F' *proAB lacIqZM15*) served as a host for recombinant plasmids used in this study. Restriction enzymes, T_4 DNA ligase and Klenow fragment were purchased from Life Technologies, Inc. (Gaithersburg, MD) or New England Biolabs (Beverly, MA) and used as recommended by the supplier. For site-directed mutagenesis, a hybrid plasmid, pDB787, was constructed by cloning a 2577-base pair *Pst*I fragment containing the *A. vinelandii nifH* gene and flanking regions and subsequently using site-directed mutagenesis to place an *Eco*RV restriction site within the *nifH*-coding sequence (Brigle *et al.*, 1985). The *EcoRV* restriction site was introduced into this hybrid plasmid at nucleotide 180 within the *nifH* gene coding sequence using site-directed mutagenesis as described by Kunkel *et al.*, 1987. The oligonucleotide: 5'CCATCATGGATATCGCTGCCGAAG 3' was used to substitute T for A at nucleotide 179, and C for G at nucleotide 182 within the *nifH*-coding sequence. The presence of the *Eco*RV site in pDB787, underlined in the above oligonucleotide, was confirmed by DNA sequence analysis and restriction enzyme digestion using the synthetic oligonucleotide 5'TCCACCACTACTCAGAAC3' as a primer.

The newly generated *Eco*RV restriction site within pDB787 was utilized in combination with an existing *Bgl*II restriction site at nucleotide 209 to excise a 27 base pair fragment from pDB787. This fragment was then substituted by a DNA cassette that was obtained by annealing two synthetic oligonucleotides having the following sequences: 5'ACCCTGCGCGAAGAAGGTGAA3' and 5'GATCTTCACCTTCTTCGCGCAGGGT3'. The hybrid plasmid constructed in this way was designated pDB790 and has a portion of the *nifH*-coding region from the *A. vinelandii nifH* gene substituted by the corresponding region of the *C. pasteurianum nifH* gene (figure 9).

This construction was then transferred to the *A. vinelandii* chromosome by using pDB790 to transform strain DJ525 to prototrophy. DJ525 contains a deletion which spans the N-terminal-coding portion of *nifH* and extends from a *Mst*II site located upstream from the *nifH* initiation codon to the *Bgl*II restriction site within the

nifH–coding sequence. This deletion results in a strictly Nif$^-$ phenotype. Thus, the *nifH* region encoding the hybrid Fe protein construction was introduced into the chromosome by transforming DJ525 with pDB790 and directly selecting for the Nif$^+$ phenotype. A more detailed description of procedures used in similar constructions can be found in Robinson *et al.* (1986) and Jacobson *et al.* (1989b). Transformation of *A. vinelandii* was performed as described by Page and von Tigerstrom (1979).

Wild-type *A. vinelandii* and DJ911 were cultured at 30° C in a modified, liquid Burk media (Strandberg and Wilson, 1968). Growth was monitored using a Summerson-Klett meter equipped with a no. 66 filter. Large scale culture of wild-type and DJ911 was accomplished using a 24L fermentor (New Brunswick, Edison, NJ). The nitrogenase component proteins were purified from *A. vinelandii* as previously described (Burgess *et al.*,1980a) except that Q-Sepharose was substituted for DEAE-cellulose during anion exchange chromatography and Sephacryl-300 was substituted for Sephacryl-200 in gel filtration chromatography. Also, Av1 was further purified by substituting hydrophobic interaction chromatography (Phenyl-Sepharose) and gel filtration chromatography (Sephacryl-300) for the crystallization step. The purified component proteins were concentrated using an Amicon pressure dialysis apparatus and purity was monitored by SDS-PAGE as described by Laemmli (1970) and stained with Coomassie Blue. SDS-PAGE molecular weight markers were purchased from Bio–Rad (Melville,NY). The Mo content of Av1 was determined to be 1.9 ± 0.1 g atom Mo per mol by inductively coupled plasma atomic emission spectrometry using a simultaneous spectrometer (Jarrell-Ash ICAP 9000) and a sequential scanning spectrometer (Jarrell-Ash Atomscan 2400).

Purified Fe protein was assayed at 30°C in 9 ml calibrated vials, fitted with butyl rubber serum stoppers and metal caps. The assay mixture contained 25 mM Hepes/HCl, 25 units of creatine phosphokinase, 30 mM phosphocreatine, 2.5 mM ATP, 5 mM $MgCl_2$ and unless otherwise stated 20 mM Na–dithionite in a 1ml assay volume. The gas chromatographs were calibrated by using standards containing 1.0% H_2 or 1000 ppm ethylene (Scotty Specialty Gases, Durham, NC). H_2 and ethylene were quantified by analyzing 200 µl of a gas sample from the reaction vial. H_2 evolution was determined using

a Shimadzu GC-8a katharometer with a molecular sieve 5A column, argon as carrier gas and a thermal conductivity detector. Ethylene was analyzed using a Shimadzu GC-14a chromatograph, a fused silica capillary column with helium as carrier gas and a flame ionization detector. Acetylene was prepared by the action of water on calcium carbide and 10% v/v was added to steady state assays. All assays were determined in the presence of 50 mM NaCl unless indicated otherwise. MgATP hydrolysis activity was determined colorimetrically by measuring the production of creatine using the method of Ennor (1957) after the pretreatment of assay samples as described by Dilworth *et al.* (1992). The strain which produces the hybrid Fe protein (AvCp2) was grown on two separate occasions and the resulting nitrogenase proteins purified independently. Both preparations exhibited the same biochemical properties. All data shown is representative of at least three separate experiments.

Flavodoxin (FldII) was isolated from N_2-fixing *A. vinelandii* cells as described previously by Klugkist *et al.* (1986). FldII, the known electron donor to the Fe protein, was reduced to the hydroquinone state (FldIIHQ) with an excess of Na–dithionite at pH 8 in an anaerobic chamber. After incubation for approximately 15 minutes to ensure complete reduction, unreacted dithionite and its reduction products were removed on a gel filtration column (0.5 x 5 cm) packed with P-6DG (Biorad) and equilibrated with anaerobic 25 mM Hepes, 10 mM $MgCl_2$. The same procedure was employed to remove dithionite ion from nitrogenase proteins used in stopped-flow spectrophotometry, with the addition that the MoFe protein elution buffer contained 150 mM NaCl to avoid tailing on the resin. Protein concentrations were determined by the colorometric method of Lowry *et al.* (1951).

Stopped-flow spectrophotometry was performed using a commercially available SF-61 instrument equipped with a kinetic data acquisition analysis and curve fitting system (Hi-Tech, Salisbury, Wilts., UK). The SHU-61 sample handling unit was installed inside an anaerobic chamber operating at less than 1 ppm. Oxygen concentration was monitored with a Teledyne Analytical Instruments series 316 trace oxygen analyzer (Vacuum Atmospheres Co., Hawthorne, Ca.). Sample flow components were thermostatted by

closed circulation of water by a Techne C-85D circulator (Techne Ltd, Duxford, Cambridge, UK) attached to a FC-200 Techne flow cooler situated outside the anaerobic chamber. All stopped-flow reactions were studied at 23°C in 25 mM Hepes buffer, pH 7.4 containing 10 mM $MgCl_2$ and either 50 or 175 mM NaCl. The oxidation of Av2 and AvCp2 was monitored at 430nm and fitted to a single exponential function. Syringe A contained Av1 (10 μM), Av2(40 μM), and 10 mM Na dithionite. Syringe B contained 20 mM MgATP and 10 mM Na-dithionite. The oxidation of FldIIHQ was monitored at 580nm and fitted to a linear function. Syringe A contained Av2 (5 μM), Av1 (1.25 μM) and syringe B contained FldIIHQ(30 μM), and 10 mM MgATP.

Results and Discussion

Comparison of the primary sequences of Av2 and Cp2 reveals an overall 69% conservation in sequence identity (Hausinger and Howard, 1982). Although this conservation is distributed relatively evenly throughout the two proteins, there is particularly strong sequence identity located within the Fe_4S_4 cluster ligand domains (Hausinger and Howard, 1983, Howard *et al.*, 1989) and the proposed MgATP binding site (Robson,1984; Seefeldt *et al.*, 1992; Wolle *et al.*,1992a). The most striking diversity between the two proteins is located at the carboxy terminus, Av2 being elongated by 13 amino acids in comparison to Cp2. Our previous results have shown that these differences are unlikely to account for the tight, inactive complex formed when Av1 and Cp2 are mixed in heterologous reconstitution experiments (Jacobson *et al.*, 1990). In the present study we constructed a strain of *A. vinelandii*, DJ911, which produces a hybrid Fe protein, hereafter, referred to as AvCp2, where residues 59 through 67 in the Av2 primary sequence were replaced by the corresponding Cp2 residues. AvCp2 has 9 amino acids from Av2 substituted by 7 residues corresponding to the Cp2 primary sequence (figure 9). DJ911 exhibits diazotrophic growth, having a doubling time of 5 hours compared to the 2 hour doubling time of the wild-type strain. Thus, *in vivo* complex formation between AvCp2 and Av1 is not sufficiently tight as to cause a dramatic lowering in the diazotrophic

growth rate. Nevertheless, the decrease in the diazotrophic growth rate exhibited by DJ911 indicates some alteration in the catalytic properties of AvCp2 when compared to Av2, thus meriting its biochemical characterization.

AvCp2 produced by DJ911 was purified in parallel with Av2 produced by the parental wild-type strain. Similar yields were obtained from both strains indicating that AvCp2 could be purified using the normal purification procedure without significant loss in activity. The predicted minor difference in molecular weight between Av2 and AvCp2 could be detected by SDS-PAGE of the purified proteins providing evidence for the correct substitution of the Av2 primary sequence by the corresponding Cp2 sequence in AvCp2 (figure 10). Because neither nitrogenase component protein exhibits any catalytic activity in the absence of the other, specific activities of the purified components are typically assessed by titrating one component protein versus the other (Shah *et al.*, 1972; Thorneley and Lowe, 1984b). Figure 11 shows the maximum catalytic activity obtained by titrating increasing amounts of purified Av2 or AvCp2 against a constant amount of Av1. These measurements show that saturating levels of AvCp2 were able to support only about 50% of the maximum Av1 activity supported by Av2, which is in agreement with the lowered diazotrophic growth rate of DJ911. Because maximum activity occurs when all the available Av2 or AvCp2 is present in a form complexed with Av1, the rate of substrate reduction becomes limited by the rate of complex dissociation. The decreased maximum activity for the AvCp2-dependent activity could, therefore, reflect a change in the rate of protein complex dissociation. The reciprocal titration yields considerably more complex results and is discussed later.

Deits and Howard (1990) have shown that concentrations of NaCl greater than 50 mM cause a dead-end inhibition of nitrogenase activity. Evidence that such inhibition occurs by interference with ionic interactions between the nitrogenase components was provided by experiments where NaCl was shown to inhibit the susceptibility of the component proteins to specific cross-linking (Willing *et al.*, 1989). Also, substitution of the Av2 Arg^{100} residue, targeted as providing an ionic interaction with Av1, results in an altered Av2 that exhibits hypersensitivity to NaCl and also exhibits MgATP hydrolysis

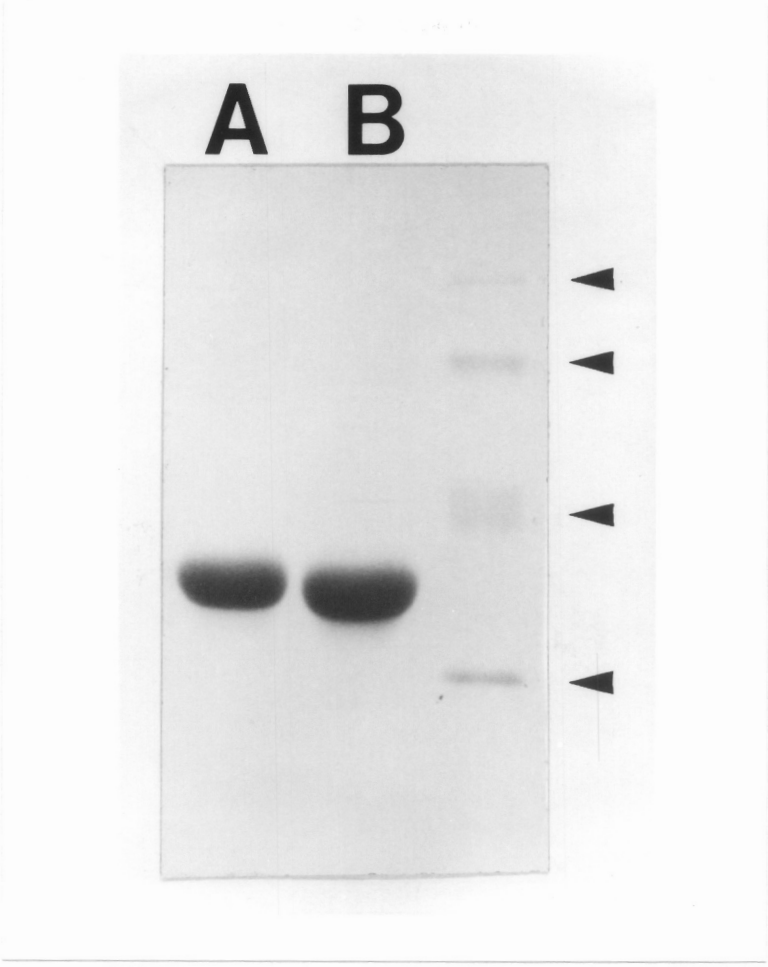

Figure 10. Coomassie-blue stained SDS-PAGE (15%) of approximately 10 μg purified Av2 (lane A) protein and purified AvCp2 (lane B). Molecular weight standards include, (phosphorylase b, 97,400; bovine serum albumin, 66,200; ovalbumin, 42,699; and carbonic anhydrase, 31,000).

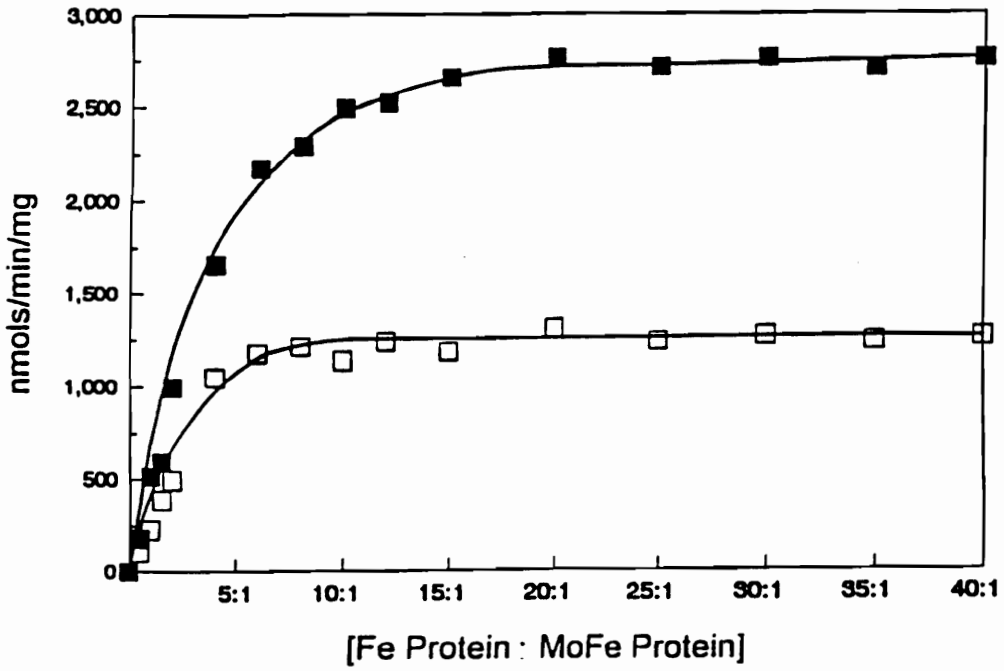

Figure 11. Determination of the maximum MoFe protein (Av1) proton reduction specific activity that can be supported by titration with increasing amounts of Fe protein (Av2 or AvCp2). Because neither MoFe protein nor Fe protein exhibits catalytic activity in the absence of the complementary component, this curve is analogous to a substrate saturation curve where Fe protein may be considered as the substrate. The curve was obtained by nitrogenase assays where 0.2 mg of Av1 was titrated with increasing amounts of Av2 (filled squares) or AvCp2 (open squares). The Av1 specific activity was determined as nmoles H_2 evolved per min per mg Av1 in the reaction vial assayed under an Ar atmosphere and is plotted as a function of the Fe protein–MoFe protein molar ratio. Data points were collected by using the standard assay procedure described in Experimental Procedures.

uncoupled from electron transfer (Wolle *et al.*, 1992b). Similar results were also obtained with a mutant produced by *K. pneumoniae* (Lowery *et al.*, 1989). Thus, we investigated the susceptibility of AvCp2 activity to inhibition by NaCl because residues 59 through 67 include a patch of anionic residues, which the Rees–Howard model predicts to participate in component protein interaction.

H_2 formation catalyzed in the AvCp2–dependent assay was not inhibited by the addition of up to 175 mM NaCl (figure 12). Rather, in this NaCl range, a modest, but reproducible, increase in specific activity was recognized. Marked inhibition of AvCp2–dependent activity, however, was recognized above 200 mM NaCl. In contrast, Av2 activity was gradually inhibited over the entire range of increasing NaCl and these results are in excellent agreement with those published by Deits and Howard (1990) and Wolle *et al.* (1992b). A simple explanation of the data is that a specific ionic interaction which occurs between Av2 and Av1 during catalysis, and which is inhibited by NaCl over the 50-175mM range, has been compromised in the analogous interaction between AvCp2 and Av1. Although not intuitively obvious, this hypothesis is in line with previous work where it was shown that substitutions placed at the Av2 Arg^{100} position lead to nitrogenase activity that is hypersensitive to NaCl. Interpretation of the hypersensitivity of altered Av2 having substitutions at the Arg^{100} position is that this residue normally provides a *dominant* ionic interaction with Av1 (Wolle *et al.*, 1992b). Consequently, elimination of this ionic interaction renders other, weaker, ionic interaction sites more susceptible to disruption by NaCl. On the other hand, the AvCp2 protein appears to have only a modest alteration in its ionic interaction with Av1, a property manifested in a lower total activity that is insensitive to the addition of up to 175 mM NaCl, but remains sensitive to higher NaCl concentrations. In other words, nitrogenase catalysis involving AvCp2 might not be inhibited at levels of NaCl up to 175 mM because a relatively weak ionic interaction, which is otherwise sensitive to such levels of NaCl, has already been disrupted in the altered protein. It should be noted that this phenomenon need not necessarily be associated with a specific ionic attraction between the component proteins during the initial docking event, but could just as well involve an electrostatic repulsion

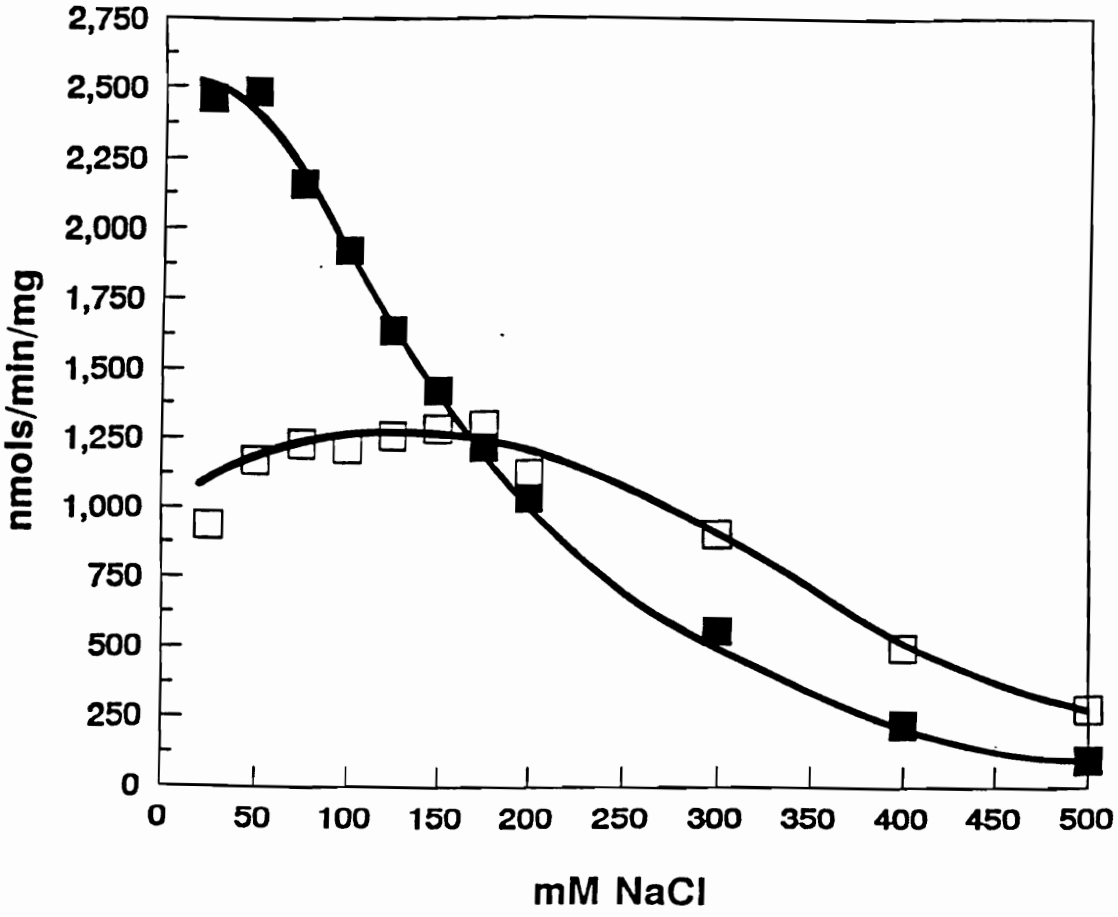

Figure 12. Effect of NaCl concentration on nitrogenase catalyzed H_2 formation. Comparison of the effect of increasing NaCl concentration on the H_2 evolution activity of Av2-dependent (filled squares) activity and AvCp2-dependent activity (open squares). Assays were performed as described in Experimental Procedures, and contained a final concentration of 0.5 mg of total component proteins at an Fe protein to MoFe protein molar ratio of 2.1:1. Activity is expressed in nmols of H_2 formed/min/mg of Fe protein.

associated with component protein dissociation.

The dependence of H_2 evolution on the component ratio, where an increasing amount of Av1 was titrated against a fixed amount of Av2 or AvCp2, is shown in figure 13. For the AvCp2-dependent reaction, maximum activity was obtained at an Av1 to AvCp2 molar ratio of 1-to-2. Because two, independent, Av2-binding sites are located on each Av1 molecule (Emerich *et al.*, 1978; Kim and Rees, 1994), this ratio corresponds to a one-to-one stoichiometry of the respective component protein interaction sites. Increasing titration beyond this ratio resulted in a dramatic loss in activity and a corresponding uncoupling of MgATP hydrolysis from substrate reduction (figure 13). In contrast, Av1 inhibition of the Av2-dependent reaction was recognized only at much higher levels of Av1. Indeed, Av1 inhibition of the Av2-dependent reaction is not readily apparent in figure 13, although it has been reported by other investigators (Ljones and Burris, 1972; Hageman and Burris, 1978a; Wherland *et al.*, 1981). The extent of this inhibition is dependent on the protein concentration and the ratio of component proteins.

In the case of the unaltered component proteins, why does a very high molar excess of MoFe protein relative to Fe protein result in lowered activity? When MoFe protein is present under these conditions, an accumulation of a catalytically-incompetent, one-electron reduced MoFe protein species must occur (Hageman and Burris, 1978b). Thus, because the accumulation of at least two electrons is required for reduction of any substrate, it is possible that the one-electron reduced form of the MoFe protein subsequently competes with dithionite for the available $Av2_{ox}(MgADP)_2$ (Thorneley and Lowe, 1984b). This phenomenon is hereafter referred to as "the back-reaction" because it involves non-productive association of *oxidized* Fe protein with the MoFe protein (see k_3 in scheme 1) which should, in principle, result in a lowering of the overall rate of substrate reduction. Experimental evidence for the back-reaction is based, in part, on the fact that increasing the dithionite concentration in the reaction, or decreasing the total protein concentration, partially suppresses the inhibitory effect that excess MoFe protein has on catalytic activity (Hageman and Burris, 1978a; Thorneley and Lowe, 1984b). This effect was also observed in the present work in the AvCp2-dependent reaction when

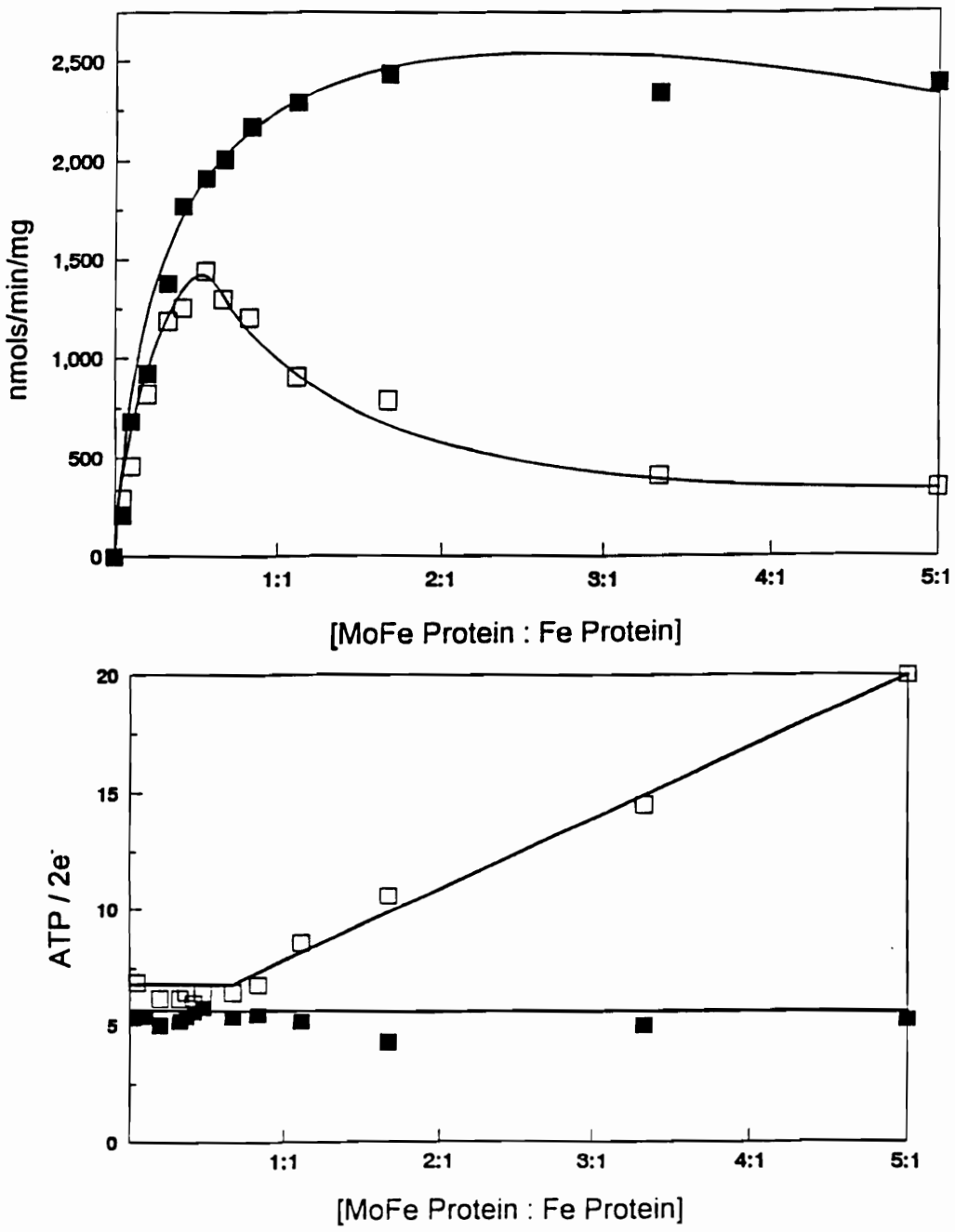

Figure13. Dependence of nitrogenase H_2 evolution and MgATP hydrolysis on the Av1:Av2 or AvCp2 molar ratio. 0.1 mg of either Av2 (filled squares), or AvCp2 (open squares) was titrated with increasing amounts of purified Av1. The resulting component protein molar ratio was plotted versus Av2- or AvCp2-specific activity for H_2 evolution (top panel) or the MgATP consumed per electron pair resulting in product formation (lower panel).

assayed for acetylene reduction (see below). Based on these considerations, we interpret our results to suggest that, during AvCp2-dependent catalysis, the back-reaction involving association of Av1 and $AvCp2_{ox}(MgADP)_2$ is markedly more significant than the analogous back-reaction involving $Av2_{ox}(MgADP)_2$. Thus, an increased significance of the back-reaction involving $AvCp2_{ox}(MgADP)_2$ is likely to be the consequence of its relatively higher affinity for Av1. In other words, formation of a relatively tighter AvCp2-Av1 complex, the theoretical basis for the original mutant strain construction, provides a plausible explanation for the marked inhibition of AvCp2-dependent activity when Av1 is present in molar excess. This consideration takes into account the previous suggestion of Thorneley and Lowe (1985) that only the unassociated form of MoFe protein can bind substrates and release products; a hypothesis that has been experimentally substantiated by component protein cross-linking studies (Willing *et al.*, 1989).

At least two different mechanisms can be used to explain the uncoupling of MgATP hydrolysis from substrate reduction that accompanies the dramatic Av1-specific inhibition of AvCp2-dependent activity at high Av1-to-AvCp2 ratios (see scheme 1). In the first possibility, reassociation of the one-electron reduced Av1 and $AvCp2_{ox}(MgADP)_2$ after the initial MgATP hydrolysis and electron transfer event could result in transfer of the electron back to AvCp2 with subsequent displacement of MgADP by MgATP. This scheme, previously suggested by Orme-Johnson and Davis (1977), would result in two MgATP hydrolyzed for each association-dissociation-reassociation event with no net electron transfer. One way of visualizing this mechanism for futile cycling of MgATP hydrolysis is to consider that an electron is bouncing back-and-forth between Av1 and AvCp2 with concomitant MgATP hydrolysis but no substrate reduction. An alternative route for futile cycling of MgATP is known as reductant-independent MgATP hydrolysis (Jeng *et al.*, 1970). This mechanism proposes that the component protein complex can catalyze MgATP hydrolysis independent from any electron transfer event. Although our present results do not distinguish between either of these two mechanisms, both possibilities are compatible with the idea that uncoupling of MgATP hydrolysis from substrate reduction observed at high Av1-to AvCp2 ratios reflects a

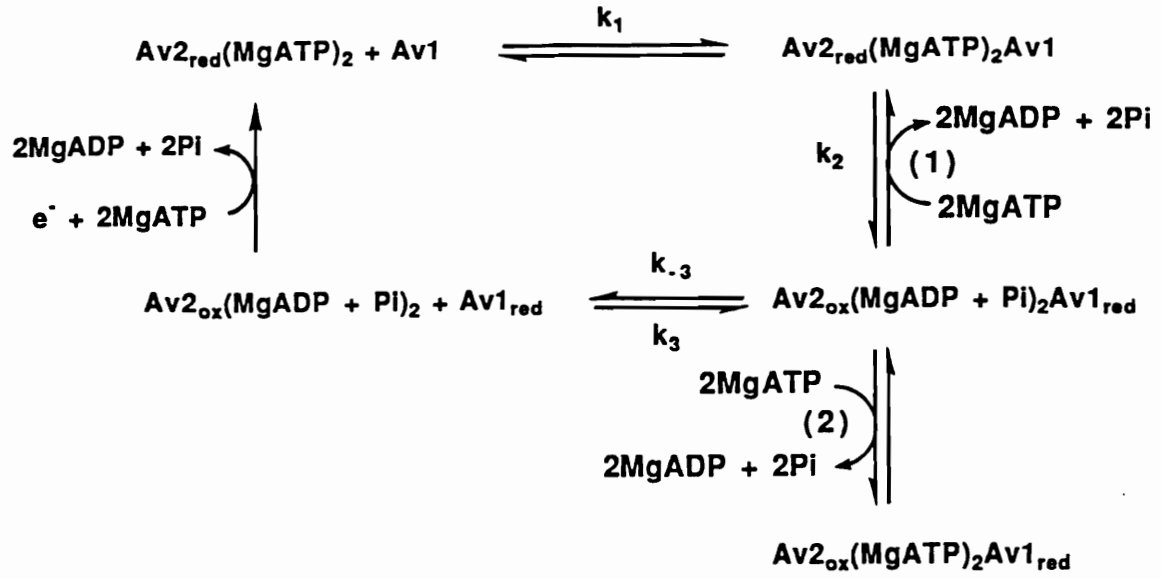

Scheme 1. Kinetic scheme showing MgATP–induced electron transfer from Av2 to Av1. The different redox states of Av1 and Av2 are indicated with subscripts as ox (oxidized) and red (one–electron reduced). Av1 with no subscripts represents the "as isolated" dithionite–reduced resting state. The scheme is based on the Lowe–Thorneley Av2 cycle (Lowe and Thorneley, 1984). In this case, Av1 is depicted as one of two independently functioning halves of the heterotetrameric structure and each $\alpha\beta$–dimer is assumed to contain one FeMo–cofactor and one Av2–binding site. The scheme has been annotated to highlight the two possible routes proposed to be responsible for uncoupling MgATP hydrolysis from substrate reduction: (1) reversible electron transfer from one–electron reduced Av1 to $Av2_{ox}(MgADP + Pi)_2$ and replacement of 2MgADP by 2MgATP (Orme–Johnson and Davis, 1977), and (2) reductant independent MgATP hydrolysis (Jeng *et al.*, 1970; Thorneley *et al.*, 1991).

relatively higher affinity of Av1 for $AvCp2_{ox}(MgADP)_2$ when compared to Av1's affinity for $Av2_{ox}(MgADP)_2$.

The dependence of ethylene formation on the component ratio, where increasing amounts of Av1 were titrated against fixed amounts of Av2 or AvCp2, is shown in figure 14. The trend of the titrations was the same as that observed for proton reduction assayed under argon (figure 13). In the case of the Av1 titration against AvCp2, however, there was an even more dramatic inhibition of substrate reduction and an increased uncoupling of MgATP hydrolysis from substrate reduction. For example, in the presence of a 5 molar excess of Av1, acetylene reduction was almost eliminated and 25 MgATP were consumed per $2e^-$ transferred to substrate. Because acetylene is reported to enhance formation of the inactive complex at high protein concentration (Lowe *et al.*, 1990), this result is consistent with the interpretation that there is an increase in the back-reaction involving the association of Av1 and $AvCp2_{ox}(MgADP)_2$. We also found that the uncoupling of MgATP hydrolysis to substrate reduction, apparent when Av1 was present in molar excess relative to AvCp2, was lowered by either increasing the concentration of dithionite in the reaction or by decreasing the protein concentration in the assay. For example, increasing the dithionite concentration from 20 mM to 50 mM resulted in a four-fold increase in total product formation in the AvCp2-dependent reaction when Av1 was present in 5 molar excess. Total product formation for the Av2-dependent reaction was unchanged under the same conditions. This result can be explained by a decrease in the unproductive association of Av1 and $AvCp2_{ox}(MgADP)_2$ under these conditions (Thorneley and Lowe, 1984b) owing to the more efficient reduction of $AvCp_{ox}(MgADP)_2$ by increased levels of dithionite, and is consistent with the hypothesis that Av1 has a higher affinity for $AvCp2_{ox}(MgADP)_2$ than for $Av2_{ox}(MgADP)_2$.

Another feature associated with the dramatic lowering in ethylene formation when assayed under a 10% acetylene atmosphere and at high Av1-to-AvCp2 molar ratios is the large increase in the percentage of electrons diverted to H_2 evolution (figure 15). When Av1 was present in 5 molar excess, the AvCp2-dependent reaction diverted almost 90% of electron flux to H_2 evolution, whereas, under the same conditions, the Av2-dependent

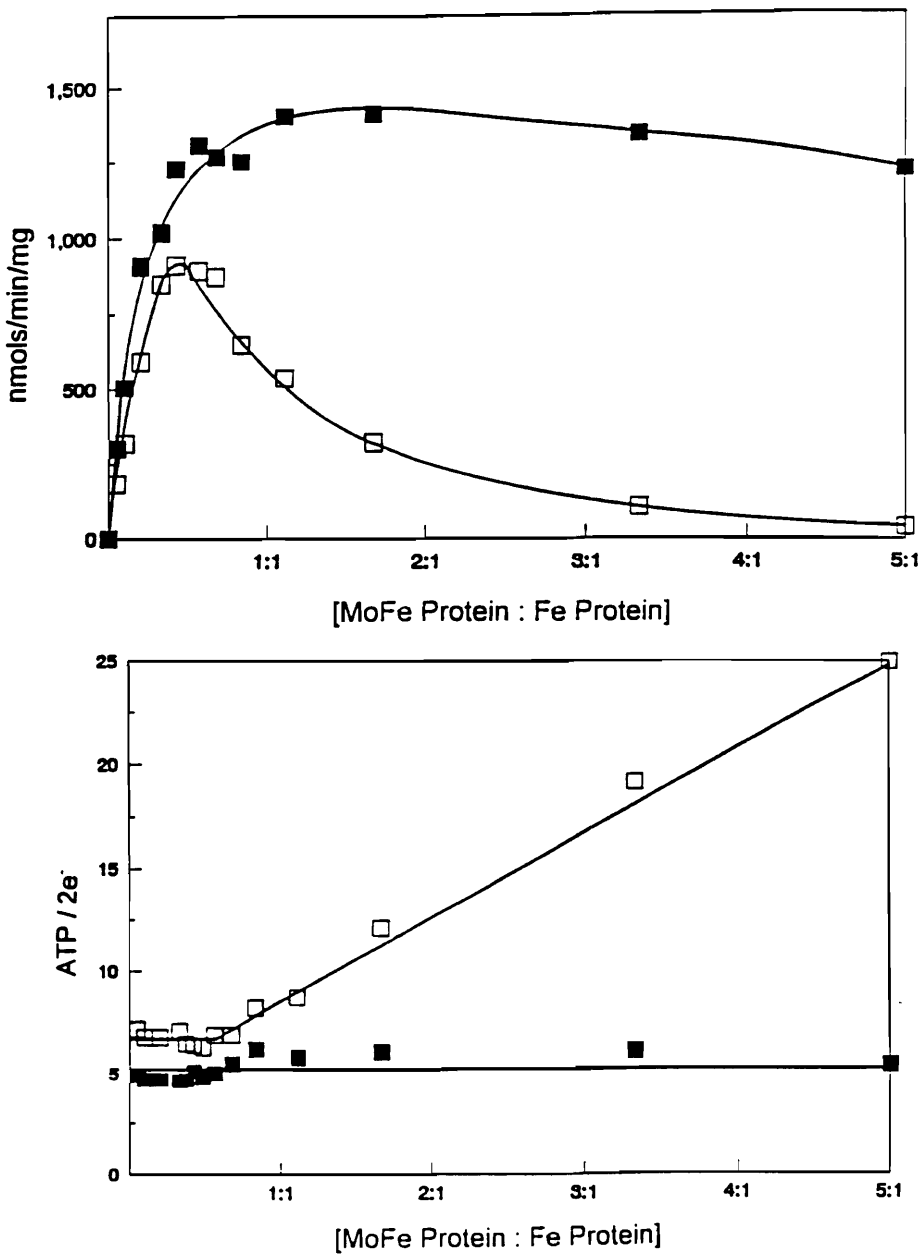

Figure 14. Dependence of nitrogenase ethylene formation and MgATP hydrolysis on the Av1:Av2 or AvCp2 molar ratio. 0.1mg of either Av2 or AvCp2 was titrated with increasing amounts of Av1. The resulting molar ratio was plotted versus Av2 (filled squares) or AvCp2 (open squares) specific activity of ethylene formation (top panel) and the ATP utilized per electron pair resulting in product formation (lower panel). Total electron pairs used in the determination of ATP/2e⁻ were calculated using both the ethylene formation and H_2 evolution activities in the acetylene reduction assays.

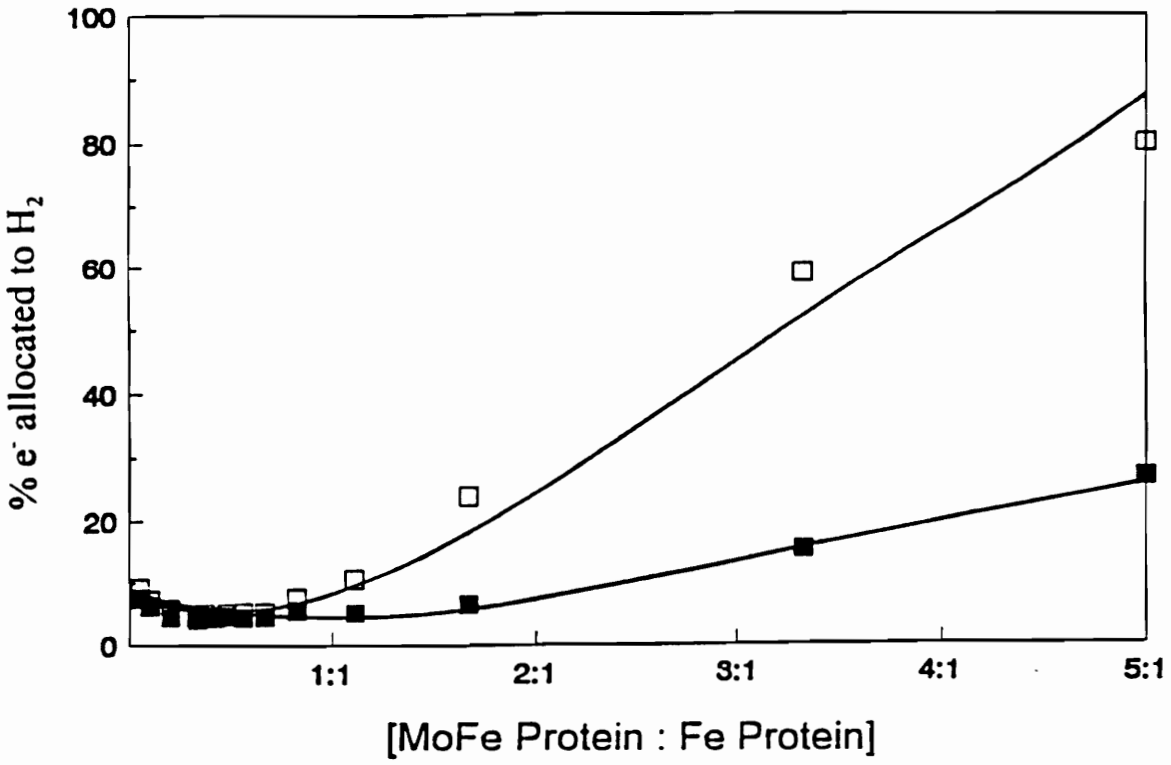

Figure 15. Percentage of total electron flux through nitrogenase diverted to H_2 formation under 10% acetylene as a function of component protein ratio. The titration was the same shown in Figure 6 except both ethylene and H_2 formation were measured. Each data point represents the percentage of total electron flux (H_2 plus ethylene formation) diverted to H_2 formation at a particular component ratio. Av2 (filled squares); AvCp2 (open squares).

reaction diverted only about 20% of electron flux to H_2 evolution. Such redistribution of electron flux to H_2 evolution under conditions of very high MoFe protein–to–Fe protein molar ratios has been previously reported and was suggested to reflect limiting conditions of electron flux resulting from a low availability of reduced Fe protein with respect to MoFe protein (Hageman and Burris, 1980).

The effect of NaCl concentration on the rate of primary electron transfer from Av2 and AvCp2 to Av1 and the respective rates of protein complex dissociation were determined using stopped-flow spectrophotometry (table 1). The dissociation of oxidized Fe protein [either $AvCp2_{ox}(MgADP)_2$ or $Av2_{ox}(MgADP)_2$] from MoFe protein was assumed to be the rate limiting step for substrate reduction under these conditions (Thorneley and Lowe, 1983). Conditions chosen were those that give minimal (50 mM NaCl) and intermediate (175 mM NaCl) inhibition of specific activity during the steady-state of the Av2–dependent reaction which is not inhibited by excess Av1. The observed first-order rate constants for the MgATP–dependent oxidation of Av2 and AvCp2 at 430 nm were similar at 50 mM NaCl (k_{obs}=140s^{-1} and 170s^{-1} respectively) and essentially the same as those previously reported for component proteins isolated from *K. pneumoniae* (Thorneley, 1975). Our data were obtained from experiments in which 40 μM Av2 or AvCp2, 10 μM Av1, 10 mM $MgCl_2$ and 10 mM Na–dithionite were pre-equilibrated in one stopped-flow drive syringe while the other syringe contained 18 mM MgATP, 10 mM $MgCl_2$ and 10 mM Na–dithionite. Both syringes also contained NaCl so that the final concentration in each syringe was 50 mM. These conditions were chosen because they gave the expected amplitude for the single exponential absorbance change associated with the oxidation of $Av2(MgATP)_2$ by Av1 ($\Delta\epsilon_{430}$=5.5 $mM^{-1}cm^{-1}$). The rate of electron transfer within AvCp2-Av1 and Av2-Av1 decreased as the concentration of NaCl was increased from 50 mM to 175 mM with all other conditions remaining constant. The change in the amplitude was equivalent in each reaction. It is evident from table 1 that there is an approximate 65% decrease in the rate of oxidation of Av2 (k_{obs}=50s^{-1}) compared with only a 45% decrease in the AvCp2 (k_{obs}=95s^{-1}) system. This result is consistent with the rate of Av2–Av1 complex formation being more significantly affected

Table 1. Measured rate constants for primary electron transfer (k_2) and component protein complex dissociation (k_{-3}) in the presence of 50mM and 175mM sodium chloride at 23°C at pH7.4. The reactions are defined by Scheme 1.

[NaCl] (mM)	Fe protein species	Primary electron transfer (s^{-1})	complex dissociation (s^{-1})
50	AvCp2	170 ± 10	3.7 ± 0.1
50	Av2	140 ± 10	6.3 ± 0.1
175	AvCp2	95 ± 5	3.8 ± 0.1
175	Av2	50 ± 5	2.8 ± 0.1

at 175 mM NaCl, however, the determination of the rate of complex association at different salt concentrations is beyond the scope of the present work. It is apparent that, even with an electron transfer rate of k_{obs}=50s^{-1}, this reaction is still 10 times faster than the rate-limiting step (k_{-3} = 6.4±0.8s^{-1}), which involves dissociation of $Av2_{ox}(MgADP_2)$ from Av1 (Thorneley and Lowe, 1983). Therefore, the decrease in k_{obs} seen at 175 mM NaCl in the Av2–dependent reaction cannot be responsible for the observed inhibition of steady-state specific activity.

We also investigated NaCl inhibition of nitrogenase activity by measuring the rate of protein complex dissociation. Although it is possible to determine the rate limiting step from the steady-state rate of substrate reduction in the typical *in vitro* assay, the values obtained are artificially low when dithionite is used as reductant, because the re-association of $Av2_{ox}(MgADP)_2$ with reduced Av1 (k_3 in the Thorneley–Lowe kinetic model) competes with the re-reduction of Av2 by dithionite (Thorneley and Lowe, 1984b). This problem can be circumvented by using the hydroquinone–form of flavodoxin II, the physiological electron donor for nitrogenase, as the source of reducing equivalents in *in vitro* assays because it reduces $Av2_{ox}(MgADP)_2$ more efficiently (Thorneley and Deistung, 1988) and, therefore, causes k_3 to become much less significant. Using the hydroquinone–form of AvFldII as the reductant also has an advantage in that the amount of available reducing species is dependent only on the concentration and percentage of the protein in the hydroquinone state and does not depend on a dissociation constant as is the case for dithionite (K_D=1.6x10^{-9} ± 0.2x10^{-9} M, Thorneley and Lowe, 1983). Thus, stopped-flow spectrophotometry was used to continuously monitor the oxidation of the hydroquinone form of AvFldII (15 μM) to the semiquinone state at 580 nm by catalytic amounts of Av1 (0.6 μM) with Av2 (2.5 μM) and MgATP (5 mM) in the absence of dithionite. After mixing, complex formation of the nitrogenase proteins is initiated by MgATP and electron transfer occurs within the complex. The hydroquinone form of AvFldII is then oxidized to the semiquinone as it rapidly transfers its electron to the oxidized Fe protein that forms upon complex dissociation. Therefore, the rate of semiquinone formation is a direct indication of the rate of complex dissociation. This

procedure was previously developed and used in the Sussex Lab (Thorneley, R.N.F., unpublished results). Calculation of the turnover numbers (based on the Mo content of the Av1 and a $\Delta\epsilon_{580}$=5.7 $mm^{-1}cm^{-1}$ for AvFldIIHQ/SQ, Klugkist *et al.*, 1986) under conditions of 50 mM NaCl gave values of 6.3 and 3.7s^{-1} for the Av2-dependent and AvCp2-dependent reaction, respectively. The value of k_{-3} for the $Av2(MgATP)_2$-Av1 complex is in excellent agreement with that determined previously using extensive computer analyses and the inhibition of the SO_2^- reduction of $Kp2_{ox}(MgADP)_2$ by Kp1 (k_{-3}=6.4±0.8s^{-1}, Thorneley and Lowe, 1983). From these results we conclude that 50 mM NaCl does not affect the dissociation of $Av2_{ox}(MgADP)_2$ from Av1, which implies that the lowered rate observed with the AvCp2-dependent reaction at 50 mM is due to its tighter binding to Av1. As a consequence of increasing the salt concentration to 175 mM, the value of k_{-3} for the Av2-dependent reaction was lowered to a value that correlated well with the measured decrease in steady-state specific activity as shown in figure 4. This data is also consistent with that of Deits and Howard (1990), who observed an approximate 50% inhibition of proton and acetylene reduction at 175 mM NaCl. At 175 mM NaCl no measurable change in the AvCp2-Av1 protein dissociation rate was detected and this was reflected in a uniform specific activity in the steady-state.

In summary, we have tested the Rees-Howard model for docking of the nitrogenase component proteins by constructing a hybrid Fe protein, which based on the model and biochemical complementation experiments, was predicted to form a tighter complex with the MoFe protein. Our results show that substitution of residues 59 through 67 of the Av2 primary sequence by the corresponding Cp2 sequence results in an AvCp2 protein that dissociates more slowly from Av1 during the electron transfer cycle. Evidence for this conclusion is based on the following observations. First, the maximum specific activity of the AvCp2 protein is about half that of Av2 and is insensitive to inhibition by up to 175 mM NaCl. This result is interpreted to indicate that a specific ionic interaction, which normally occurs between Av2 and Av1, and, which could involve component protein dissociation, has been compromised in AvCp2. Second, when present in molar excess, Av1 was found to be a potent inhibitor of the AvCp2-dependent reaction

and results in the uncoupling of MgATP hydrolysis from electron transfer. Finally, the effect of NaCl concentration on the rate of primary electron transfer and the respective rates of protein complex dissociation were measured by stopped-flow spectrophotometry. These results show that the dissociation rate for the AvCp2-Av1 complex is about half that of the Av2-Av1 complex, which is consistent with the steady state activity of AvCp2-dependent catalysis, the diazotrophic growth rate of the mutant strain, and is also in line with the current view that complex dissociation is the rate-limiting step in nitrogenase catalysis. Although our results provide strong evidence for the Rees-Howard model, it is interesting that AvCp2 does not form a tight, inactive complex with Av1. This result was not unexpected as inspection of the model shows that there are other regions within Av2 likely to be involved in component protein interaction which bear primary sequence differences when compared to Cp2. The most notable of these is a region which includes Glu^{112}, which has been identified as the Av2 residue susceptible to cross-linking with Av1. Success in the present work encourages us to analyze these other regions, singly and in various combination with the available construct, by using the hybrid Fe protein strategy.

CHAPTER II.

Fe protein-MoFe protein interaction and intermolecular electron transfer: Role of the α-subunit aspartate-161 residue.

This chapter represents a manuscript in preparation which will be authored by Limin Zheng, Karl Fisher, myself, William E. Newton, and Dennis R. Dean. Although the experimental results represent the combined efforts of Limin Zheng, Karl Fisher and myself, the majority of the experimental work was performed by Limin Zheng. EPR spectroscopy was performed by Richard Dunham (University of Michigan).

Summary

Nitrogenase catalysis involves the interaction of the Fe protein and the MoFe protein in a manner which couples hydrolysis of MgATP to electron transfer. Previous studies involving the salt sensitivity of nitrogenase catalysis indicated that electrostatic interactions are involved in component protein complex formation (Deits and Howard, 1990; Wolle *et al.*, 1992b). A docking model has been proposed which places the Fe_4S_4 cluster of the Fe protein in close proximity to the MoFe protein P cluster (Kim and Rees, 1992b; Howard, 1993, see figure 1a and b). Mutagenesis studies have demonstrated that several amino acid residues of the Fe protein, which are located at the proposed component protein docking interface, contribute to electrostatic interactions which promote complex formation (Wolle *et al.*, 1992b; Seefeldt, 1994). In this study, the contribution of MoFe protein amino acid residues to component protein interaction was probed by placing amino acid substitutions at α-Asp^{161}, α-Asp^{162}, β-Asp^{160} and β-Asp^{161}, which, within the proposed docking model, are likely to interact with the Fe protein during complex formation. Analysis of mutant strains having altered MoFe proteins with either α-Asp^{162}, β-Asp^{160} or β-Asp^{161} replaced by Asn indicates that the charged amino acid side chains of these residues are not important for nitrogenase catalysis and are therefore not

likely to be involved in electrostatic interactions which are important for complex formation. However, substitution of α-Asp^{161} by Asn results in an altered MoFe protein with only 3 to 5 percent of the wild-type catalytic activity. A detailed biochemical characterization of this altered MoFe indicated that the remaining catalytic activity was hypersensitive to inhibition by NaCl and that the inhibition could not be overcome to any extent by increasing Fe protein concentration. In addition, MgATP hydrolysis was highly uncoupled from electron transfer to substrate. These results indicate that, although α-Asp^{161} is not involved in an initial interaction which promotes complex formation, it is likely that this residue has a role in an electrostatic interaction which occurs as a result of reciprocal conformational changes of both component protein partners within the complex induced by MgATP hydrolysis.

Introduction

The process of biological nitrogen fixation, the reduction of dinitrogen to ammonia, is catalyzed by the complex metalloenzyme nitrogenase. Nitrogenase is composed of two easily separable component proteins, termed the Fe protein and the MoFe protein, which reflect the metal content of their respective associated metalloclusters. The Fe protein is a γ_2-homodimer ($M_r \approx 63{,}000$, encoded by *nifH*) with one single Fe_4S_4 cluster bridging its two identical subunits, and the MoFe protein is an $\alpha_2\beta_2$-heterotetramer ($M_r \approx 230{,}000$, encoded by *nifDK*) having two kinds of metalloclusters, which are referred to as P clusters and iron-molybdenum cofactors (FeMocos). Each αβ-dimer of the MoFe protein is considered as functioning independently, and contains a P cluster (Fe_8S_8) located at its αβ-unit interface and an FeMoco (Fe_7S_9Mo-homocitrate) completely contained within the α-subunit. For recent reviews of the structural aspects of both component proteins and their associated metalloclusters see Dean *et al.*, 1993; Mortenson *et al.* 1993; Rees *et al.*, 1993a; Eady and Leigh, 1994; Howard and Rees, 1994; Kim and Rees, 1994.

During nitrogenase catalysis, electrons are transferred from the Fe protein to the

MoFe protein in a process that involves component protein complex formation and MgATP hydrolysis. The MoFe protein P clusters are believed to initially accept the electron before transferring it to the FeMoco upon which is located the site of substrate binding and reduction (Shah and Brill, 1977; Hawkes *et al.*, 1984; Liang *et al.*, 1990; Scott *et al.*, 1990; Scott *et al.*, 1992). Under optimum conditions *in vitro*, the stoichiometry for the reaction is normally as indicated by the following equation.

$$N_2 + 8e^- + 8H^+ + 16\ MgATP \rightarrow 2NH_3 + H_2 + 16\ MgADP + 16Pi$$

In addition to the six electron reduction of N_2 to ammonia, nitrogenase also catalyzes a number of other reductions, among them the reduction of acetylene to ethylene and protons to H_2. The quantitative correlation between MgATP hydrolysis and electron transfer has been intensively studied with the wild-type system and it is generally accepted that 4-5 MgATP molecules are hydrolyzed per pair of electrons transferred to substrate (Watt *et al.*, 1975; Ashby *et al.*, 1987; Dilworth *et al.*, 1992). Since neither component protein hydrolyzes MgATP alone (Imam and Eady, 1980), MgATP hydrolysis is a property of the Fe protein-MoFe protein complex. The efficiency of the electron transfer and thus the catalytic rate of the nitrogenase reaction are strongly related to the interaction of the component proteins. Previous studies have suggested that the rate of proton reduction depends on the ratio and absolute concentration of the component proteins (Thorneley and Lowe, 1984b). Using conditions of limiting electron flux, it has been shown that the rate of protein-protein association and electron transfer from the Fe protein to the MoFe protein are independent of the level of reduction of the MoFe protein (Fisher *et al.*, 1991). It has also been shown that high concentrations of salt inhibit nitrogenase activity in *Azotobacter vinelandii* (Deits and Howard, 1990). Chemical cross-linking experiments determined that residue Glu^{112} of the Fe protein is at the interface of the component protein interaction (Willing and Howard, 1990) and mutagenesis studies have shown that Arg^{140}, Lys^{143} (Seefeldt, 1994) and Arg^{100} (Wolle *et al.*, 1992b) of the Fe protein are involved in the ionic interactions associated with component protein complex

formation. A region from residue 59 to 67 of Av2 has been implicated in component protein interaction by substitution with the same region from Cp2 (see Chapter I).

Because each electron is transferred from the Fe_4S_4 cluster of the Fe protein to the P cluster of the MoFe protein, and the Fe_4S_4 cluster is bridged between the identical γ_2-subunits of the Fe protein (Georgiadis *et al.*, 1992), we expected that the P cluster environment of the MoFe protein should have certain symmetry too. Comparing the primary structures of the α-and β-subunits of the MoFe protein it is clear that the residues around the P cluster ligand residues, α-Cys^{62}, α-Cys^{88}, α-Cys^{154}, β-Cys^{95} and β-Cys^{153}, β-Cys^{188} (Dean and Jacobson, 1992), are homologous to each other, suggesting that the structure of the α- and β-subunits in this region are pseudo-symmetrical (Dean and Jacobson, 1992). This suggestion is supported by the x-ray crystallographic data (Kim and Rees, 1992b). Certain charged residues are conserved in both the α- and β-subunits of the MoFe protein and are located at the proposed docking interface and thus may be involved in the ionic interaction between the component proteins (Kim and Rees, 1992b).

In the present study, α-Asp^{161}, α-Asp^{162}, β-Asp^{160}, and β-Asp^{161} were substituted singly and in combination to ascertain their possible contribution to component protein interaction and nitrogenase catalysis. The results of the biochemical characterization of an altered MoFe protein with α-Asp^{161} substituted by Asn are discussed in the context of a model for intermolecular electron transfer in which conformational changes induced by MgATP hydrolysis on the Fe protein are transduced to the MoFe protein to enable intermolecular electron transfer to occur.

Experimental Procedures

Oligonucleotides were synthesized using an Applied Biosystems Model 381A DNA synthesizer. Restriction enzymes, T_4 DNA ligase, and Sequenase were purchased from Life Technologies Inc.(Gaithersburg, MD), New England Biolabs (Beverly, MA) or United States Biochemical (Cleveland, Ohio). Other chemicals and enzymes were purchased from Sigma (St. Louis, Missouri).

For site-directed mutagenesis, the 1.4 kb *Eco*RI fragment of *A. vinelandii nifD* gene and the 1.0 kb *Hind*III-*Kpn*I fragment of *nifK* gene were cloned individually into pUC119 (Vieira and Messing, 1987). Oligonucleotide-directed mutagenesis was accomplished using the oligonucleotides listed in table 2 as described previously by Kunkel *et al.*, (1987). The mutations in *nifD* were transferred to the *A. vinelandii* chromosome by using the appropriate plasmid construction to transform DJ100 to prototrophy. DJ100 contains a deletion in the *nifD* gene spanning the region corresponding to α-subunit residues 103 to 376 and is therefore phenotypically nif-. The mutations in *nifK* were transferred to the chromosome in a manner analogous to the mutations in *nifD* except DJ727 was used for transformation. DJ727 is a phenotypically nif- strain in which a Kanamycin resistant marker has been inserted at a position of the *nifK* gene which corresponds to β-Asp^{161} of the MoFe protein. The construction of Av1(α-Asn^{161}) and Av1(α-Asn^{161} + α-Asn^{162}) mutants, which result in a nif- phenotype, involves congression using a Rifampicin resistance determinant as a marker in selection. A more detailed description of the construction of similar mutant strains can be found in Robinson *et al.* (1986) and Jacobson *et al.* (1989b). Diazotrophic growth was accomplished as described by Strandberg and Wilson (1968). The mutant strains that have been constructed during this investigation are shown in table 2.

All enzyme manipulations were performed under anaerobic conditions achieved by using a Schlenk line manifold connected to a vacuum and a purified argon source. All MoFe proteins and Fe proteins used in this study were purified using the method described by Burgess *et al.* (1980a) with the following changes. Q-Sepharose chromatography using a continuous gradient of 0.1 to 1 M NaCl was substituted for DEAE cellulose chromatography. The samples were subsequently concentrated on a Q-Sepharose column (1.0 x 20 cm) and the Fe proteins were further purified with a gel filtration step using a Sephacryl S300HR column (5 x 30 cm) equilibrated with 25 mM Tris-HCl, pH 7.4 buffer with 100 mM NaCl and 1 mM $Na_2S_2O_4$. MoFe protein purification was accomplished by substituting hydrophobic interaction chromatography (Phenyl Sepharose) for the

Table 2. Construction of *Azotobacter vinelandii* mutant strains with amino acid substitutions at α-Asp^{161}, α-Asp^{162}, β-Asp^{160}, and β-Asp^{161}.

Plasmid	Mutant Strain	Substitution[a]	Oligonucleotide[b]
pDB700	DJ725	α-Asn^{161}	CTGATCGGC<u>A</u>ACGACATCG
pDB701	DJ722	α-Asn^{162}	CGGCGAC<u>A</u>ACATCGAATCC
pDB702	DJ723	α-Glu^{162}	CGGCGACGA<u>G</u>ATCGAATCC
pDB703	DJ726	α-Asn^{161} + α-Asn^{162}	CTGATCGGC<u>A</u>AC<u>A</u>ACATCGAATCC
pDB704	DJ724	α-Glu^{161} + α-Glu^{162}	CGGCGA<u>G</u>GA<u>G</u>ATCGAATCC
pDB705	DJ738	β-Asn^{160}	GGTCATCGGT<u>A</u>ACGACCTC
pDB706	DJ739	β-Glu^{160}	CATCGGTGA<u>G</u>GACCTCAAC
pDB707	DJ740	β-Asn^{161}	CATCGGTGAC<u>A</u>ACCTCAAC
pDB708	DJ741	β-Glu^{161}	CGGTGACGA<u>G</u>CTCAACGCC
pDB784	DJ929	β-Asn^{160} + β-Asn^{161}	CATCGGT<u>A</u>AC<u>A</u>ACCTCAAC
pDB709	DJ742	β-Glu^{160} + β-Glu^{161}	CATCGGTGA<u>G</u>GA<u>G</u>CTCAACG

[a]α-Asn^{161} represents substitution of Asp at α−subunit residue position 161 by Asn. Also see abbreviations.

[b]Nucleotide mismatches are underlined.

crystallization step. Phenyl sepharose chromatography was accomplished using a continuous gradient 0.4 to 0 M NH_4SO_4. The purified component proteins were concentrated using an Amicon Pressure Filtration Concentrator and purity was monitored by Coomassie Blue stained SDS-PAGE (Laemmli, 1970). The concentrations of the purified component proteins were determined by the method essentially based on the Lowry or Folin-Ciocalteau procedure (Lowry *et al.*, 1951) using bovine serum albumin as a standard. The molybdenum and iron content of the MoFe proteins were determined by inductively coupled plasma atomic emission spectrometry using a simultaneous spectrometer (Jarrell-Ash ICAP 9000) and a sequential scanning spectrometer (Jarrell-Ash Atomscan 2400). The wild-type and α-Asn^{161} MoFe proteins contained 1.9 and 1.57 g atom Mo (mol protein)$^{-1}$ respectively and both contained 26 g atom Fe (mol protein)$^{-1}$.

Nitrogenase component proteins were assayed at 30°C in 9 ml calibrated vials fitted with butyl rubber serum stoppers and metal caps. The 1 ml reaction mixture contained 25 mM Hepes-NaOH buffer, pH 7.4, 25 units of creatine phosphokinase, 30 mM phosphocreatine, 2.5 mM ATP, 5 mM $MgCl_2$ and 20 mM $Na_2S_2O_4$. Vials were degassed and filled with purified argon gas for H_2 evolution assays or 8.6 % acetylene in argon for acetylene reduction assays. $Na_2S_2O_4$ was added to degassed assays, followed by Av2 and the reaction was started by the syringe addition of Av1 to give the desired molar ratio of the two proteins. The concentration of each component protein in the assay is indicated in the figure legends or in the text. Assays were terminated by the addition of 0.25 ml 0.4 M Na-EDTA. H_2 evolution was analyzed by gas chromatography using a Shimadzu GC-8A gas chromatograph fitted with a thermal conductivity detector and 5A molecular sieve column, by injecting 200 µl from the gas-phase of each vial, with a pressure-lock syringe. Samples were similarly analyzed for C_2H_4 (the product of acetylene reduction) by using a Shimadzu GC-14A gas chromatograph linked to a flame ionization detector. Gas chromatographs were calibrated by using standards containing 1% H_2 in N_2 or 1000 ppm C_2H_4 in He (Scotty Specialty Gases, Durham, NC). MgATP hydrolysis was determined indirectly by measuring the production of creatine using the colorimetric method of Ennor (1957). Small columns (2.5 cm x 6 mm diameter) of Dowex-AG 1-x2

resin (Cl^- form; 200-400 mesh) were prepared in glass wool plugged Pasteur pipettes to remove inhibitory components from the assays (Dilworth *et al*, 1992). Creatine was determined colorimetrically at 530 nm using a calibration curve prepared with creatine.

Stopped-flow measurements were made with a Hi-Tech SF61 stopped-flow spectrophotometer equipped with a data acquisition and analysis system (Salisbury, Wilts, U.K.). To ensure complete anaerobicity, the SHU-61 sample handling unit was installed inside an anaerobic chamber operating at less than 0.5 ppm O_2. A Teledyne Analytical Instruments series 316 trace oxygen analyzer (Vacuum Atmospheres Co., Hawthorne, CA) was used to continually monitor oxygen concentration during experimentation. Reactants were thermostatted to 23±0.1°C by closed circulation of water by a Techne C-85D circulator (Techne Ltd., Duxford, Cambridge, U.K.) attached to a FC-200 Techne flow cooler. Both the cooler and circulator were situated outside the anaerobic chamber. All stopped-flow reactions were performed in 25 mM Hepes buffer, pH 7.4, containing 10 mM $MgCl_2$ and unless otherwise stated 10 mM $Na_2S_2O_4$. The oxidation of Av2 and AvCp2 was monitored at 430 nm and fitted to a single exponential function.

Results and Discussion

Previous studies involving salt inhibition of nitrogenase have indicated that electrostatic interactions are important in productive Fe protein-MoFe protein complex formation (Deits and Howard, 1990, Wolle *et al.*, 1992b). Examination of the x-ray crystal structure of the MoFe protein reveals that residues α-Asp^{161}, α-Asp^{162}, β-Asp^{160} and β-Asp^{161} lie at the pseudo-symmetrical component protein docking interface (Kim and Rees, 1992b, see figure 5). These residues are closely linked to the P cluster ligands, α-Cys^{154} and β-Cys^{153} through short α-helixes. The side chains of α-Asp^{162} and β-Asp^{161} are on the surface of the MoFe protein and exposed to the solvent (Kim and Rees, 1992b). Similarly, the side chain of α-Asp^{161} is solvent exposed; however, its corresponding pseudo-symmetric partner, β-Asp^{160}, is not.

Each of these Asp residues were substituted by Asn and Glu singly and in

combination in an effort to ascertain their possible contribution to component protein interaction and nitrogenase catalysis. The diazotrophic growth rates and nitrogenase activities of crude extracts of the resulting mutant strains is shown in table 3. Nitrogenase activities in crude extracts can only be compared qualitatively because of variability in the levels of nitrogenase derepression. A comparison of the Fe protein specific activities in these crude extracts is an indication of that variability (table 3). Substitution of α-Asp^{162}, β-Asp^{160}, or β-Asp^{161} either singly or in combination by Asn or Glu had no significant effect on diazotrophic growth or MoFe protein crude extract activity of the resulting mutant strains. Similarly, substitution of α-Asp^{161} by Glu was of no consequence in terms of diazotrophic growth and MoFe protein acitvity in crude extracts. A mutant strain with α-Asp^{161} substituted by Asn, however, was unable to grow diazotrophically and was almost devoid of MoFe protein activity in crude extracts. It was not unexpected that there is no significant contribution by β-Asp^{160} in component protein interaction, since it is not among those residues mentioned as being solvent exposed at the docking interface (Kim and Rees, 1992b). It was surprising, however, that substitution of α-Asp^{162} or β-Asp^{161} by Asn did not result in any phenotypic or biochemical alterations, indicating that the acidic side chains of these residues, which are entirely solvent exposed, are not involved in electrostatic interactions with the Fe protein. The possibility remains that these residues could hydrogen bond with residues of the Fe protein by virtue of their carbonyl groups which would be conserved upon substitution by Asn. Elimination of charge at α-Asp^{161} results in an almost complete loss of MoFe protein activity (table 3) indicating that this residue is involved in some electrostatic interaction that is important for catalysis. The observation that the analogous substitution of α-Asp^{161}'s pseudo-symmetric partner, β-Asp^{160}, has no apparent effect in terms of MoFe protein activity suggests that although there is significant conservation of structure between the α- and β-subunits, there is not necessarily conservation of function in terms of the role of individual amino acid side chains. This is consistent with the results of chemical cross-linking experiments in which the Fe protein is specifically cross-linked to only the β-subunit of the MoFe protein (Willing *et al.*, 1989).

Table 3. Diazotrophic growth rates and acetylene reduction activities in crude extracts of *Azotobacter vinelandii* mutant strains with amino acid substitutions at α-Asp^{161}, α-Asp^{162}, β-Asp^{160}, and β-Asp^{161} of the MoFe protein.

Strain	Substitution	Diazotrophic growth rate (doubling time)	Nitrogenase Activity in Crude Extract	
			MoFe	Fe
		h	*nmol/min/mg*	
Trans	none	2.5	107.0	27.5
DJ725	α-Asn^{161}	-	0.7	23.2
DJ63	α-Glu^{161}	2.5	120.0	40.7
DJ722	α-Asn^{162}	2.5	76.9	20.4
DJ723	α-Glu^{162}	2.5	55.4	20.6
DJ726	α-Asn^{161} + α-Asn^{162}	-	0.1	24.6
DJ724	α-Glu^{161} + α-Glu^{162}	2.5	103.6	33.5
DJ738	β-Asn^{160}	2.5	110.6	24.0
DJ739	β-Glu^{160}	2.5	63.2	16.4
DJ740	β-Asn^{161}	2.5	76.1	11.2
DJ741	β-Glu^{161}	2.5	108.5	35.4
DJ929	β-Asn^{160} + β-Asn^{161}	2.5	104.3	41.4
DJ742	β-Glu^{160} + β-Glu^{161}	2.5	60.2	13.5
DJ921	α-Asn^{162} + β-Asn^{161}	2.5	73.4	17.1

Very low but detectable levels of α-Asn^{161} MoFe protein [Av1(α-Asn^{161})] activity was detected in crude extracts indicating a more in depth biochemical characterization would be possible upon purification. Av1(α-Asn^{161}) could be purified by the same procedure as is used for the purification of wild-type MoFe protein (Av1). Similar yields were observed in comparison to a typical wild-type purification indicating that the protein was stable to purification. Av1(α-Asn^{161}), under optimal conditions, exhibited 3 to 5% of hydrogen evolution and acetylene reduction activities of Av1(data not shown) which correlates well with the activities observed in crude extracts (table 3). The S=3/2 EPR signal of the Av1(α-Asn^{161}) was identical to that of Av1 in intensity, line shape and g-value indicating no alteration in the structure of the FeMoco or its associated polypeptide environment (substrate binding site).

In an effort to further implicate the involvement of α-Asp^{161} in component protein interaction, biochemical complementation experiments were used to test whether a previously characterized Fe protein altered in component protein interaction could somewhat suppress the low activity observed in Av1(α-Asn^{161}) dependent nitrogenase reactions. Nitrogenase activity in reactions in which the AvCp hybrid Fe protein (AvCp2) was used as the electron donor for Av1(α-Asn^{161}) was increased 3 to 5 fold in comparison to the activity observed in analogous reactions in which wild-type Fe protein (Av2) was used as the electron donor (data not shown).

By titration of increasing amounts of Fe protein with MoFe protein and measuring MoFe protein specific activities, the apparent affinity of the MoFe protein for the Fe protein can be determined. The apparent affinities of Av1(α-Asn^{161}) and Av1 for either AvCp2 (K_{AvCp2}) or the Av2 (K_{Av2}) are shown in table 4. The K_{Av2} of Av1(α-Asn^{161}) is 4 fold higher than that of Av1 representing a decrease in the apparent affinity; however, the K_{AvCp} of Av1(α-Asn^{161}) is essentially equal to that of Av1 and also equivalent to its observed K_{Av2}. These results indicate that Av1(α-Asn^{161}) has a higher apparent affinity for AvCp2 than Av2. Interestingly, the interpretation of the results of the biochemical characterization of AvCp2 is that this protein is altered in its ability to dissociate from the MoFe protein (discussed in Chapter I). This might suggest that Av1(α-Asn^{161}) is altered

Table 4. Kinetic constants for Av1-Av2, Av1-AvCp2, Av1(α-Asn^{161})-Av2, and Av1(α-Asn^{161})-Av2 dependent reactions.

MoFe protein	[a]K_{Av2}	[a]K_{AvCp2}	[b]$k_{2(Av2)}$	[b]$k_{2(AvCp2)}$
	μM	μM	s^{-1}	s^{-1}
Av1	3.7	2.5	168	180
Av1(α-Asn^{161})	15.9	4.2	23.5	25.5

[a]Apperant K_m's were determined with 0.885 μM of Av1 or Av1−α161DN. Av2 or AvCp2 concentrations varied from 0.0885 to 35.4 μM. The salt concentration was adjusted to 50 mM by addition of NaCl.
[b]Rate constants for primary electron transfer.

in component protein dissociation as well. However, other biochemical characteristics normally associated with an alteration in component protein dissociation, such as increased inhibition at high MoFe protein to Fe protein molar ratios, are not observed in Av1(α-Asn^{161})-Av2 dependent reactions (figure 16A). The inhibition of Av1(α-Asn^{161})-AvCp2 dependent specific activity at high MoFe protein to Fe protein molar ratios (figure 16A) is similar to that observed in Av1-AvCp2 dependent reactions (Peters *et al.*, 1994). The inhibition of activity at high MoFe protein to Fe protein ratios in the Av1-AvCp2 dependent reactions has been interpreted to be due to an increased significance of the back reaction involving association of the oxidized form to the Fe protein with the MoFe protein leading to inactive complex formation (Peters *et al.*, 1994; Chapter I).

One of the most striking characteristics of Av1(α-Asn^{161}) is the dramatic uncoupling of MgATP hydrolysis to electrons transferred to substrate observed in Av1(α-Asn^{161})-Av2 dependent reactions. The ratio of MgATP hydrolyzed to electrons transferred to substrate (ATP/2e$^-$) in these reactions ranges from 50 under high flux conditions to 80 under low flux conditions (figure 16B). Under these same conditions ATP/2e$^-$ of Av1-Av2 dependent reactions were approximately 5 over the entire range of flux conditions. These results suggest that a significant amount of the apparent reduction in the rate of substrate reduction occurs as a result of the inability of the Av1(α-Asn^{161})-Av2 complex to effectively couple MgATP hydrolysis to electron transfer. The ATP/2e$^-$ ratios observed in Av1(α-Asn^{161})-AvCp2 reactions were as much as 3 fold lower than that of Av1(α-Asn^{161})-Av2 reactions under certain flux conditions (figure 16B) which is consistent with the difference in the kinetic constants (table 4) and the increase in maximum activities. High ATP/2e$^-$ ratios have been reported previously to occur among nitrogenase reactions involving Fe proteins altered in initial docking (Wolle *et al.*, 1992b; Seefeldt, 1994). The increase in ATP/2e$^-$ ratios as a function of increasing MoFe protein to Fe protein molar ratio in the Av1(α-Asn^{161})-AvCp2 dependent reactions (figure 16B) has been observed previously in Av1-AvCp2 dependent reactions (Peters *et al.*, 1994). The uncoupling of MgATP hydrolysis to substrate reduction observed in the Av1-AvCp2 dependent reactions is believed to be associated with the increased significance of the

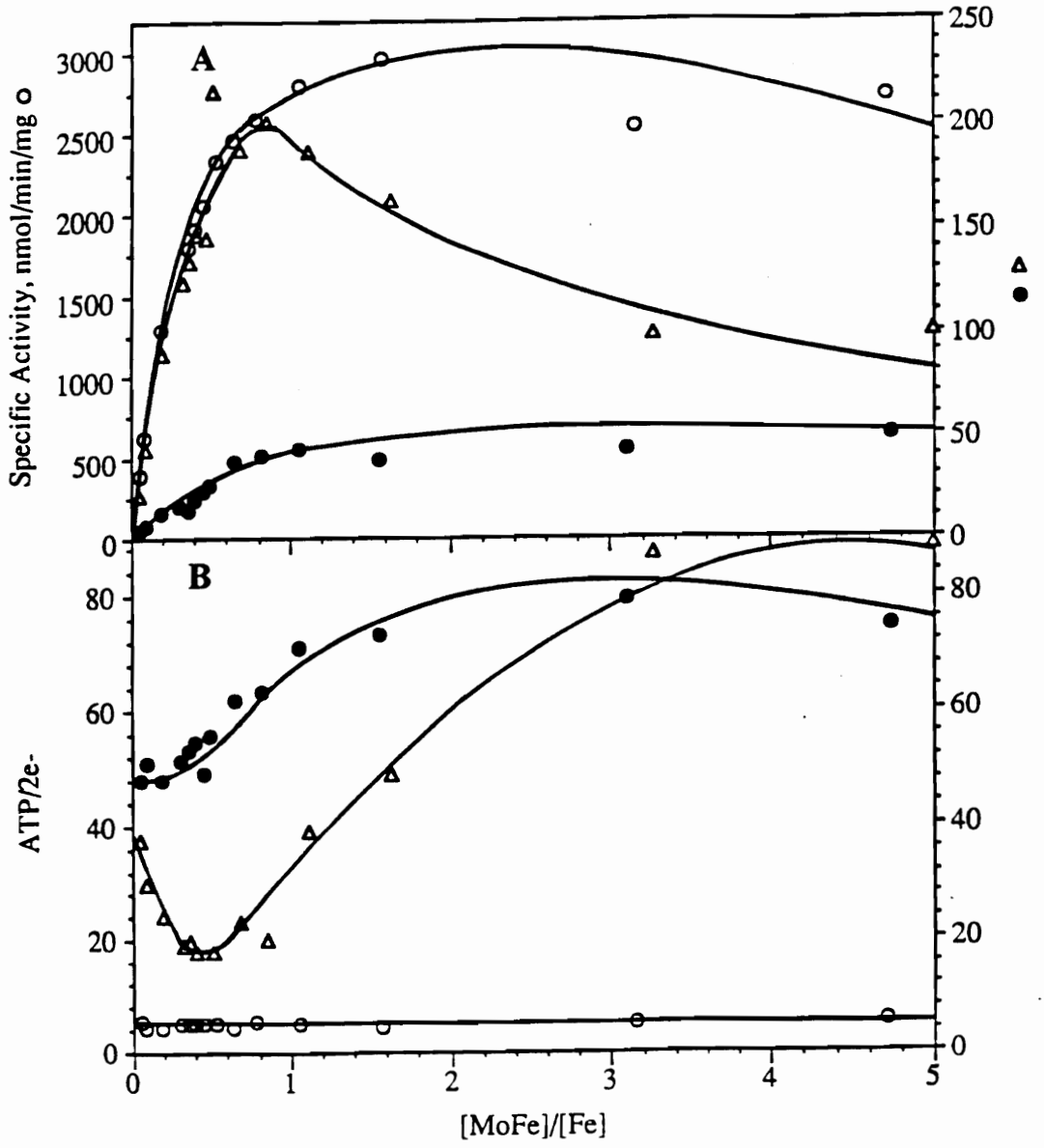

Figure 16. H_2 production and MgATP hydrolysis of nitrogenase at different component protein ratios. In this experiment, [Av2] = 1.7 μM, [AvCp2] = 1.6 μM. The salt concentration was adjusted to 50 mM by addition of NaCl. Panel A, nitrogenase catalyzed H_2 evolution. Panel B, values of ATP/2e$^-$ at different component protein ratios. The symbols for the Av1-Av2, Av1(α-Asn^{161})-Av2, and Av1(α-Asn^{161})-AvCp2 reactions are open circles, filled circles, and triangles, respectively.

back reaction involving association of oxidized Fe protein with the MoFe protein (Peters *et al.*, 1994; Chapter I). It is unclear why the ATP/2e$^-$ ratios increase at very low MoFe protein to Fe protein molar ratios in the Av1(α-Asn^{161})-AvCp2 dependent reactions (figure 16b).

Another very distinguishing characteristic among Fe proteins altered by substitution of amino acid residues involved in initial docking is the hypersensitivity to inhibition by NaCl (Wolle *et al.*, 1992b; Seefeldt, 1994). The interpretation of this hypersensitivity is that substitutions of certain residues involved in initial docking results in the elimination of dominant electrostatic interactions involved in component protein interactions (Wolle *et al.*, 1992b). The result of the elimination of the dominant reactions would render the remaining weaker interactions more sensitive to inhibition by NaCl. Figure 17, A and B, shows the effects of increasing NaCl concentration on the hydrogen evolution activities of the Av1-Av2, Av1(α-Asn^{161})-Av2, and Av1(α-Asn^{161})-AvCp2 dependent reactions under conditions of high and low electron flux. The Av1(α-Asn^{161})-Av2 dependent reactions are markedly more sensitive to NaCl inhibition than either the Av1-Av2 or the Av1(α-Asn^{161})-AvCp2 dependent reactions under either flux condition (figure 17, A and B). This result is consistent with α-Asp^{161} being involved in initial docking; however, a more detailed analysis of the NaCl sensitivity in figure 17, A and B, indicates that this is not the case. A comparison of NaCl sensitivity at high and low electron flux under all three reaction conditions indicates that Av1-Av2 and Av1(α-Asn^{161})-AvCp2 dependent reactions are sensitive to flux but the Av1(α-Asn^{161})-Av2 dependent reactions are not. The inhibition of nitrogenase catalysis by NaCl has been attributed to its ability to compete with charged residues involved in interactions of Av2 with Av1 and therefore inhibiting complex formation. By definition, competitive inhibition can be overcome to some degree by increasing the concentration of substrate, in this case Fe protein, with respect to inhibitor. In the Av1-Av2 and Av1(α-Asn^{161})-AvCp2 dependent reactions, inhibition by increasing NaCl is significantly lowered under high flux conditions (high Av2-to-Av1 molar ratio) when compared to low flux conditions (low Av2-to-Av1 molar ratio). In contrast, there is no change in the observed NaCl sensitivity

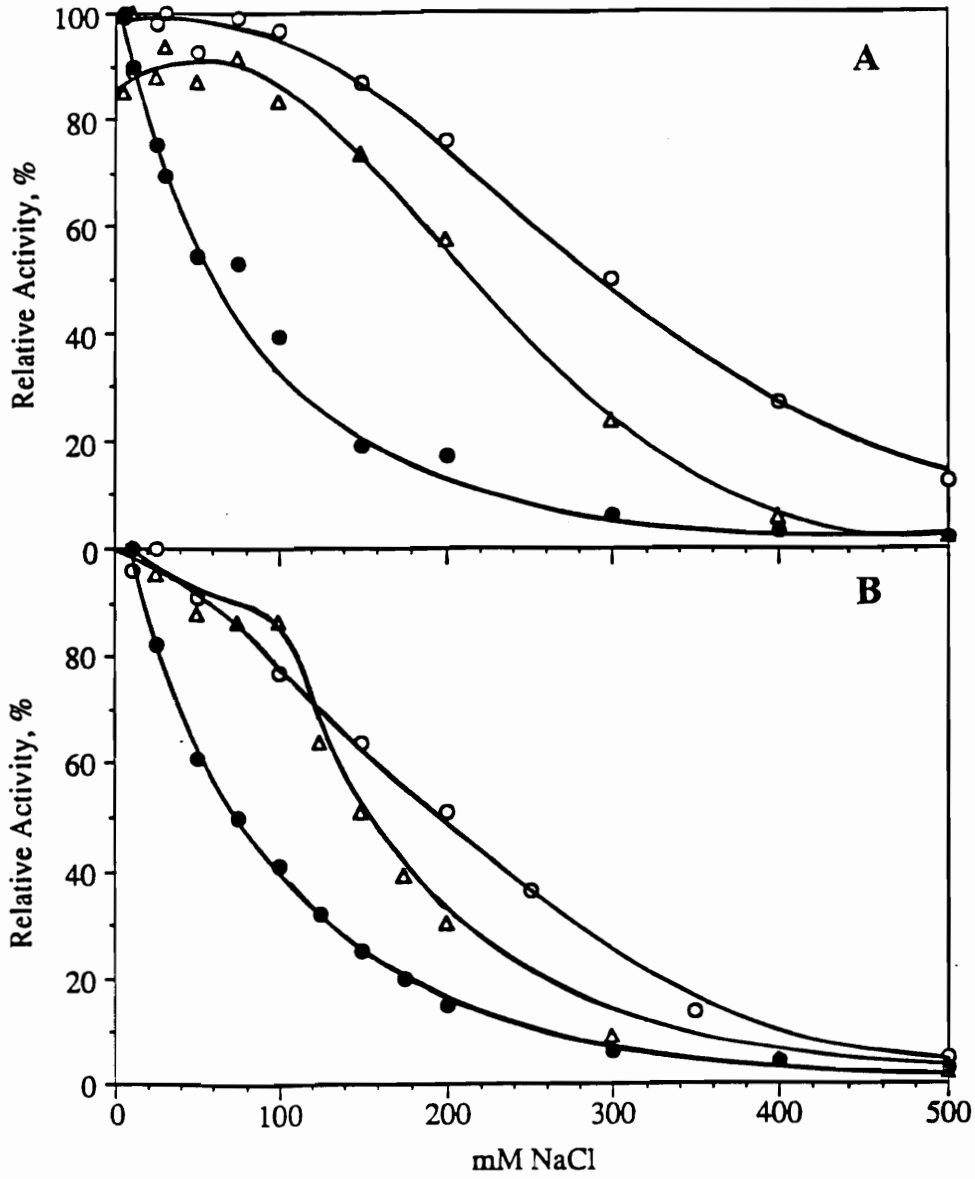

Figure 17. Effect of NaCl concentration on the native and altered nitrogenase-catalyzed H_2 formation. The data are normalized to 100 % at the highest activities. Panel A, [Av1] = 0.43 μM [Av1(α-Asn^{161})] = 0.41 μM, [Av2] = 14.4 μM, [AvCp2] = 15.1 μM. The 100 % activities of the Av1-Av2 (open circles), Av1(α-Asn^{161})-Av2 (filled circles) and Av1(α-Asn^{161})-AvCp2 (triangles) reaction were 2250, 105 and 179 nmol of H_2 formed/min/mg MoFe protein, respectively. Panel B, [Av1] = 1.45 μM, [Av1(α-Asn^{161})] = 1.51 μM, [Av2] = 2.69 μM, [AvCp2] = 2.50 μM. The 100 % activities of the Av1-Av2, Av1(α-Asn^{161})-Av2 and Av1(α-Asn^{161})-AvCp2 (symbols are the same as in A) reaction were 2030, 43.3, and 197 nmol of H_2 formed/min/mg MoFe protein, respectively.

in the Av1(α-Asn^{161})-Av2 dependent reactions in response to increasing flux. This suggests that substitution of Asp^{161} by Asn results in the elimination of a dominant electrostatic interaction involved in some process other than initial component protein docking. It is likely, therefore, that Av1(α-Asn^{161}) is altered in an electrostatic interaction that is brought about by conformational changes which may occur as a result of MgATP hydrolysis.

Stopped-flow spectrophotometry was used to measure the primary electron transfer rate, the delivery of the first electron from the Fe protein, in Av1-Av2, Av1(α-Asn^{161})-Av2, and Av1(α-Asn^{161})-AvCp2 dependent reactions. The rates for primary electron transfer (table 4) observed in the Av1(α-Asn^{161})-Av2 and Av1(α-Asn^{161})-AvCp2 dependent reactions, 23.5 s^{-1} and 25.5 s^{-1}, respectively, are significantly lower than primary electron transfer in Av1-Av2 dependent reactions (168 s^{-1}). However, the slower primary electron transfer is not rate limiting and therefore cannot account for the observed reduction in maximum activity in Av1(α-Asn^{161})-Av2 and Av1(α-Asn^{161})-AvCp2 dependent reactions, since component protein dissociation in the Av1-Av2 dependent reactions has been shown to occur more slowly (6 s^{-1}) (Thorneley and Lowe, 1983).

The amplitude of the absorbance change at 430 nm associated with Av1(α-Asn^{161})-Av2 dependent primary electron transfer is significantly less than the corresponding change observed during Av1-Av2 dependent primary electron transfer (figure 18). This indicates that there are fewer primary electron transfer events occurring from Av2 to Av1(α-Asn^{161}) compared to the analogous electron transfer from Av2 to Av1 before reaching the steady-state. Increasing the amount of Fe protein present did not result in an increase in the amplitude of this electron transfer reaction (data not shown). The amplitude of the absorbance change during Av1(α-Asn^{161})-AvCp2 primary electron transfer is significantly higher than that of Av1(α-Asn^{161})-Av2; however, in both cases as the steady-state is approached the absorbance decreases dramatically to almost its initial value. A similar absorbance decrease has been observed in stopped-flow experiments involving an altered MoFe protein from *Klebsiella pneumoniae* with β-Phe^{124} substituted by Ile (Thorneley *et al.*, 1993). The analogous residue in *A. vinelandii* (β-Phe^{125}) is

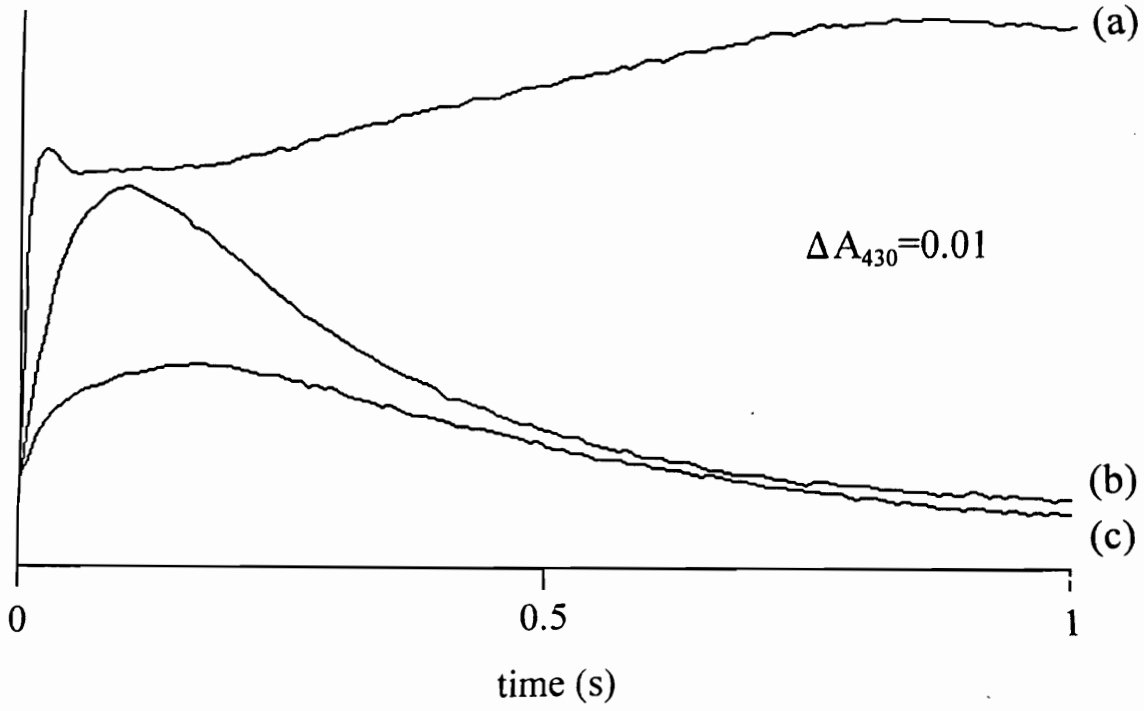

Figure 18. MgATP dependent electron transfer from the Fe protein to the MoFe protein and ensuing absorbance changes as the steady-state is attained. The traces were obtained by stopped-flow spectrophotometry at 430 nm when pre-equilibrated nitrogenase component proteins (20 μM Av1 or Av1(α-Asp^{161}) and 120 μM Av2 or AvCp2) were mixed with MgATP (18 mM) in 25 mM Hepes buffer, pH 7.4. Both syringes contained 10 mM $Na_2S_2O_4$. The trace in (a) shows a typical wild-type Av2 oxidation with an amplitude (ΔA) of 0.108 and a rate of primary electron transfer (k_2) of 165 s^{-1}. Traces (b) k_2=25 s^{-1}, ΔA=0.059 and (c) k_2=23 s^{-1}, ΔA=0.02 show the electron transfer from AvCp2 and Av2 to Av1(α-Asp^{161}) respectively.

located at the proposed docking interface (figure 5). The interpretation of the absorbance decrease in experiments involving Kp1(β-Phe^{124}) was that in the steady state a higher percentage of Av2 is in the reduced state. In the case of Av1(α-Asn^{161})-Av2 dependent reactions the high percentage of reduced Av2 in the steady state together with the observed uncoupling of MgATP hydrolysis to electron transfer suggests that in the Av1(α-Asn^{161})-Av2 complex, MgATP hydrolysis can only very infrequently induce the conformational changes necessary to effect electron transfer from the Fe protein to the MoFe protein.

In summary, we have probed component protein interaction by substituting charged residues at the proposed Fe protein-MoFe protein docking interface (Howard, 1993; Kim and Rees, 1992b). The charged amino acid side chains of α-Asp^{162}, β-Asp^{160}, and β-Asp^{161} were not important for nitrogenase catalysis and thus are unlikely to be involved in electrostatic interactions associated with component protein interaction. However, elimination of charge at α-Asp^{161} by its substitution by Asn resulting in an altered MoFe protein the could only support 3 to 5 percent of the wild-type MoFe protein activity. The results of NaCl sensitivity studies involving purified Av1-α-Asn^{161} indicate that a dominant electrostatic interaction which might arise as a result of conformational changes within the complex has been eliminated. Results of stopped-flow spectrophotometry suggest that MgATP hydrolysis is inefficient in bringing about conformational changes that facilitate electron transfer from the Fe protein to the MoFe protein. The ability of AvCp2 to complement to some degree the effects observed in Av1-(α-Asn^{161}) may suggest that electron transfer normally occurs in the conformational state of the component protein complex in which dissociation occurs (dissociative state). This is possible because the observed rate of wild-type component protein dissociation (6 s^{-1}) is 30 times slower than the primary electron transfer rate (200 s^{-1}) (Thorneley *et al.*, 1993). AvCp2 has been suggested to have a higher affinity for Av1 in the dissociative state than does Av2. This higher affinity could drive the conformational changes to the dissociative state, thereby accounting for the increase in productive electron transfer coupled to MgATP hydrolysis.

Together the results described in this study suggest an overall mechanism for electron transfer from the Fe protein to the MoFe protein in which conformational changes induced by MgATP hydrolysis on the Fe protein are transduced to the MoFe protein in order to facilitate electron transfer. Such conformational changes within the MoFe protein may be required to structurally alter the P cluster so it may act as an electron acceptor (Rees *et al.*, 1993a; Howard and Rees, 1994). Additional mutagenesis studies designed to dissect the pathway of conformational changes within the MoFe induced by MgATP hydrolysis will undoubtedly provide insight into their contribution to intermolecular electron transfer.

CHAPTER III.

Intramolecular electron transfer within the nitrogenase MoFe protein: Role of the β-subunit tyrosine-98 residue

This chapter represent a manuscript in preparation that will be authored by myself, Karl Fisher, William E. Newton, and Dennis R. Dean. Karl Fisher performed all pre-steady-state stopped-flow experiments. EPR spectroscopy was performed by Richard Dunham (University of Michigan) and MCD spectroscopy was performed by Micheal K. Johnson (University of Georgia). Limin Zheng and Jaccobus Flipson were involved in strain construction.

Summary

Nitrogenase is the catalytic component of biological nitrogen fixation and it is comprised of two component proteins called the Fe protein and MoFe protein. The Fe protein contains a single Fe_4S_4 cluster and the MoFe protein contains two metallocluster types called the P cluster and FeMo-cofactor. During turnover a metallocluster-to-metallocluster-to-substrate flow of electrons occurs where electrons are delivered one at a time from the Fe protein to the MoFe protein in a reaction coupled to component protein association-dissociation and MgATP hydrolysis. Under conditions of optimum activity the rate of component protein dissociation is rate limiting. The Fe protein's Fe_4S_4 cluster is the redox entity responsible for intermolecular electron delivery to the MoFe protein and FeMo-cofactor provides the substrate reduction site. In contrast, the role of the P cluster in catalysis is not well understood although it is believed to be involved in accumulating electrons delivered from the Fe protein and brokering their intramolecular delivery to the substrate reduction site. A nitrogenase component protein docking model, based on the crystallographic structures of the component proteins, and which pairs the two-fold symmetric surface of the Fe protein with the exposed surface of the MoFe protein's pseudo-symmetric αβ interface is now available. In this model the P

cluster is placed between the Fe protein's Fe_4S_4 cluster and FeMo-cofactor during component protein interaction, an arrangement consistent with the possibility that the P cluster is involved in mediating intramolecular electron transfer. In the present study evidence supporting the idea that the P cluster has such a role in catalysis was obtained by demonstrating it is possible to alter intramolecular electron transfer between the P cluster and FeMo-cofactor without necessarily compromising the biophysical features of the individual metalloclusters. These experiments were guided by the available crystallographic model for the MoFe protein and the experimental rationale involved substituting the β-subunit tyrosine-98 residue (β-Tyr^{98}) by phenylalanine, leucine, and histidine. The β-Tyr^{98} residue was chosen for substitution because this residue is located on a helix which spans the P cluster and FeMo-cofactor and its side-chain is situated directly between the two cluster types. In control experiments, the α-Tyr^{91} residue was also substituted by phenylalanine, leucine, and histidine. The α-Tyr^{91} residue is the pseudo-symmetric homolog of the β-Tyr^{98} residue, and it is also located on a helix which spans the P cluster and FeMo-cofactor, but its side chain is directed away from rather than between the two cluster types. The isolated MoFe protein which has the β-subunit tyrosine-98 residue substituted by histidine (β-His^{98} MoFe protein) exhibited the following features when compared to the wild-type MoFe protein: (i) the magnetic circular dichroism and electron paramagnetic resonance spectroscopic features of the β-His^{98} MoFe protein were identical to the wild-type MoFe protein, (ii) a lower level of Fe protein was required to achieve maximum specific activity in the reaction catalyzed by the β-His^{98} MoFe protein which is approximately 50% the maximum activity exhibited by the wild-type MoFe protein, (iii) MgATP hydrolysis became partially uncoupled from substrate reduction in the reaction catalyzed by the β-His^{98} MoFe protein, (iv) the rates of primary and secondary intermolecular electron transfer from the Fe protein to the β-His^{98} MoFe protein were identical to the wild-type MoFe protein, (v) in pre-steady state experiments the rate of Fe protein turnover (i.e. apparent rate of component protein dissociation) in the reaction catalyzed by the β-His^{98} MoFe protein was the same as the wild-type MoFe protein for the first 300 milliseconds but after this brief initial period the

Fe protein turnover rate was slowed approximately two-fold. These results are explained by a model where the steady state activity of the β-His^{98} MoFe protein is limited by the rate of intramolecular electron transfer between the P cluster and FeMo-cofactor rather than by an alteration in either the nature of component protein interaction or in the biophysical properties of the metalloclusters. Also, the biphasic nature of the turnover rate measured in the pre-steady state analysis of the β-His^{98} MoFe protein indicates that at least two electrons may be accumulated by the P cluster, a result consistent with the possible role of the P cluster as an electron storage unit.

Introduction

The MgATP-dependent reduction of nitrogen gas to yield ammonia is called biological nitrogen fixation. A minimal stoichiometry for the reaction is usually indicated as:

$$N_2 + 8e^- + 8H^+ + 16MgATP \rightarrow 2NH_3 + H_2 + 16MgADP + 16\ Pi.$$

The reaction is catalyzed by nitrogenase which is comprised of two component proteins called the Fe protein, a homodimer, and the MoFe protein, an $\alpha_2\beta_2$ heterotetramer (reviewed by Dean *et al.*, 1993; Howard and Rees, 1994; Kim and Rees, 1994; see figure 1a and b for structural models). Turnover requires the sequential delivery of single electrons from the Fe protein to the MoFe protein and involves the association and dissociation of the protein partners in a process where MgATP hydrolysis is coupled to electron transfer. One independent substrate reduction site is located within each MoFe protein αβ-unit. Three different metal clusters are believed to be involved in electron transfer and substrate reduction. These include an Fe_4S_4 cluster that is bridged between the identical subunits of the Fe protein and two pairs of unusual metal clusters, called the P cluster and FeMo-cofactor, both of which are contained within the MoFe protein. There is one P cluster and one FeMo-cofactor within each MoFe protein αβ-unit. Each

P cluster is comprised of two Fe_4S_4 subcluster fragments linked by a corner-to-corner disulfide bond and is bridged between the α- and β-subunits of the MoFe protein at a region exhibiting pseudo-two-fold symmetry between the two subunits. The P cluster is coordinated to the protein by residues α-Cys^{62}, α-Cys^{88}, α-Cys^{154}, β-Cys^{70}, β-Cys^{95}, β-Cys^{153} and β-Ser^{188} (numbers refer to the primary sequences of the component proteins from *Azotobacter vinelandii*). A novel feature of the P cluster is that two of the coordinating cysteines, α-Cys^{88} and β-Cys^{95}, connect the Fe_4S_4 subcluster fragments by each binding two Fe atoms, one from each subcluster. FeMo-cofactor contains a metal-sulfide core (Fe_7S_9Mo) and one molecule of (R)-homocitrate. The metal-sulfide core is constructed from two partial cubes, one each of $MoFe_3S_3$ and Fe_4S_3 subcluster fragments, joined by a ring of three sulfide bridges connecting pairs of opposing Fe atoms. FeMo-cofactor is contained entirely within the α-subunit and is covalently attached to the protein through a thiolate ligand provided by α-Cys^{275} to an Fe atom at one end of the molecule and by the side-chain nitrogen atom of α-His^{442} to the Mo atom at the opposite end.

There is compelling evidence that the Fe protein's Fe_4S_4 cluster is the obligate electron donor to the MoFe protein and that it cycles between the 1^+ and 2^+ redox state during the sequential single electron deliveries which occur during turnover (Smith and Lang, 1974; Stephens, 1985; Lindahl *et al.*, 1985). It is also well established that FeMo-cofactor provides the substrate reduction site (Shah and Brill, 1977; Hawkes *et al.*, 1984; Scott *et al.*, 1990; Scott *et al.*, 1992; Kim *et al.*, 1995). In contrast, the specific role of the P cluster in catalysis is much less certain, but it is believed to be involved in accumulating electrons delivered from the Fe protein and brokering their intramolecular delivery to the substrate reduction site. Thus, questions attached to the potential role of the P cluster include: (i) is the P cluster involved in mediating the delivery of electrons from the Fe protein's Fe_4S_4 cluster to the FeMo-cofactor; (ii) if so, how many electrons are accumulated by the P cluster prior to their delivery to the substrate reduction site; and (iii) what is the path for intramolecular electron delivery between the P cluster and FeMo-cofactor?

The availability of a structural model for the MoFe protein (Kim and Rees, 1992b) now permits the design of biochemical–genetic experiments aimed at deciphering the intramolecular electron pathway and the role of the P cluster in that process. Namely, residues located within potential intramolecular electron transfer pathways can be identified and targeted for amino acid substitution and the consequences of such substitutions can be determined by characterizing the biochemical and kinetic features of the altered proteins. Kim and Rees have previously recognized four helices that are oriented in parallel and located between the P cluster and FeMo–cofactor that could participate in electron transfer between the two clusters (Kim and Rees, 1992b). The β–Tyr^{98} residue is located on one of these helices and is situated in a direct line between the two clusters (figure 19). This residue is also included among a group of hydrophobic residues which provide the non–contacted polypeptide environment of the P cluster. Furthermore, β–Tyr^{98} approaches the terminal carboxyl of the homocitrate moiety of FeMo–cofactor and may indirectly interact with it by hydrogen bonding through water. The analogous residue within the α–subunit, α–Tyr^{91}, is also found on a helix located between the clusters but its side–chain is directed away rather than towards the FeMo–cofactor (figure 19). As an approach to assess the potential role of the P cluster and β–Tyr^{98} in intramolecular electron transfer this residue was substituted by Phe, Leu and His and the catalytic, kinetic, and spectroscopic properties of the altered MoFe proteins were examined. In control experiments, the α–Tyr^{91} residue was also substituted by Phe, Leu, and His and the catalytic and kinetic properties of the altered α–His^{91} MoFe protein were examined as well.

Experimental Procedures

Methods for site–directed mutagenesis, gene replacement, and the isolation of mutant strains were performed as described or cited previously (Brigle *et al.*, 1987a; Jacobson *et al.*, 1989b). Oligonucleotides used for mutagenesis, hybrid plasmids used for strain constructions, and strain designations are shown in table 5. For site–directed

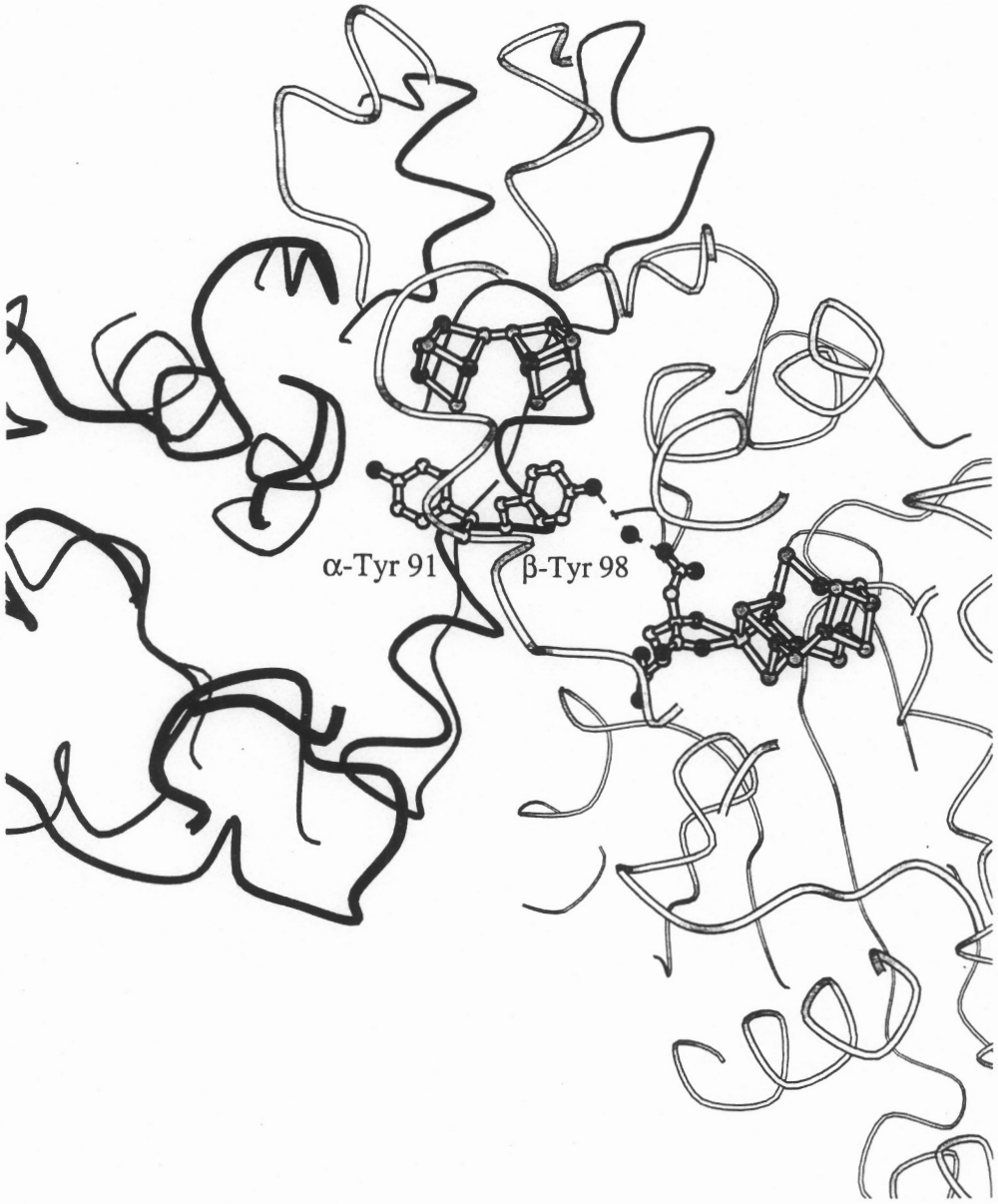

Figure 19. Cut away α-carbon trace of the MoFe protein showing the location of α-subunit 91 and β-subunit 98 tyrosine residues relative to the P cluster and iron-molybdenum cofactor. The MoFe protein α-carbon traces of the α and β-subunits are represented as open coil and filled coils, respectively. The P cluster, iron-molybdenum cofactor and the amino acid side chains of α-Tyr ^{91} and β-Tyr^{98} are represented as ball and stick models. A dashed line represents hydrogen bonding of β-Tyr^{98} to a terminal carboxyl of the homocitrate moiety of the iron-molybdenum cofactor through water.

Table 5. Construction and diazotrophic growth of *Azotobacter vinelandii* mutant strains

Strain	Oligonucleotide	Plasmid	Substitution	Doubling Time (Hr)
Wild-Type	-	-	None	3.0
DJ1038	TGCGGCCAGCACTCGCGCGCCG	pDB880	α-His^{91}	3.5
DJ931	TGCGGCCAGCTGTCGCGCGCCG	pDB814	α-Leu^{91}	3.5
DJ933	TGCGGCCAGTTCTCGCGCGCCG	pDB809	α-Phe^{91}	3.5
DJ939	TGCGTCGCCCACTTCCGCT	pDB797	β-His^{98}	6.0
DJ1028	TGCGTCGCCCTGTTCCGCTCCT	pDB860	β-Leu^{98}	4.0
DJ982	GCGTCGCCTTCTTCCGCTC	pDB796	β-Phe^{98}	4.0

mutagenesis of the *A. vinelandii nifD* gene, encoding the MoFe protein α−subunit (Brigle *et al.*, 1985), an approximately 1.4 kb DNA fragment containing the *nifD* gene was cloned into *Eco*RI digested pUC119 (Viera & Messing, 1987). This plasmid was designated pDB697 and is the one from which plasmids pDB880, pDB809, pDB814 were derived (table 5). For site-directed mutagenesis of the *nifK* gene (Brigle *et al.*, 1985), encoding the MoFe protein β−subunit, an approximately 1 kb *Hind*III−*Kpn*I DNA fragment containing the 5' half of the *A. vinelandii nifK* gene was cloned into *Hind*III−*Kpn*I−digested pUC118 (Vieira & Messing, 1987). This plasmid was designated pDB698 and is the one from which plasmids pDB796, pDB797, and pDB860 were derived (table 5).

Wild-type and mutant strains of *A. vinelandii* were cultured at 30° C in a modified, liquid Burk media (Strandberg and Wilson, 1968). Nitrogenase was purified and assayed according to the methods described by Burgess *et al.* (1980) with the modifications described by Peters *et al.* (1994) and references cited therein. Purity of protein samples (figure 20) was determined by denaturing gel electrophoresis using modifications of the procedure described by Laemmli (1970) as discussed by Scott *et al.* (1992). Flavodoxin (FldII) used in stopped−flow spectrophotometric experiments was isolated from *A. vinelandii* cells as described by Klugkist *et al* (1986). The Mo content of the isolated wild-type and β−His^{98} MoFe protein was determined to be 1.9 ± 0.1 and 1.8 ± 0.1 g atom Mo per mol by inductively coupled plasma atomic emission spectrometry using a simultaneous spectrometer (Jarrell-Ash ICAP 9000) and a sequential scanning spectrometer (Jarrell-Ash Atomscan 2400). Acetylene Km values for both the wild−type and the β−His^{98} MoFe proteins were obtained from Lineweaver−Burk plots as described by Kim *et al.* (1995). Maximum specific activities shown in table 6 as well as kinetic experiments were performed with saturating levels of Fe protein (at least a 40:1 Fe protein to MoFe protein molar ratio). Except for stopped−flow experiments described below all nitrogenase assays contained a total of 0.5 mg of the nitrogenase component proteins in a final assay volume of 1 ml. Protein concentrations were determined by the method of Lowry *et al.* (1951). Experimental results were reproducible and all data shown are

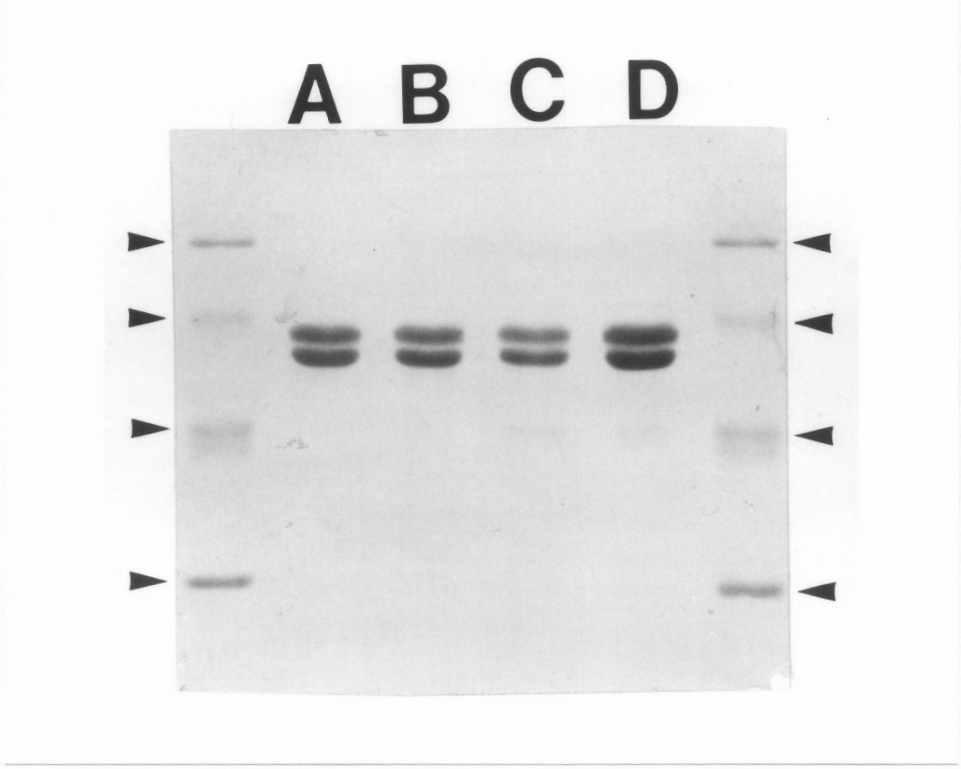

Figure 20. Coomassie-blue stained SDS-PAGE (12%) of approximately 10 μg of purified MoFe proteins (lanes A-D): wild-type - β-Tyr^{98}(lane A), β-His^{98} (lane B), β-Leu^{98} (lane C), β-Phe^{98} (lane D). Molecular weight standards include, (phosphorylase b, 97,400; bovine serum albumin, 66,200; ovalbumin, 42,699; and carbonic anhydrase, 31,000).

representative of at least three separate experiments.

Stopped-flow spectrophotometric techniques used to measure the rates of primary and secondary electron transfer from the Fe protein to the MoFe protein and the rate of dissociation of the Fe protein-MoFe protein ternary complex have been pioneered by Lowe, Thorneley and colleagues. Primary electron transfer refers to the transfer of a single electron from Fe protein in the 1^+ redox state to the semi-reduced as-isolated MoFe protein, whereas, secondary electron transfer refers the transfer of a second electron to the one-electron reduced MoFe protein. Methods used to determine the rates of primary and secondary electron transfer are described in detail in the original publications (Thorneley, 1975; Fisher *et al.*, 1991), however, the underlying principle involved is that oxidation of Fe protein's Fe_4S_4 cluster results in an increased absorbance at 430 nm which may be monitored by visible spectroscopy. Stopped-flow spectrophotometry was performed using a commercially available SF-61 instrument equipped with a kinetic data acquisition analysis and curve fitting system (Hi-Tech, Salisbury, Wilts., UK). The SHU-61 sample handling unit was installed inside an anaerobic chamber operating at less than 1 ppm O_2. Sample flow components were thermostatted by closed circulation of water by a Techne C-85D circulator (Techne Ltd, Duxford, Cambridge, UK) attached to a FC-200 Techne flow cooler situated outside the anaerobic chamber. All stopped-flow reactions were studied at 23° C in 25 mM Hepes buffer, pH 7.4 containing 10 mM $MgCl_2$ and 50 mM NaCl. For primary electron transfer determinations syringe A contained 10 μM MoFe protein, 40 μM Fe protein and 10 mM $Na_2S_2O_4$ and syringe B contained 20 mM MgATP and 10 mM $Na_2S_2O_4$. For determination of the rate of secondary electron transfer (Fisher *et al.*, 1991), conditions of low electron flux were initiated by the addition of 18 mM MgATP, 18 mM creatine phosphate, and 60 μg creatine phosphokinase to a mixture of 40 μM MoFe protein 0.4 μM Fe protein in a stopped-flow drive syringe via a mixing block as described by Fisher *et al.* (1991). The second drive syringe contained 80 μM Fe protein. The first stopped-flow trace was recorded after the premixing procedure and successive stopped-flow traces were obtained at time intervals up to 60 min.

The rate of Fe protein turnover was also measured by stopped-flow

spectrophotometry but in a different way. In these experiments the physiological electron donor to the Fe protein, flavodoxin (product of the *nifF* gene), was used as reductant rather than the artificial reductant, $Na_2S_2O_4$, used in routine assays. Reduction of oxidized Fe protein by the hydroquinone form of flavodoxin to yield the semiquinone form is accompanied by an increase in absorbance at 580 nm. Thus, under turnover conditions, the reduced hydroquinone form of flavodoxin is oxidized to the semiquinone form as it rapidly transfers its electron to the oxidized Fe protein upon its dissociation from the MoFe protein. In this way the consumption of reducing equivalents which occurs during Fe protein turnover can be continuously monitored by following the increased absorbance at 580 nm. Under normal conditions the Fe protein turnover rate estimated by the rate of oxidation of flavodoxin provides an indirect measure of the rate of component protein dissociation because that is the rate limiting step in catalysis (Thorneley and Lowe, 1983). In the analysis of the altered β-His^{98} MoFe protein, however, where the Fe protein turnover rate might ultimately be limited by intramolecular electron transfer, the observed change in optical density was used to calculate an "apparent" dissociation rate because the component protein dissociation rate was not measured directly. For these experiments flavodoxin, the known electron donor to the Fe protein, was reduced to the hydroquinone state by using an excess of $Na_2S_2O_4$ at pH 8 in an anaerobic chamber. After incubation for approximately 15 minutes to ensure complete reduction, unreacted dithionite and its reduction products were removed on a gel filtration column (0.5 x 5 cm) packed with P-6DG (Biorad, Melville, NY) and pre-equilibrated with anaerobic 25 mM Hepes pH 7.4, 10 mM $MgCl_2$. The same procedure was employed to remove dithionite from nitrogenase proteins used in these experiments, with the addition that the MoFe protein elution buffer contained 150 mM NaCl to avoid tailing on the resin.

Samples for electron paramagnetic resonance (EPR) spectroscopy of wild-type and altered MoFe proteins were exchanged into 25 mM Tris-HCl pH 7.4, 100 mM NaCl, and 5 mM $Na_2S_2O_4$ using Biogel P-6DG gel-filtration resin (Biorad, Melville, NY). The purified protein samples were concentrated to at least 10 mg/ml and packed in EPR tubes in an anaerobic chamber. EPR spectra were recorded at 9.22 GHz and 20 mW on a

Varian Associates E-line spectrometer with a modulation amplitude of 2.5 mT at 100 kHz. The temperature was maintained at 12 K by liquid helium boil-off. The setup and procedure for performing magnetic circular dichroism (MCD) spectrophotometry performed as previously described by Johnson (1988).

Results and Discussion

Structural, kinetic and biochemical evidence that the P cluster is the primary acceptor of electrons from the Fe protein and that the P cluster subsequently brokers the intramolecular delivery of electrons to the FeMo-cofactor can be considered in the context of the proposed structural models for the nitrogenase component proteins from *A. vinelandii* (Georgiadis *et al.*, 1992; Kim and Rees, 1992b). A docking model based on the structures of the individual component proteins (Kim and Rees, 1992b; Howard, 1993) and which takes into account amino acid substitution studies (Wolle *et al.*, 1992b) and chemical cross-linking experiments has been proposed (Willing *et al.*, 1989; Willing and Howard, 1990). This model (see figure 1a and b) pairs the 2-fold symmetric surface of the Fe protein homodimer with the exposed surface of a MoFe protein pseudo-symmetric $\alpha\beta$-unit interface (figure 1a and b). In this arrangement the Fe protein's Fe_4S_4 cluster is positioned in the closest possible proximity to the MoFe protein's P cluster and, during the docking event, places the P cluster between the Fe protein's Fe_4S_4 cluster and FeMo-cofactor. Evidence supporting the docking model has come from biochemical and kinetic analyses of altered component proteins having one or more amino acid substitutions located within the respective docking sites (Wolle *et al.*, 1992b, Kim *et al.*, 1993a; Thorneley *et al.*, 1993; Peters *et al.*, 1994; Seefeldt, 1994). For example, substitution of the *Klebsiella pneumoniae* MoFe protein β-Phe^{124} residue by β-Ile^{124} results in an approximately 70% reduction in the rate of primary electron transfer. Protease susceptibility studies have revealed that β-Phe^{124} is located at the exposed surface (Fisher *et al.*, 1993) and the structural model places the analogous residue from *A. vinelandii*, β-Phe^{125}, at the $\alpha\beta$-pseudo-symmetric interface within the proposed docking

site and near the mouth of a channel leading directly to the P-cluster (figure 5). Inspection of the Fe protein structural model also reveals a crown of positively charged residues, Arg^{100}, Arg^{140}, and Lys^{143}, that are located within the proposed docking interface, and which surround the Fe protein's Fe_4S_4 cluster. Altered Fe proteins having Arg^{100} substituted by His^{100} (Wolle *et al.*, 1992b), Lys^{140} substituted by Gln^{140} or Lys^{143} substituted by Gln^{143} (Seefeldt, 1994), all share similar biochemical phenotypes exhibiting various levels of increased inhibition of catalytic activity by salt and various levels of uncoupling of MgATP hydrolysis from substrate reduction. These results have been interpreted to indicate that such substitutions disrupt reciprocal ionic interactions that are involved in bringing the Fe protein's Fe_4S_4 cluster and a site on the MoFe protein, presumably the P cluster, in the proper juxtaposition to accomplish effective primary electron transfer (Wolle *et al.*, 1992b). One of the complementary ionic interaction sites located on the MoFe protein might be provided by residue α-Asp^{161} because substitution of this residue by α-Asn^{161} also results in salt sensitivity and MgATP hydrolysis that is uncoupled from electron transfer (Kim *et al.*, 1993a, discussed in Chapter II). The α-Asp^{161} residue is also located at the $\alpha\beta$-pseudo-symmetric interface within the proposed docking site and is connected to the P cluster coordinating residue α-Cys^{154} through a short helix (figure 5). Finally, a series of substitutions located within a region of the Fe protein, which, according to the docking model, is proposed to interact with the MoFe protein (Howard, 1993), leads to a slower rate of Fe protein-MoFe protein complex dissociation (Peters *et al.*, 1994; see Chapter I).

There is also biochemical-genetic evidence that the P cluster is involved in the intramolecular transfer of electrons to the substrate reduction site. Evidence for this role was provided by assaying an altered MoFe protein, for which the P cluster coordinating residue β-Cys^{153} was substituted by β-Ser^{153}, under conditions of both high flux and low flux (May *et al.*, 1991). The electron flux through nitrogenase can be controlled by manipulating the Fe protein-MoFe protein molar ratio in enzyme assays (Hageman and Burris, 1980; Wherland *et al.*, 1981). At high Fe protein to MoFe protein molar ratios the flux through nitrogenase is greatest and specific activity is maximized and is limited by the

rate of complex dissociation (Thorneley and Lowe, 1983). In contrast, a low Fe protein to MoFe protein molar ratio results in a condition of low flux and the specific activity is relatively lower because catalysis becomes limited by the availability of Fe protein that can participate in the delivery of electrons to the MoFe protein. The altered β−Ser^{153} MoFe protein was found to exhibit approximately the same specific activity as the unaltered β−Cys^{153} MoFe protein under conditions of low flux but only about 50% of the normal activity when assayed under conditions of high flux. The interpretation offered for these results was that, under conditions of high flux, the reaction catalyzed by the altered β−Ser^{153} protein is limited by intramolecular electron transfer between the P cluster and the substrate reduction site owing to a rearrangement in the P cluster polypeptide environment (May *et al.*, 1991). Evidence supporting this view has been obtained by magnetic circular dichroism spectrophotometric analysis of the altered β−Ser^{153} MoFe protein which reveals substantial changes in the magnetic properties of its P cluster (K. Fisher, D. Dean, W. Newton, M. Johnson, unpublished data).

In the present work the possibility that β−Tyr^{98} is involved in intramolecular electron transfer was investigated because this residue is located on a helix which spans the P cluster and FeMo−cofactor, yet, does not directly contact either the P cluster or FeMo−cofactor (figure 19). Thus, the primary objective was to determine whether or not it is possible to alter intramolecular electron transfer between these cluster types without disrupting either of their respective polypeptide environments. Three different amino acid residues, Phe, Leu, and His, were substituted for the β−Tyr^{98} residue (table 5). The rationale for choosing these substituting amino acids was as follows: (i) substitution by β−Phe^{98} was designed to determine whether or not the hydroxyl group of β−Tyr^{98}, which apparently interacts with the homocitrate moiety of FeMo−cofactor through water, is necessary for intramolecular electron transfer; (ii) substitution by β−Leu^{98} was designed to determine whether or not an aromatic group is required for intramolecular electron transfer; and (iii) substitution by β−His^{98} was designed to determine if a charged group at this position would affect intramolecular electron transfer. In another set of experiments the α−subunit residue analogous to the β−Tyr^{98} residue, α−Tyr^{91}, was also substituted by

α-Phe^{91}, α-Leu^{91}, and α-His^{91} (table 5). These latter experiments were intended to serve as a control because the side chain of the α-Tyr^{91} residue is directed away rather than towards the FeMo-cofactor (figure 19) and substitutions at this position were, therefore, considered less likely to have an effect on intramolecular electron transfer.

Mutant strains which produce altered MoFe proteins having substitutions at the α-Tyr^{91} position exhibit only a small increase in diazotrophic doubling time (table 5). Also, the isolated α-His^{91} MoFe protein exhibited kinetic and catalytic properties nearly identical to the wild-type MoFe protein confirming that this substitution does not have a discernible effect on intramolecular electron transfer (data not shown). Similarly, the diazotrophic doubling time of mutant strains which produce the altered β-Phe^{98} and the β-Leu^{98} MoFe proteins were comparable to the wild-type (table 5) and the altered MoFe proteins exhibit catalytic activities only moderately lower than the wild-type MoFe protein (table 6). A lower level in all substrate reduction properties was observed for the β-Leu^{98} MoFe protein, but even the lowest level was still approximately 70% that of the wild-type. The simple interpretation of these results is that neither the hydroxyl group nor the aromatic feature of the β-Tyr^{98} residue is critical for productive intramolecular electron transfer. It should be noted, however, that intramolecular electron transfer rates measured for certain other proteins (reviewed by Farid *et al.*, 1993) are orders of magnitude faster than reported for nitrogenase component protein dissociation (Thorneley and Lowe, 1983), the rate limiting step in nitrogenase catalysis. Consequently, a dramatic decrease in the rate of intramolecular electron transfer might be necessary in order for this process to become rate limiting and, thus, in the absence of an ability to directly measure the rate of intramolecular electron transfer within the MoFe protein, it is premature to conclude that neither the hydroxyl group nor the aromatic nature of the β-Tyr^{98} residue have no involvement in intramolecular electron transfer.

In contrast to mutant strains which produce the α-Phe^{91}, α-Leu^{91}, α-His^{91}, β-Phe^{98} and β-Leu^{98} MoFe proteins, the mutant which produces the β-His^{98} MoFe protein shows a more significant increase in its diazotrophic doubling time and a corresponding decrease in the maximum specific activity of its altered MoFe protein (table

Table 6. Maximum activities and MgATP hydrolysis of altered MoFe proteins with amino acid substitutions at β-Tyr^{98} of the MoFe protein.

MoFe protein	Addition	Product	[a]Atmosphere: 10% C_2H_2, 90%Argon	[a]Atmosphere: 100% Argon	[a]Atmosphere: 100% N_2
wild-type (β-Tyr^{98})	None	H_2	290	2331	566
		C_2H_4	2196	0	0
		NH_3	0	0	930
		[b]Total 2e$^-$	2486	2331	1961
		[d]ATP/2e$^-$	5.5	5.4	5.4
	[c]CO	H_2	2460	2442	1930
		C_2H_4	0	0	0
		NH_3	0	0	0
		Total 2e$^-$	2460	2442	1930
		ATP/2e$^-$	5.6	5.3	5.1
β-Phe^{98}	None	H_2	207	2245	650
		C_2H_4	2374	0	0
		NH_3	0	0	722
		Total 2e$^-$	2581	2245	1733
		ATP/2e$^-$	5.2	6.2	4.6
	CO	H_2	2544	2260	2105
		C_2H_4	0	0	0
		NH_3	0	0	0
		Total 2e$^-$	2544	2260	2105
		ATP/2e$^-$	5.0	5.7	4.8
β-Leu^{98}	None	H_2	126	1775	415
		C_2H_4	1483	0	0
		NH_3	0	0	844
		Total 2e$^-$	1609	1775	1680
		ATP/2e$^-$	5.5	6.0	6.1
	CO	H_2	1917	2067	1670
		C_2H_4	0	0	0
		NH_3	0	0	0
		Total 2e$^-$	1917	2067	1670
		ATP/2e$^-$	5.2	5.9	5.4
β-His^{98}	None	H_2	61	1142	362
		C_2H_4	703	0	0
		NH_3	0	0	456
		Total 2e$^-$	764	1142	1046
		ATP/2e$^-$	11.3	8.1	7.8
	CO	H_2	1335	1197	1275
		C_2H_4	0	0	0
		NH_3	0	0	0
		Total 2e$^-$	1335	1197	1275
		ATP/2e$^-$	6.5	7.7	5.4

[a]Specific activity is expressed in nmols of product formed min^{-1} mg^{-1} of purified MoFe protein under the atmosphere indicated and the conditions specified in the Experimental Procedures.

[b]Total 2e$^-$ represents the electron pairs derived from all products in a particular experiment to allow direct comparisons among substrates. 1 nmol of C_2H_2 or H_2 is equivalent to 1 nmol of 2e$^-$ and 1 nmol of NH_3 is equivalent to 1.5 nmol of 2e$^-$.

[c]Approximately 10 % carbon monoxide (CO) was added, which is sufficient for complete inhibition.

[d]ATP/2e$^-$ represents the nmols of MgATP hydrolyzed per electron pair transferred to substrate.

5). A number of experiments were performed to determine whether or not the lower specific activities observed for the β−His^{98} MoFe protein can be attributed to an alteration in intramolecular electron delivery. Component protein ratio titrations involving the β−His^{98} MoFe protein revealed that its specific activity maximized at a lower Fe protein to MoFe protein ratio than that of the analogous titration involving the wild−type MoFe protein (figure 21). For the wild−type MoFe protein a maximum specific activity of 2250 nmols H_2 formed/min/mg MoFe protein was achieved at an Fe protein/MoFe protein molar ratio of greater than 10:1 under conditions of proton reduction, whereas under the same conditions, a maximum specific activity of 1100 nmoles/H_2 formed/min/mg MoFe protein was observed for the β−His^{98} MoFe protein, which was achieved at a lower molar ratio of approximately 5:1 (figure 21, upper panel). This effect was even more apparent in the analogous titration performed under conditions of acetylene reduction (figure 21, lower panel). Because the primary and secondary rates of intermolecular electron transfer were found to be identical for the altered β−His^{98} MoFe protein and the wild−type MoFe protein (figure 22, discussed below), the reduction in steady state maximum activity observed for the β−His^{98} MoFe protein must be a consequence of an alteration in electron transfer that occurs after these events. Also, the fact that substitution of β−Tyr^{98} by β−His^{98} has no apparent effect on component interaction, i.e. primary electron transfer, is consistent with the location of this residue within the interior of the polypeptide rather than at the exposed surface. Thus, the component protein titration experiments can be best explained by a model where, under high flux conditions (i.e. high Fe protein to MoFe protein ratios), substrate reduction catalyzed by the β−His^{98} MoFe protein becomes limited by intramolecular electron transfer rather than complex dissociation. In other words, the amount of Fe protein required to achieve maximum β−His^{98} specific activity is lowered in the titration experiment shown in figure 21 because the maximum flux through the system is limited as a consequence of a defect in intramolecular electron transfer per se.

The difference between the interpretation of the present results and similar data involving the consequences of substituting the β−Cys^{153} residue by β−Ser^{153} (May *et al.*,

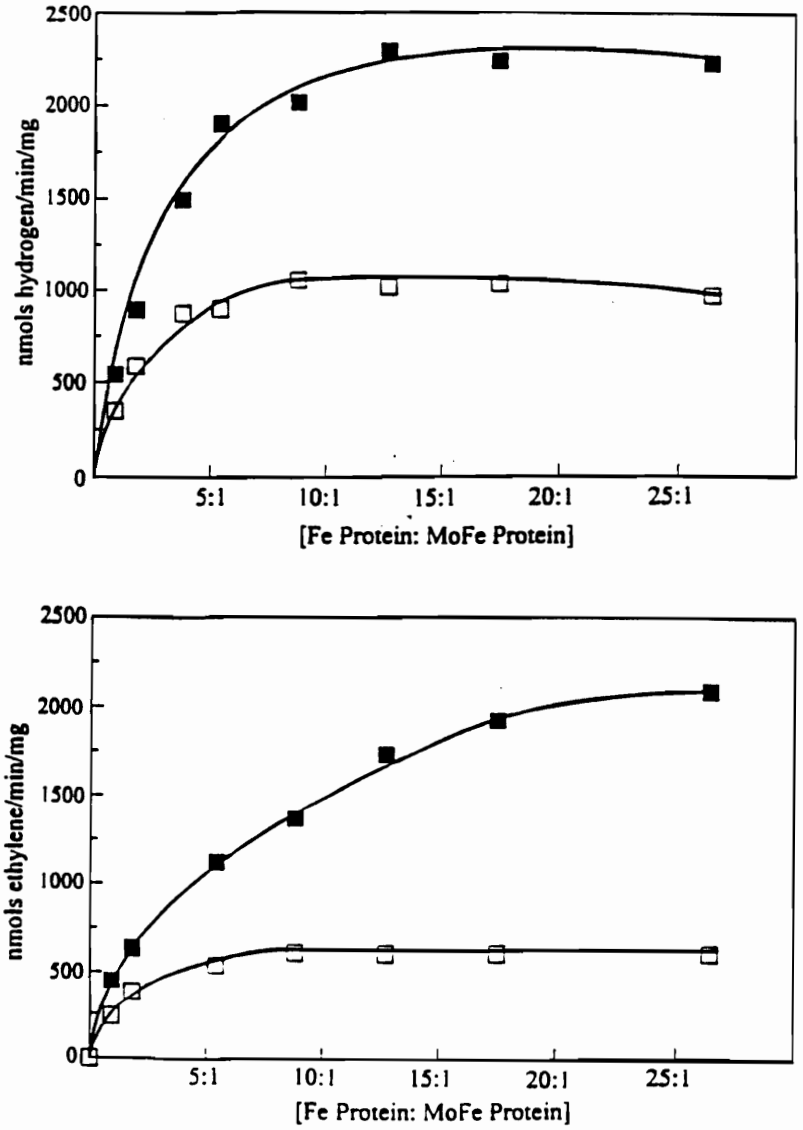

Figure 21. Titration of wild-type and β-His[98] MoFe protein with wild-type Fe protein. The component protein molar ratios were varied while the total protein concentration (0.5 mg) was kept constant. The upper panel shows the titrations in which the assays were performed under H_2 evolution conditions. In this curve activities are expressed as the nmols of H_2 produced/min/mg of MoFe protein. The lower panel shows the analogous titrations in which the assays were performed under acetylene reduction conditions. Activities in this curve are expressed as the nmols of ethylene formed/min/mg of MoFe protein. The assays were performed as described in the Experimental Procedures.

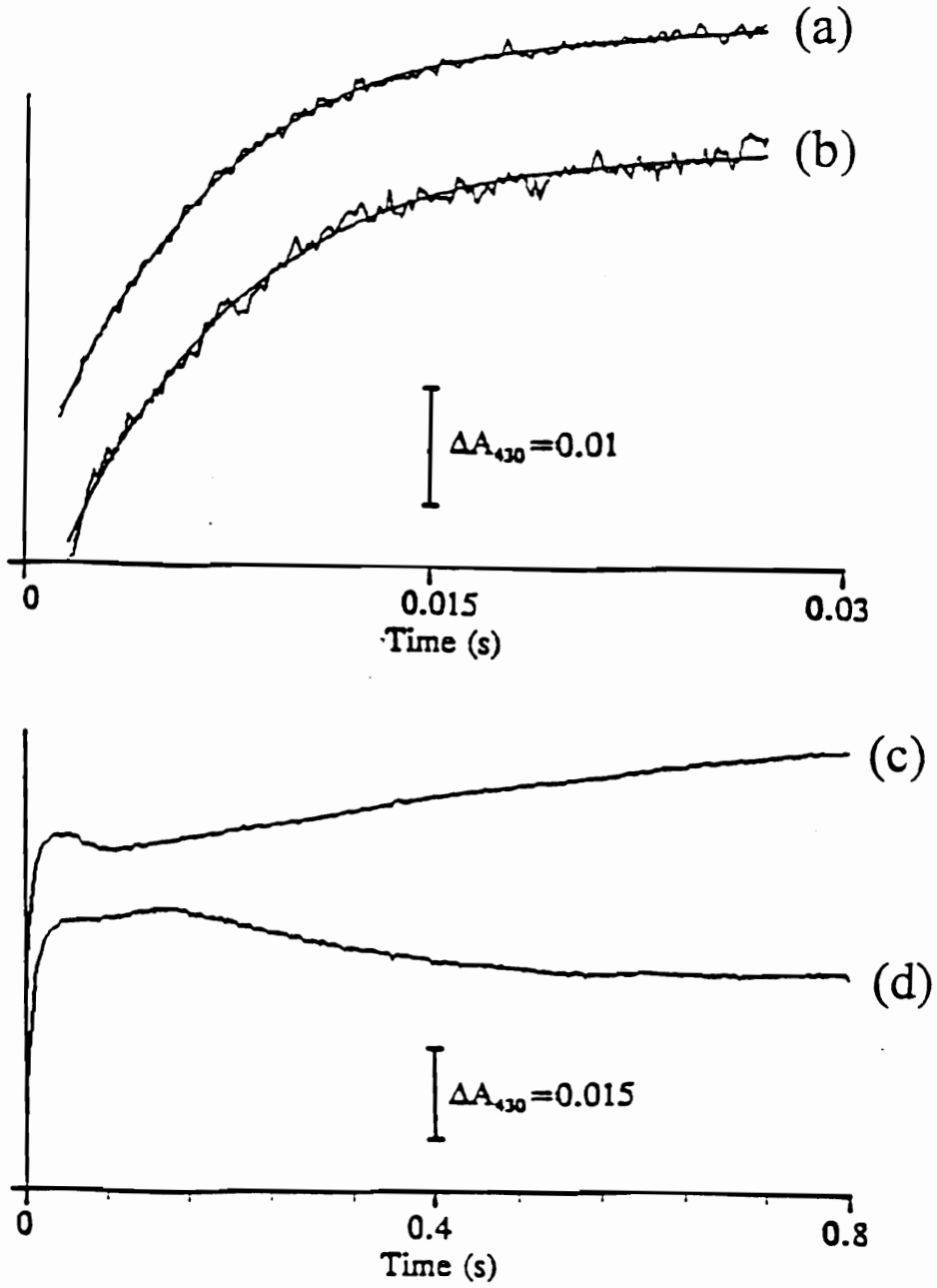

Figure 22. Electron transfer from the Fe protein to wild-type and β-His^{98} MoFe protein and subsequent absorbance changes occurring after primary electron transfer. The top panel is a comparison of stopped-flow spectrophotometry traces of (a) β-His^{98} and (b) wild-type MoFe protein dependent Fe protein oxidation. The traces are an enlargement of the initial 0.03 s of the lower trace. The calculated rate of primary electron transfer to β-His^{98} and wild-type MoFe protein was 157 s^{-1} and 160 s^{-1} respectively. The lower panel is an expanded trace (0.8 s) to show the absorbance changes that occur after primary electron transfer. Trace (c) was obtained with wild-type MoFe protein and is typical of that reported previously (Lowe *et al.*, 1993). The β-His^{98} dependent reaction (d) shows a single exponential absorbance decrease (k_{obs}=2.5 s^{-1}) after primary electron transfer.

1991) is that the latter was explained by structural changes in the P cluster polypeptide environment which was also interpreted to affect the rate of intramolecular electron transfer. Unlike the β−Cys^{153} residue, the β−Tyr^{98} residue does not participate in covalent ligation to the P cluster and, therefore, substitutions placed at this position are less likely to cause significant changes in the spatial arrangement of the P cluster within the polypeptide matrix. This conclusion is supported by MCD spectrophotometric analysis of the altered β−His^{98} MoFe protein, which, in contrast to the altered β−Ser^{153} MoFe protein, was unchanged when compared to the wild-type, indicating no apparent changes in the P cluster structure or its electronic environment (M. K. Johnson, personal communication).

The possibility that the reduction in maximum specific activity supported by the β−His^{98} MoFe protein might be explained by a perturbation in FeMo−cofactor's polypeptide environment was also explored. Previous studies have shown that substitution of amino acids in the polypeptide environment of FeMo−cofactor can result in various changes in the properties of the altered MoFe proteins that allow them to be distinguished from the wild-type MoFe protein (Scott *et al.*, 1990; Scott *et al.*, 1992; Kim *et al.*, 1995). Among these alterations are included changes in the characteristic S =3/2 EPR signal and changes in substrate reduction properties, such as; (i) alteration in the distribution of electron flux to different substrates, (ii) the four electron reduction of acetylene to yield ethane, and (iii) CO inhibition of proton reduction. No difference in the S =3/2 EPR spectra was observed for any of the altered MoFe proteins when compared to the wild−type spectrum (data not shown). Also, none of the altered MoFe proteins having substitutions at the β−Tyr^{98} position exhibited any of the characteristic changes associated with perturbation of FeMo−cofactor's polypeptide environment (table 6). These results, together with comparable Km values for acetylene binding for both the wild−type MoFe protein (0.0055 atm) and the β−His^{98} MoFe protein (0.0040 atm), indicate that the lowered maximum specific activity for the β−His^{98} MoFe protein under conditions of high flux are unlikely to occur as a result of an alteration in the substrate reduction site.

Effective nitrogenase catalysis requires the coordinate hydrolysis of about two MgATP for each electron transferred to substrate. However, MgATP hydrolysis can

become partially uncoupled from electron transfer under certain conditions such as extremely low flux (Ljones and Burris, 1972), high or low pH (Jeng *et al.*, 1970), and high or low temperature (Watt *et al.*, 1975; Watt and Burns, 1977). Certain amino acid substitutions that alter either component–protein interaction (Wolle *et al.*, 1992b; Seefeldt, 1994) or the substrate reduction site (Kim *et al.*, 1995) have also been shown to uncouple MgATP hydrolysis from electron transfer. In the present work it was found that MgATP hydrolysis is also partially uncoupled from substrate reduction in nitrogenase assays catalyzed by the β–His^{98} MoFe protein (table 6). A reasonable explanation for this result is that by slowing the rate of intramolecular electron transfer, electrons are accumulated on the P cluster to capacity, such that upon component protein interaction and subsequent MgATP hydrolysis, electron transfer from the Fe protein to the MoFe protein cannot occur because the P cluster is unable to act as an electron acceptor.

The possibility that the β–His^{98} MoFe protein is unable to easily transfer an electron from the P cluster to FeMo–cofactor such that intramolecular electron transfer is rate limiting was also investigated using two different types of continuous stopped–flow spectrophotometric experiments. In the first series of experiments the Fe protein turnover rates for catalysis involving the wild-type MoFe protein and the β–His^{98} MoFe protein was monitored over a continuous period of about 3 seconds. Such measurements provide an indirect measurement of the apparent component protein dissociation rate. In these experiments the wild–type nitrogenase dependent oxidation of flavodoxin was found to exhibit a single linear function having a calculated turnover rate of 6.3 s^{-1}. This value, calculated from the rate in absorbance change, the $\Delta\epsilon_{580}$ = 5.7 mm^{-1} cm^{-1} for the hydroquinone form of flavodoxin (Klugkist *et al.*, 1989), and the Mo content of the isolated MoFe protein, is in agreement with the value of 6.4 s^{-1} previously reported for the dissociation rate of the *Klebsiella pneumoniae* nitrogenase component proteins determined using steady state data (Thorneley and Lowe, 1983). In the reaction catalyzed by the β–His^{98} MoFe protein the apparent rate of component protein dissociation was also 6.3 s^{-1}, but only for approximately the first 300 ms. After this brief initial time period the apparent rate of component protein dissociation in the β–His^{98} catalyzed reaction was

slowed approximately two-fold to a linear rate of 2.5 s^{-1}. The biphasic nature of the apparent dissociation rate indicates that the reaction catalyzed by the β-His^{98} MoFe protein occurs in two stages in the pre-steady state. Namely, it appears that electron transfer to the P cluster of the β-His^{98} MoFe protein occurs at an initial rate comparable to the wild-type only until its capacity for storing electrons is reached, at which time the apparent component protein dissociation rate becomes substantially lowered owing to a defect in intramolecular electron transfer (figure 23). This interpretation is consistent with the results of a second series of pre-steady state analyses that were used to determine the rates of primary and secondary electron transfers from the Fe protein to the MoFe protein.

The rates of both primary and secondary intermolecular electron transfers to both the wild-type and β-His^{98} MoFe proteins were found to be the same (≈160 s^{-1}, figure 22; note, data for determination of the secondary electron transfer rate are not shown) and within the range previously reported (Thorneley, 1975; Fisher *et al.*, 1991). However, pre-steady state optical changes at 430 nm that are observed after the initial 150 ms are dramatically different for the β-His^{98} MoFe protein dependent reaction when compared to wild-type. Although details of the events associated with the optical changes that occur after approximately 150 ms are not well understood, P cluster oxidation, which presumably results from the intramolecular transfer of electrons to the substrate reduction site, has been proposed to be a major contributor to the absorbance increase after this period. (Lowe *et al.*, 1993). In contrast to the wild-type MoFe protein, the reaction involving the β-His^{98} MoFe protein exhibits a gradual decrease in optical absorbance after about 150 ms in the pre-steady state experiment. Thus, according to the model of Lowe *et al.* (1993), it appears that P cluster oxidation within the β-His^{98} MoFe protein occurs only at a relatively slow rate which is in line with the hypothesis that the altered MoFe protein is unable to achieve effective intramolecular electron transfer between its P cluster and FeMo-cofactor.

Because the amount of all the reactants are known in the continuous stopped-flow experiments and the time-dependent oxidation of flavodoxin was monitored, it was possible to calculate how many electrons were delivered to the MoFe protein prior to the

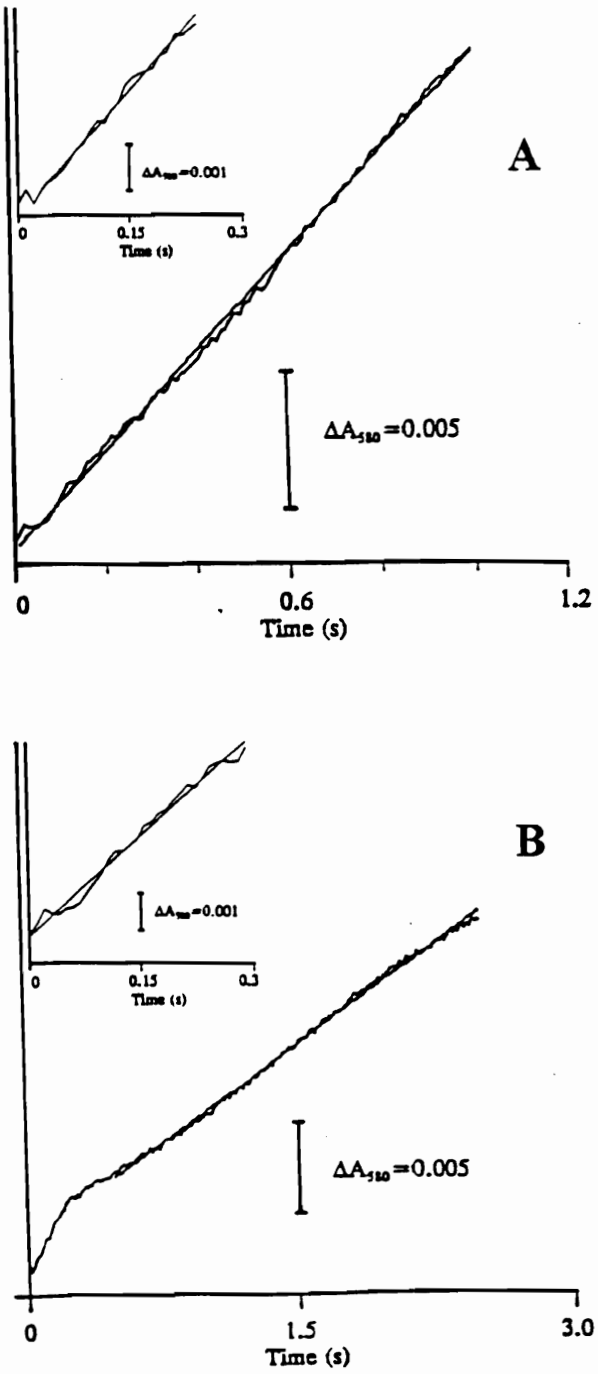

Figure 23. Stopped-flow spectrophotometric traces of the oxidation of the hydroquinone form of flavodoxin ($\Delta\epsilon_{580}$=5.7 mM^{-1} cm^{-1}) as a function of time. The rate of oxidation of the hydroquinone form of *A. vinelandii* flavodoxin II is a direct indication of the rate of complex dissociation (see Experimental Procedures). Panel A and Panel B represent the wild-type and β-His^{98} MoFe protein dependent reactions respectively. The calculated turnover rates from a linear fit are 6.3 s^{-1} for the wild-type and the first phase of the β-His^{98} MoFe protein dependent reactions and 2.5 s^{-1} for the second phase of the β-His^{98} MoFe protein dependent reaction.

observed lowering in Fe protein turnover rate. This value was found to be 2.4 and indicates that the P cluster is probably able to accumulate at least two electrons prior to the intramolecular electron delivery event. The apparent ability of the P cluster to accumulate at least two electrons is consistent with the proposed role of the P cluster as an electron storage unit and the proposed corner to corner disulfide link between the P cluster subfragments (Rees *et al.*, 1993a). Although the present results do not provide insight as to whether the P cluster donates single electrons or electron pairs (or both) to the substrate reduction, they do provide some credence to the possibility that a two electron transfer from the P cluster to the substrate reduction site could occur during turnover.

In summary, we report here compelling evidence supporting that electron transfer from the Fe protein's Fe_4S_4 cluster to the FeMo-cofactor on the MoFe protein involves the MoFe protein's P cluster as an intermediate. The MoFe protein β-Tyr^{98} was targeted for substitution because it is located in the region of the MoFe protein separating the P cluster and the FeMo-cofactor. The biochemical characterization of an altered MoFe protein with β-Tyr^{98} substituted by His revealed several features which indicated a deficiency in its ability to transfer electrons within the MoFe protein from the P cluster to the FeMo-cofactor. First, maximum activities of this altered MoFe protein were achieved at lower Fe protein to MoFe protein molar ratios than the wild-type indicating that overall flux through the altered MoFe protein was limited. Since primary and secondary electron transfer rates were unaltered, the limitation in flux is unlikely to occur during intermolecular electron transfer. Second, the pre-steady-state absorbance increase at 430 nm normally observed in reactions involving the wild-type MoFe protein after 150 ms are absent in the analogous reactions involving the β-His^{98} MoFe protein. This absorbance increase occurs after the Fe protein oxidation-reduction cycle reaches the steady-state and has been previously attributed to P cluster oxidation (Lowe *et al.*, 1993) suggesting that P cluster oxidation occurs more slowly in reactions involving the β-His^{98} MoFe protein. Third, a reduction in Fe protein turnover after 300 ms interpreted in the context of the aforementioned results suggests that the P cluster can accept electrons at the normal rate

only until its capacity is reached At this point, the acceptance of additional electrons requires reciprocal transfer from the P cluster to the FeMo-cofactor, a process which we believe to be rate limiting in reactions involving the β-His^{98} MoFe protein. In the context of this interpretation, it was determined that at least 2 electrons can be transferred to the P cluster which supports the role of the P cluster in storing electrons and is in line with the proposed mechanism of reduction involving breakage of the disulfide which connects the two Fe_4S_4 subfragments (Rees *et al.*, 1993a). The implications of these results on the overall mechanism of nitrogenase catalyzed electron transfer reactions are included in the Discussion section.

DISCUSSION

The pathway of electron transfer in nitrogenase begins with the delivery of electrons from the Fe protein to the MoFe protein. During catalysis the component proteins associate and dissociate in a process that couples the transfer of a single electron from the Fe protein to the MoFe protein to the hydrolysis of at least two molecules of MgATP. Since multiple electrons are required for substrate reduction, several electrons must be delivered and stored within the MoFe protein and there must be a mechanism to maintain unidirectional electron flow directed toward substrate reduction. The current view on component protein docking pairs the two-fold symmetry of the Fe protein with the pseudo-two-fold axis of the MoFe protein's $\alpha\beta$-subunit interface, placing the Fe protein's Fe_4S_4 cluster in close proximity to the MoFe protein's P cluster (Howard, 1993; Kim and Rees, 1992b, see figure 1a and b). The P cluster is believed to function in the acceptance, storage, and subsequent transfer of electrons to the iron-molybdenum cofactor at the site of substrate binding and reduction.

Nitrogenase-catalyzed substrate reduction is initiated by the delivery of an electron from the Fe protein to the MoFe protein in a series of events termed the "Fe protein cycle" (see scheme 1). Since this process requires component protein complex formation, there must be some specific mechanism of recognition by which the component proteins associate in a productive manner to facilitate electron transfer. Upon reduction and subsequent nucleotide displacement (MgATP for MgADP), the Fe protein undergoes a conformational change that is reflected in changes in redox potential (Watt *et al.*, 1986), spectroscopic properties (Zumft *et al.*, 1974) and susceptibility of its Fe_4S_4 cluster to chelation (Walker and Mortenson, 1974). This change in Fe protein conformation is believed to reflect the switch from the dissociative mode of the Fe protein to the associative mode that is competent for electron transfer. It has been suggested that association occurs in a two step process which involves an initial recognition facilitated by weak interactions followed by the formation of a more specific tighter bound complex in which electron transfer and MgATP hydrolysis occur (Howard, 1993). Results of

chemical cross-linking studies have shown that the Fe protein and MoFe protein can be specifically linked using the water soluble reagent, 1-ethyl-3-dimethylaminopropyl-carbodiimide (Willing *et al.*, 1989). Cross-linking occurs between Fe protein Glu^{112} and MoFe protein β-subunit Lys^{399} and is sensitive to inhibition by salt but not affected by the presence of MgATP. The observation that the cross-linking is not sensitive to MgATP in the reaction led to the interpretation that this site represents an early stage of interaction that precedes the precise interactions that facilitate electron transfer. The site of cross-linking is consistent with the current view of component protein docking. However, this docking model is based primarily on the x-ray crystal structures of the respective components, which represent singular static states of proteins that are believed to undergo coordinated conformational changes. Since MgATP hydrolysis is believed to trigger a conformational change in the complex, it is unlikely that primary interactions involving the MoFe protein and the reduced, MgATP bound form of the Fe protein would be common with interactions involved in the dissociation of the MgADP bound oxidized form of the Fe protein from the MoFe protein. A more plausible interpretation of the cross-linking phenomenon may be that the cross-linking occurs in the dissociative state of the complex. The presence of MgATP would not affect cross-linking because it would be rapidly turned over by the complex. This interpretation is also consistent with our view that catalysis involving the *C. pastuerianum* Fe protein and the *A. vinelandii* MoFe protein cannot occur because they are tightly bound in the dissociative mode. A primary sequence comparison indicates that Glu^{112} of the *A. vinelandii* Fe protein is substituted by Leu in the *C. pastuerianum* Fe protein.

Studies involving the salt sensitivity of both wild-type and altered nitrogenases have been interpreted to indicate that component protein association occurs by a mechanism of electrostatic attraction (Deits and Howard, 1989; Wolle *et al.*, 1992b). Salt inhibition was suggested to occur by competing with electrostatic groups and effectively preventing complex formation. A crown of positively charged residues surround the Fe_4S_4 cluster of the Fe protein on the face that, within the current docking model, would interact with the MoFe protein. Nitrogenase catalysis involving Fe proteins that have been

altered by substitution of these residues has been observed to occur at only a small fraction of the wild-type rate (Wolle *et al.*, 1992b; Seefeldt, 1994). Also characteristic to reactions involving these proteins was a marked hyper-sensitivity to NaCl and MgATP hydrolysis that is not coordinated with electron transfer. It was also shown that these Fe proteins were ineffective in their interaction with the MoFe protein because they failed to compete with wild-type Fe protein dependent catalysis. The interpretation of the results of studies involving these altered Fe proteins was that a dominant electrostatic interaction has been eliminated and that residual interactions are more sensitive to salt inhibition.

Since MgATP hydrolysis only occurs when both components are present and the sites for nucleotide binding and hydrolysis are located on the Fe protein, there must be a signal initiated by the interaction of the Fe protein with the MoFe protein which leads to MgATP hydrolysis. This signal may occur when the components are in the proper alignment so that a conformational change driven by the hydrolysis of MgATP can effect electron transfer from the Fe protein to the MoFe protein. This is consistent with the results obtained using stopped-flow calorimetry which indicate that MgATP hydrolysis precedes electron transfer (Thorneley *et al.*, 1989). However, proton release during MgATP hydrolysis has been shown to occur more slowly than electron transfer (Mensink *et al.*, 1992). These two results are compatible if MgATP hydrolysis precedes electron transfer but protons remain captured by the Fe protein until after component protein dissociation and subsequent reduction and nucleotide displacement of the Fe protein at the beginning of the next "Fe protein cycle". This is a reasonable scenario since the observed rates of proton release (Mensink *et al.*, 1992) and component protein dissociation (Thorneley and Lowe, 1983) are similar and Fe protein reduction and nucleotide displacement are not rate-limiting. Whether or not MgATP hydrolysis precedes electron transfer, the result of MgATP hydrolysis most certainly is a change in the conformation of the complex to one in which the interactions between the component proteins facilitate dissociation.

The rate-limiting step in nitrogenase catalysis is the dissociation of the Fe protein-MoFe protein complex which occurs after the transfer of each electron. Experiments

described in chapter I show that nitrogenase turnover is reduced two-fold with the addition of 175mM NaCl (table 1). Although the rate of primary electron transfer at this NaCl concentration was reduced, it was found to be at least 10-fold higher than the observed turnover rate. Since primary electron transfer and therefore protein association are not rate-limiting, the observed decrease in enzyme turnover rate must be due to a change in the rate-limiting step, component protein dissociation. The observation that the rate of component protein dissociation can be lowered with the addition of NaCl indicates that this process must occur by a mechanism which involves electrostatic repulsion. The biochemical characterization of a hybrid *A. vinelandii-C. pasteurianum* Fe protein, the details of which are discussed in Chapter I, indicated that this Fe protein was altered by the elimination of electrostatic interactions that normally facilitate dissociation resulting in a tighter binding dissociative complex. The hybrid Fe protein was constructed by replacement of a region of the *A. vinelandii* Fe protein termed the "variable region", which within the docking model is likely to interact with the MoFe protein and is considerably divergent in primary sequence with respect to the corresponding *C. pasteurianum* region (Howard, 1993). The substituted region is located on the same face of the Fe protein as the residues discussed previously as being involved in association of the Fe protein-MoFe protein complex. These residues, however, are located near the Fe_4S_4 cluster and the subunit interface and the variable region is located more distant with respect to the cluster (figure 4).

The location of these various residues and their proposed involvement suggests a dynamic model for the Fe protein cycle (see figure 4). The first feature of this model is that upon reduction and nucleotide displacement the Fe protein adopts a conformation in which the Fe_4S_4 cluster and the crown of positively charged residues are exposed for interaction and the variable region, which is involved in dissociation, is not. One can imagine that this can be easily accomplished by bending of the Fe protein at the Fe_4S_4 cluster to bring the subunits closer together near the MgATP binding site, thereby forcing residues proximal to the Fe_4S_4 cluster toward the docking face and more distal residues away from the docking face. This conformation of the Fe protein has increased affinity

and can now productively transfer electrons to the MoFe protein. The second feature is that productive component protein complex formation triggers MgATP hydrolysis causing a conformational change in the Fe protein. This conformational change moves the residues involved in electrostatic attraction away from the docking interface and the "variable region", which is involved in electrostatic repulsion, toward the docking interface, thereby facilitating dissociation. The third feature is that component protein dissociation, facilitated by electrostatic repulsion, releases the Fe protein to undergo another reduction and nucleotide replacement, which begins the next " Fe protein cycle". It is important to note that although this model describes the interaction of the Fe protein and the MoFe protein that facilitates electron transfer between them, it is unclear at what point in this process electron transfer actually occurs. A more in-depth discussion of the role of MgATP hydrolysis in electron transfer will follow.

The current view of component protein docking places the Fe_4S_4 cluster of the Fe protein in close proximity to the MoFe protein's P cluster (Howard, 1993; Kim and Rees, 1992b). It is generally accepted that the P cluster functions in the acceptance, storage, and ultimate transfer of electrons originating from the Fe protein to the substrate reduction site. In support of this docking model are chemical cross-linking studies mentioned previously and mutagenesis studies that involved the biochemical characterization of altered MoFe proteins with substitutions at β-subunit residue Phe^{124}, which is positioned at the docking interface in *K. pneumoniae* nitrogenase (Thorneley *et al.*, 1993). It has been suggested the corresponding *A. vinelandii* residue (β-Phe^{125}) and its pseudo-symmetric partner (α-Phe^{125}) could interact specifically with hydrophobic residues of surface helices on the Fe protein (Howard, 1993, see figure 5).

One problem with the role of the P cluster as the initial electron acceptor in the MoFe protein is that in the "as isolated dithionite reduced resting state" of the enzyme all Fe sites in the P cluster are observed to be in the ferrous state (Surerus *et al.*, 1992). The disulfide bridge that links the two Fe_4S_4 components of the P cluster is a potential electron acceptor, however in the as isolated protein the two sulfurs are too close to allow non-covalent contact (Howard and Rees, 1994; Rees *et al.*, 1993a). This suggests that the

MoFe protein may undergo a conformational change upon its interaction with the Fe protein, that causes the two Fe_4S_4 constituents of the P clusters to separate a sufficient distance to allow the reduction of the disulfide bridge (Rees *et al.*, 1993a; Howard and Rees, 1994). In this scenario, the hydrolysis of MgATP on the Fe protein of the complex initiates conformational changes in the Fe protein that are then transduced to the MoFe protein by virtue of their intimate contact. These conformational changes could then make electron transfer from the Fe protein's Fe_4S_4 to the MoFe protein's P cluster more favorable, therefore this model of electron transfer supports the view that MgATP hydrolysis precedes electron transfer. In the context of the previous discussion of the Fe protein cycle, this suggests that electron transfer occurs when the Fe protein is in its dissociative conformation. This is possible because the primary electron transfer event is observed to occur at a rate that is 30 times (200 s^{-1}) faster than component protein dissociation 6 s^{-1}. However it is also plausible that reduction of the MoFe protein at the P cluster causes conformational changes within the MoFe protein that can be transduced to the Fe protein making dissociation more favorable.

Although there is no direct experimental evidence to support this scenario of intermolecular electron transfer, the experimental results in Chapter II concerning the biochemical characterization of the α-Asn^{161} can be discussed in its context. The biochemical phenotype of nitrogenase catalysis involving this altered MoFe protein is very similar, in many respects, to that of Fe proteins which have been altered in initial docking. Namely, catalysis involving either these altered Fe proteins or the α-Asn^{161} MoFe protein is hypersensitive to inhibition by NaCl and exhibits MgATP hydrolysis that is uncoupled to electrons transferred to substrate (figures 16 and 17). However, unlike the altered Fe proteins, this altered MoFe protein retains the ability to compete with its wild-type component protein equivalent during catalysis. In addition, the NaCl inhibition of nitrogenase catalysis involving the α-Asn^{161} MoFe protein and the wild-type Fe protein was insensitive to increasing flux. Inhibition of nitrogenase catalysis by NaCl has been suggested to occur through its competition with electrostatic groups involved in the interaction of the Fe protein with the MoFe protein (Deits and Howard, 1990; Wolle *et*

al., 1992b). Therefore, increasing flux or increasing the Fe protein concentration in the reaction relative to the NaCl concentration can normally overcome, to some extent, the inhibition by NaCl. Since NaCl inhibition is not sensitive to flux in the α-Asn^{161} MoFe protein catalyzed reactions (figure 16), it is very likely that a dominant electrostatic interaction involved in some process other than component protein interaction has been altered, rendering the remaining weaker interactions more NaCl sensitive. These results can be interpreted to suggest that the α-Asn^{161} MoFe protein is altered in a dominant electrostatic interaction that is either: 1) involved in the transducing mechanism of conformational change brought about by component protein interaction and subsequent MgATP hydrolysis or, 2) in electrostatic interactions between the component proteins that arise as a result of reciprocal conformational changes. Uncoupling of MgATP hydrolysis to electron transfer to substrate is observed in catalysis involving this altered MoFe protein, which in the context of the preceding interpretation suggests that the nature of these conformational changes induced by MgATP hydrolysis are critical to the effective electron transfer.

The mechanism of electron transfer to the P cluster involving reduction of its disulfide will allow for the acceptance and storage of at most two electrons before additional electron transfer events must be accompanied by reciprocal transfers to the substrate reduction site (Rees *et al.*, 1993a; Howard and Rees, 1994). Since the P cluster is edge-to-edge approximately 14 Å from the iron-molybdenum cofactor (Kim and Rees, 1992b) it is unlikely that the two metal centers come into contact during catalysis. An intramolecular electron transfer between these two centers must therefore involve the polypeptide matrix which separates them. Described in Chapter III is a detailed discussion of mutagenesis studies involving the substitution of tyrosine residues located within or nearby this intervening region of the protein. The results indicate that substitution of β-subunit Tyr^{98} by His results in an altered MoFe protein that is defective in transferring electrons from the P cluster to the iron-molybdenum cofactor at the substrate reduction site. Pre-steady state experiments indicated that the overall rate of nitrogenase turnover was reduced two-fold after 2 electrons are transferred to each P cluster at the normal rate.

Additionally, pre-steady state absorbance changes that occur after 150ms, which have been suggested to occur as a result of P cluster oxidation (Lowe *et al.*, 1993), are significantly altered. In terms of nitrogenase electron transfer these results support a pathway of electron transfer that involves the P cluster as an intermediate. Significant to the overall mechanism of electron transfer is the observation that during catalysis involving the β-His^{98} MoFe protein, the P cluster appears to accept 2 electrons before the acceptance of additional electrons requires reciprocal electron transfer to the FeMo-cofactor. The ability of the P cluster to accept two electrons suggests that electron transfer from the P cluster could occur in pairs.

An obligate pair-wise electron transfer from the P cluster to the FeMo-cofactor is unlikely because experiments involving EPR have shown that reduction of the MoFe protein by a single electron causes bleaching of the EPR signal of the FeMo-cofactor (Münck *et al.*, 1975). This indicates that the single electron is not stored at the P cluster but rather is transferred to the FeMo-cofactor. The possibility that the P cluster can participate as a two-electron donor is, however, an attractive one in terms of the reduction of dinitrogen. It has been suggested that the high activation barrier involved in the two-electron reduction of dinitrogen to diimide could be side-stepped by a simultaneous four-electron reduction of dinitrogen to hydrazine (Rees *et al.*, 1993a). This could be achieved by the concurrent reduction of dinitrogen by two electrons stored at the FeMo-cofactor together with a two-electron contribution by the P cluster.

The preceding discussion describes a model for electron transfer within nitrogenase which is based on previously published works, insights gained by experimental results of this dissertation research, and personal speculation as well as the speculation of others. The mechanism can be summarized as follows: 1) reduction and subsequent nucleotide displacement causes conformational change within the Fe protein which render it competent for productive interaction and electron transfer to the MoFe protein, 2) association of the Fe protein with the MoFe protein is facilitated by the contribution of electrostatic attraction, 3) complex formation provides the signal for MgATP hydrolysis, 4) MgATP hydrolysis causes conformation changes in the Fe protein which are transduced

to the MoFe protein by virtue of their intimate contact, effectively altering the structure of the P cluster so it may act as an electron acceptor, 5) the resulting conformation changes that drive electron transfer align amino acid side chains involved in complex dissociation, 6) electrostatic repulsion contributes to complex dissociation, 7) the MoFe protein P cluster can accept up to two electrons, 8) electron transfer from the P cluster to the FeMo-cofactor can occur either as single electrons or in pairs, 9) pair-wise electron transfer from the P cluster to the FeMo-cofactor only occurs when required to overcome the high activation barrier involved in the reduction of dinitrogen.

The benefits of a detailed understanding of the mechanism of electron transfer events in nitrogenase are of broader significance than the obvious application to the improvement of the process of biological nitrogen fixation. Both structural (Schulz, 1992) and primary sequence comparisons (Koonin, 1993) have revealed that the nitrogenase Fe protein is a member of a broad class of nucleotide binding proteins that link the energy from nucleotide hydrolysis to a variety of molecular machinery. Included in this group are ras p21 (Pai *et al.*, 1990; Tong *et al.*, 1991), elongation factor Tu (Jurnack, 1985; Kjeldgaard and Nyborg, 1992), and recA-protein (Story and Steitz, 1992). A fundamental understanding of how conformational changes induced by MgATP hydrolysis drive electron transfer in nitrogenase might shed some light on how conformational changes that occur as a result of nucleotide hydrolysis act in processes such as cellular regulation, protein synthesis, and DNA recombination. Similarly, a detailed understanding of Fe protein-MoFe protein complex formation and dissociation can be applied to other processes involving protein-protein interactions such as electron transfer pathways and regulation. Nitrogenase might also be a good model system for electron transfer reactions that occur between redox centers that are located within the same protein. The advantages of studying nitrogenase in the context of these general processes are the availability of structural models of both components, rapid and efficient methods of gene transfer and mutagenesis, and, over 20 years of literature describing various experimental methods by which individual aspects can be probed.

REFERENCES

Ashby GA, Dilworth MJ, Thorneley RNF. 1987. *Klebsiella pneumoniae* nitrogenase: Inhibition of hydrogen evolution by ethylene and the reduction of ethylene to ethane. *Biochem. J.* 247:547-54

Benyon J. Cannon M, Buchanan-Wollaston V, Cannon F. 1983. The *nif* promoters of *Klebsiella pneumoniae* have a characteristic primary structure. *Cell* 34:665-71

Bolin JT, Campobasso N, Muchmore SW, Minor W, Morgan TV, Mortenson LE. 1993a. Structure of the nitrogenase MoFe protein: spatial distribution of the intrinsic metal atoms determined by x-ray anomalous scattering. See Palacios *et al.*, 1993, pp. 89-94

Bolin JT, Campobasso N, Muchmore SW, Morgan TV, Mortenson. 1993b. Structure and environment of the metal clusters in the nitrogenase molybdenum-iron protein from *Clostridium pasteurianum*. See Stiefel *et al.*, 1993, pp. 186-95

Brigle KE, Newton WE, Dean DR. 1985. Complete nucleotide sequence of the *Azotobacter vinelandii* nitrogenase structural gene cluster. *Gene* 37:37-44

Brigle KE, Setterquist RA, Dean DR, Cantwell JS, Weiss MC, Newton WE. 1987a. Site–directed mutagenesis of the nitrogenase MoFe protein of *Azotobacter vinelandii*. *Proc. Natl. Acad. Sci. USA* 84:7066-69

Brigle KE, Weiss MC, Newton WE, Dean DR. 1987b. Products of the iron-molybdenum cofactor-specific biosynthetic genes, *nifE* and *nifN*, are structurally homologous to the products of the nitrogenase molybdenum-iron protein genes, *nifD* and *nifK*. *J. Bacteriol.* 169:1547-53

Burgess BK. 1990. The iron-molybdenum cofactor of nitrogenase. *Chem. Rev.* 90:1377-1406

Burgess BK, Jacobs DB, Stiefel EI. 1980a. Large-scale purification of high activity *Azotobacter vinelandii* nitrogenase. *Biochim. et Biophys. Acta* 614:196-209

Burgess BK, Stiefel EI, Newton WE. 1980b. Oxidation-reduction properties and complexation reactions of the iron-molybdenum cofactor of nitrogenase. *J. Biol. Chem.* 255:353-56

Burris RH. 1991. Nitrogenases. *J. Biol. Chem.* 266:9339-42

Chan MK, Kim J, Rees DC. 1993. The nitrogenase FeMo-cofactor and P-cluster pair: 2.2 Å resolution structures. *Science* 260:792-94

Chaney AL, Marbach EP. 1962. Modified reagents for determination of urea and ammonia. *Clin. Chem.* 8:130-32

Chen J, Christiansen J, George SJ, van Elp J, Tittsworth R, *et al.* 1993. Extended X-ray absorption fine structure and L-edge spectroscopy of nitrogenase molybdenum-iron protein. See Stiefel *et al.*, 1993, pp. 231-42

Conradson SD, Burgess BK, Holm RH. 1988. Flourine-19 chemical shifts as probes of the structure and reactivity of the iron-molybdenum cofactor of nitrognease. *J. Biol. Chem.* 263:13743-49

Dance IG. 1994. The binding and reduction of dinitrogen at the Fe_4 face of the FeMo cluster of nitrogenase. *Aust. J. Chem.* 47:979-90

Dean DR, Bolin JT, Zheng L. 1993. Nitrogenase metalloclusters: Structures, organization, and synthesis. *J. Bacteriol.* 175:6737-44

Dean DR, Jacobson MR. 1992. Biochemical genetics of nitrogenase. See Stacey *et al.*, 1992, pp. 763-834

Dean DR, Scott DJ, Newton WE. 1990a. Identification of FeMoco domains within the nitrogenase MoFe protein. In *Nitrogen fixation: achievements and objectives*, ed. PM Gresshoff, LE Roth, G Stacey, WE Newton, pp. 95–102. New York: Chapman and Hall. 869 pp.

Dean DR, Setterquist RA, Brigle KE, Scott DJ, Laird NF, Newton WE. 1990b. Evidence that conserved residues Cys-62 and Cys-154 within the *Azotobacter vinelandii* nitrogenase MoFe protein α–subunit are essential for nitrogenase activity but conserved residues His-83 and Cys-88 are not. *Mol. Microbiol.* 4:1505-12

Deits TL, Howard JB. 1990. Effect of salts on *Azotobacter vinelandii* nitrogenase activities. *J. Biol. Chem.* 265:3859–67

Deng H, Hoffman R. 1993. How N_2 might be activated by the FeMo-cofactor in nitrogenase. *Angew. Chem., Int. Ed. Engl.* 32:1062-65

DeRose VJ, Kim C–H, Newton WE, Dean DR, Hoffman BM. 1995. Electron spin echo envelope modulation analysis of altered nitrogenase MoFe proteins from *Azotobacter vinelandii. Biochemistry* In Press

Dilworth MJ. 1966. Acetylene reduction by nitrogen-fixing preparations from *Clostridium pasteurianum. Biochim. Biophys. Acta* 127:285-94

Dilworth MJ, Eady RR, Robson RL, Miller RW. 1987. Ethane formation from acetylene as a potential test for vanadium nitrogenase *in vivo*. *Nature* 327:167–68

Dilworth MJ, Eldridge ME, Eady RR. 1992. Correction for creatine interference with the direct indophenol measurement of NH_3 in steady-state nitrogenase assays. *Anal. Biochem.* 207:6-10

Dunham WR, Hagen WR, Braaksma A, Grande HJ, Haaker H. 1985. The importance of quantitative Mossbauer spectroscopy of the MoFe-protein from *Azotobacter vinelandii*. *Eur. J. Biochem.* 146:497-501

Eady RR, Leigh GJ. 1994. Metals in the nitrogenases. *J. Chem. Soc. Dalton Trans.* 19:2739–47

Eady RR, Smith BE, Cook KA, Postgate JR. 1972. Nitrogenase of *Klebsiella pneumoniae*: Purification and properties of the component proteins. *Biochem. J.* 128:655-75

Emerich DW, Burris RH. 1976. Interactions of heterologous nitrogenase components that generate catalytically inactive complexes. *Proc. Natl. Acad. Sci. USA* 73:4369-73

Emerich DW, Ljones T, Burris RH. 1978. Nitrogenase: Properties of the catalytically inactive complex between *Azotobacter vinelandii* MoFe protein and the *Clostridium pasteurianum* Fe protein. *Biochim. Biophys. Acta* 527:359-69

Ennor AH. 1957. Determination and preparation of N-phosphates of biological origin. *Methods in Enzymol.* 3:850-56

Farid RS, Moser CC, Dutton PL. 1993. Electron transfer in proteins. *Curr. Opin. Struct.*

Biol. 3:225-33

Fisher K, Lowe DJ, Pau RN. 1993. *Klebsiella pneumoniae* nitrogenase MoFe protein: chymotryptic proteolysis affects function by limited cleavage of the β-chain and provides high-specific-activity MoFe protein. *Biochem. J.* 291:309-14

Fisher K, Lowe DJ, Thorneley RNF. 1991. *Klebsiella pneumoniae* nitrogenase: The pre-steady-state kinetics of MoFe-protein reduction and hydrogen evolution under conditions of limiting electron flux show that the rates of association with the Fe-protein and electron transfer are independent of the oxidation level of the MoFe-protein. *Biochem. J.* 279:81-85

Georgiadis MM, Komiya H, Chakrabarti P, Woo D, Kornuc JJ, Rees DC. 1992. Crystallographic structure of the nitrogenase iron protein from *Azotobacter vinelandii. Science* 257:1653-59

Govezensky D, Zamir A. 1989. Structure-function relationships in the α−subunit of Klebsiella pneumoniae nitrogenase MoFe protein from analysis of *nifD* mutants. *J. Bacteriol.* 171:5729-35

Hageman RV, Burris RH. 1978a. Kinetic studies on electron transfer and interaction between nitrogenase components from *Azotobacter vinelandii. Biochemistry* 17:4117-24

Hageman RV, Burris RH. 1978b. Nitrogenase and nitrogenase reductase associate and dissociate with each catalytic cycle. *Proc. Natl. Acad. Sci. USA* 75:2699-2702

Hageman RV, Burris RH. 1979. Changes in the EPR signal of dinitrogenase from *Azotobacter vinelandii* during the lag period before hydrogen evolution begins. *J. Biol. Chem.* 254:11189-92

Hageman RV, Burris RH. 1980. Electron allocation to alternative substrates of *Azotobacter vinelandii* nitrogenase is controlled by the electron flux through dinitrogenase. *Biochim. Biophys. Acta* 591:63-75

Hallenbeck PC. 1983. Nitrogenase reduction by electron carriers: Influence of redox potential on activity and the ATP/2e$^-$ ratio. *Arch. Biochem. Biophys.* 220:657-60

Hausinger RP, Howard JB. 1982. The amino acid sequences of the nitrogenase-iron protein from *Azotobacter vinelandii*. *J. Biol. Chem.* 257:2483-90

Hausinger RP, Howard JB. 1983. Thiol reactivity of the nitrogenase Fe-protein from *Azotobacter vinelandii*. *J. Biol. Chem.* 258:13486-92

Hawkes TR, McLean PA, Smith BE. 1984. Nitrogenase from *nifV* mutants of *Klebsiella pneumoniae* contains an altered form of the iron-molybdenum cofactor. *Biochem. J.* 217:317-21

Holland D, Zilberstein A, Zamir A, Sussman J. 1987. A quantitative approach to sequence comparisons of nitrogenase MoFe protein α- and β-subunits including the newly sequenced *nifK* gene from *Klebsiella pneumoniae*. *Biochem. J.* 247:277-85

Hoover TR, Imperial J, Liang J, Ludden PW, Shah VK. 1988a. Dinitrogenase with altered substrate specificity results from the use of homocitrate analogues for *in vitro* synthesis of the iron-molybdenum cofactor. *Biochemistry* 27:3647-52

Hoover TR, Imperial J, Ludden PW, Shah VK. 1988b. Homocitrate cures the NifV$^-$ phenotype in *Klebsiella pneumoniae*. *J. Bacteriol.* 170:1978-79

Hoover TR, Imperial J, Ludden PW, Shah VK. 1989. Homocitrate is a component of the

iron-molybdenum cofactor of nitrogenase. *Biochemistry* 28:2768-71

Howard JB. 1993. Protein component complex formation and adenosine triphosphate hydrolysis in nitrogenase. See Stiefel *et al.*, 1993, pp. 271-89

Howard JB, Davis R, Moldenhauer B, Cash VL, Dean DR. 1989. Fe-S cluster ligands are the only cysteines required for nitrogenase Fe-protein activities. *J. Biol. Chem.* 264:11270-74

Howard JB, Rees DC. 1994. Nitrogenase: A nucleotide–dependent molecular switch. *Annu. Rev. Biochem.* 63:235–64

Hughes DL, Ibrahim SK, Querne G, Laouenen A, Talarmin J, *et al.* 1994. On carboxylate as a leaving group at the active site of Mo nitrogenase: Electrochemical reactions of some molybdenum and tungsten carboxylates, formation of mono– di–and tri–hydrides and the detection of an $MoH_2(N_2)$ intermediate. *Polyhedron* 13:3341-48

Imam S, Eady RR. 1980. Nitrogenase of *Klebsiella pneumoniae*: Reductant-independent ATP hydrolysis and the effect of pH on the efficiency of coupling of ATP hydrolysis to substrate reduction. *FEBS Lett.* 110:35-38

Jacobson MR, Brigle KE, Bennett LT, Setterquist RA, Wilson MS, *et al.* 1989a. Physical and genetic map of the major *nif* gene cluster from *Azotobacter vinelandii*. *J. Bacteriol.* 171:1017-27

Jacobson MR, Cantwell JS, Dean DR. 1990. A hybrid *Azotobacter vinelandii-Clostridium pasteurianum* nitrogenase iron protein that has *in-vivo* and *in-vitro* catalytic activity. *J. Biol. Chem.* 265:19429-33

Jacobson MR, Cash VL, Weiss MC, Laird NF, Newton WE, Dean DR. 1989b. Biochemical and genetic analysis of the *nifUSVWZM* cluster from *Azotobacter vinelandii*. *Molec. Gen. Genet.* 219:49-57

Jeng DY, Morris JA, Mortenson LE. 1970. The effect of reductant in inorganic phosphate release from adenosine 5' triphosphate by purified nitrogenase of *Clostridium pasteurianum*. *J. Biol. Chem.* 245:2809-13

Johnson MK. 1988. Variable-temperature magnetic circular dichroism studies of metalloproteins. In *Metal clusters in proteins*, ed. L Que, pp. 326-42. Washington DC: ACS Books Symposium Series. 413 pp.

Jurnack F. 1985. Structure of the GDP domain of EF-Tu and localization of the amino acids homologous to *ras* oncogene proteins. *Science* 230:32-36

Kent HM, Baines M, Gormal C, Smith BE, Buck M. 1990. Analysis of site-directed mutations in the α- and β-subunits of *Klebsiella pneumoniae* nitrogenase. *Mol. Microbiol.* 4:1497-1504

Kent HM, Ioannidis I, Gormal C, Smith BE, Buck M. 1989. Site-directed mutagenesis of *Klebsiella pneumoniae* nitrogenase. *Biochem. J.* 264:257-64

Kim C-H, Newton WE, Dean DR. 1995. The role of the MoFe protein α-subunit histidine-195 residue in FeMo-cofactor binding and nitrogenase catalysis. *Biochemistry* In Press

Kim C-H, Zheng L, Newton WE, Dean DR. 1993. Intermolecular electron transfer and substrate reduction properties of MoFe proteins altered by site-specific amino acid substitution. See Palacios *et al.*, 1993, pp. 105-10

Kim J, Rees DC. 1992a. Structural models for the metal centers in the nitrogenase molybdenum-iron protein. *Science* 257:1677-82

Kim J, Rees DC. 1992b. Crystallographic structure and functional implications of the nitrogenase molybdenum-iron protein from *Azotobacter vinelandii. Nature* 360:553-60

Kim J, Rees DC. 1994. Nitrogenase and biological nitrogen fixation. *Biochemistry* 33:389-97

Kim J, Woo D, Rees DC. 1993. X-ray crystal structure of the nitrogenase molybdenum-iron protein from *Clostridium pasteurianum* at 3.0-Å resolution. *Biochemistry* 32:7104-15

Kjeldgaard M, Nyborg J. 1992. Refined structure of elongation factor EF-Tu from *Escherichia coli. J. Mol. Biol.* 223:721-42

Klugkist J, Voorberg J, Haaker H, Veeger C. 1986. Charaterization of three different flavodoxins from *Azotobacter vinelandii. Eur. J. Biochem.* 155:33-40

Koonin EV. 1993. A superfamily of ATPases with diverse functions containing either classical or deviant ATP-binding motif. *J. Mol. Biol.* 229:1165-74

Kraulis PJ. 1991. Molscript: A program to produce both detailed and schematic plots of protein structures. *J. Appl. Crystall.* 24:946-50

Kunkel TA, Roberts JD, Zakour RA. 1987. Rapid and efficient site-specific mutagenesis without phenotypic selection. *Methods in Enzymol.* 154:367-82

Kurtz DM, McMillan RS, Burgess BK, Mortenson LE, Holm RH. 1979. Identification of iron-sulfur centers in the iron-molybdenum proteins of nitrogenase. *Proc. Natl. Acad. Sci.*

USA 76:4986-89

Laemmli UK. 1970. Cleavage of structural proteins during the assembly of the head of bacteriophage T_4. *Nature* 227:680-85

Lammers PJ, Haselkorn R. 1983. Sequence of the *nifD* gene coding for the α-subunit of dinitrogenase from the cyanobacterium *Anabaena. Proc. Natl. Acad. Sci. USA* 80:4723-27

Liang J, Madden M, Shah VK, Burris RH. 1990. Citrate substitutes for homocitrate in the nitrogenase of a *nifV* mutant of *Klebsiella pneumoniae. Biochemistry* 29:8577–81

Lindahl PA, Day EP, Kent TA, Orme-Johnson WH, Münck E. 1985. Mössbauer, EPR, and magnetization studies of the *Azotobacter vinelandii* Fe protein. *J. Biol. Chem.* 260:11160-73

Ljones T, Burris RH. 1972. ATP hydrolysis and electron transfer in the nitrogenase reaction with different combinations of iron protein and molybdenum-iron protein. *Biochim. Biophys. Acta* 275:93-101

Lowe DJ, Fisher K, Thorneley RNF. 1990. *Klebsiella pneumoniae* nitrogenase: Mechanism of acetylene reduction and its inhibition by carbon monoxide. *Biochem. J.* 272:621-25

Lowe DJ, Fisher K, Thorneley RNF. 1993. *Klebsiella pneumoniae* nitrogenase: Pre-steady state absorbance changes show that redox changes occur in the MoFe protein that depend on substrate and component protein ratio; a role for P-centres in reducing nitrogen. *Biochem. J.* 292:93-98

Lowery RG, Chang CL, Davis LC, McKenna M-C, Stephens PJ, Ludden PW. 1989. Substitution of histidine for arginine-101 of dinitrogenase reductase disrupts electron transfer to dinitrogenase. *Biochemistry* 28:1206-12

Lowry OH, Rosebrough NJ, Farr AL, Randall RH. 1951. Protein measurement with the folin phenol reagent. *J. Biol. Chem.* 193:265-75

Ludden PW, Shah VK, Roberts GP, Homer M, Allen R, et al. 1993. Biosynthesis of the iron–molybdenum cofactor of nitrogenase. See Stiefel *et al.*, 1993, pp. 196–215

Masepohl B, Angermuller S, Hennecke S, Hubner P, Moreno–Vivian C, Klipp W. 1993. Nucleotide sequence and genetic analysis of the *Rhodobacter capsulatus* ORF6–*nifU1SVW* gene region: possible role of *NifW* in homocitrate processing. *Mol. Gen. Genet.* 238:369–82

May HD, Dean DR, Newton WE. 1991. Altered nitrogenase MoFe proteins from *Azotobacter vinelandii*. *Biochem. J.* 277:457-64

McLean PA, Papaefthymiou V, Orme-Johnson WH, Munck E. 1987. Isotopic hybrids of nitrogenase: Mossbauer study of MoFe protein with selective ^{57}Fe enrichment of the P-cluster. *J. Biol. Chem.* 262:12900-03

Mensink RE, Wassink H, Haaker H. 1992. A reinvestigation of the pre–steady–state ATPase activity of the nitrogenase from *Azotobacter vinelandii*. *Eur. J. Biochem.* 208:289–94

Mortenson LE, Seefeldt LC, Morgan TV, Bolin J. 1993. The role of metal clusters and MgATP in nitrogenase catalysis. *Adv. Enzymol.* 67:299-373

Münck E, Rhodes H, Orme-Johnson WH, Davis LC, Brill WJ, Shah VK. 1975. Nitrogenase. VIII. Mössbauer and EPR spectroscopy. The MoFe protein component from *Azotobacter vinelandii* OP. *Biochim. Biophys. Acta* 400:32-53

Newton WE. 1992. Isolated iron-molybdenum cofactor of nitrogenase. See Stacey *et al.*, 1992, pp. 877-930

Orme-Johnson WH, Davis LC. 1977. Current topics and problems in the enzymolgy of nitrogenase. In *Iron-sulfur proteins*, ed. W Lovenberg, pp. 15–60. New York: Academic Press. 443 pp

Orme-Johnson WH, Holm RH. 1978. Identification of Fe-S clusters in proteins. *Methods Enzymol.* 53:268-74

Page WJ, von Tigerstrom M. 1979. Optimal conditions for transformation of *Azotobacter vinelandii. J. Bacteriol.* 139:1058–61

Pai EF, Krengel U, Petsko GA, Goody RS, Kabsch W, Wittinghofer A. 1990. Refined crystal structure of the triphosphate conformation of H-*ras* p21 at 1.35 Å resolution: implications for the mechanism of GTP hydrolysis. *EMBO J.* 9:2351-59

Palacios R, Mora J, Newton WE, eds. 1993. *New Horizons in Nitrogen Fixation.* Dordrecht: Kluwer Academic. 788 pp.

Paustian TD, Shah VK, Roberts GP. 1989. Purification and characterization of the *nifN* and *nifE* gene products from *Azotobacter vinelandii* mutant UW45. *Proc. Natl. Acad. Sci. USA* 86:6082-86

Peters JW, Fisher K, Dean DR. 1994. Identification of a nitrogenase protein-protein

interaction site defined by residues 59 through 67 within the *Azotobacter vinelandii* Fe protein. *J. Biol. Chem.* 269:28076-83

Pope MR, Murrell SA, Ludden PW. 1985. Covalent modification of the iron protein of nitrogenase from *Rhodospirillum rubrum* by adenosine diphosphoribosylation of a specific arginine residue. *Proc. Natl. Acad. Sci. USA* 82:3173:77

Rees DC, Chan MK, Kim J. 1993a. Structure and function of nitrogenase. *Adv.Inorg. Chem.* 40:89-119

Rees DC, Kim J, Georgiadis MM, Komiya H, Chirino AJ, et al. 1993b. Crystal structures of the iron protein and the molybdenum-iron protein of nitrogenase. See Stiefel *et al.*, 1993, pp. 170-85

Robinson AC, Burgess BK, Dean DR. 1986. Activity, reconstitution, and accumulation of nitrogenase components in *Azotobacter vinelandii* mutant strains containing defined deletions within the nitrogenase structural gene cluster. *J. Bacteriol.* 166:180–86

Robson RL. 1984. Identification of possible adenine nucleotide-binding sites in nitrogenase Fe- and MoFe-proteins by amino acid sequence comparison. *FEBS Lett.* 173:394-98

Sanger F, Nicklen S, Coulson R. 1977. DNA sequencing with chain-terminating inhibitors. *Proc. Natl. Acad. Sci. USA* 74:5463-67

Schöllhorn R, Burris RH. 1967. Acetylene as a competitive inhibitor of N_2 fixation. *Proc. Natl. Acad. Sci. USA* 58:213-16

Schrauzer GN, Doemeny PA, Palmer JG. 1993. The chemical evolution of a nitrogenase

model, XXII. Reduction of acetylene with catalysts derived from molybdate, homocitric acid and N-methylimidazole and a proposal concerning the active site of functional *Azotobacter* nitrogenases. *Z. Naturforsch* 48b:1295–98

Schulz GE. 1992. Binding of nucleotides by proteins. *Curr. Opin. Struct. Biol.* 2:61-67

Scott DJ, Dean DR, Newton WE. 1992. Nitrogenase-catalyzed ethane production and CO-sensitive hydrogen evolution from MoFe proteins having amino acid substitutions in an α-subunit FeMo cofactor binding domain. *J. Biol. Chem.* 267:20002-10

Scott DJ, May HD, Newton WE, Brigle KE, Dean DR. 1990. Role for the nitrogenase MoFe protein α-subunit in the FeMo-cofactor binding and catalysis. *Nature* 343:188-90

Seefeldt LC. 1994. Docking of nitrogenase iron– and molybdenum–iron proteins for electron transfer and MgATP hydrolysis: The role of arginine 140 and lysine 143 of the *Azotobacter vinelandii* iron protein. *Protein Sci.* 3:2073-81

Seefeldt LC, Morgan TV, Dean DR, Mortenson LE. 1992. Mapping the sites of MgATP and MgADP interaction with the nitrogenase of *Azotobacter vinelandii:* Lysine 15 of the Fe protein plays a major role in MgATP interaction. *J. Biol. Chem.* 267:6680-88

Seefeldt LC, Mortenson, LE. 1993. Increasing nitrogenase catalytic efficiency for MgATP by changing serine 16 of its Fe protein to threonine: Use of Mn^{++} to show interaction of serine 16 with Mg^{++}. *Protein Sci.* 2:93-102

Shah VK, Brill WJ. 1977. Isolation of an iron–molybdenum cofactor from nitrogenase. *Proc. Natl. Acad. Sci. USA*, 74:3249–53

Shah VK, Davis LC, Brill WJ. 1972. Repression and derepression of the iron-molybdenum

and iron proteins of nitrogenase in *Azotobacter vinelandii*. *Biochim. Biophys. Acta* 256:498-511

Smith BE, Buck M, Faridoon KY, Gormal CA, Howes BD, *et al.* 1993. The metallo–sulpher centres of the nitrogenase MoFe protein from wild–type and mutant strains of *Klebsiella pneumoniae*. *J. Inorg. Biochem.* 51:357

Smith BE, Eady RR. 1992. Metalloclusters of the nitrogenases. *Eur. J. Biochem.* 205:1-15

Smith BE, Eady RR, Lowe DJ, Gormal C. 1988. The vanadium-iron protein of vanadium nitrogenase from *Azotobacter chroococcum* contains an iron-vanadium cofactor. *Biochem. J.* 250:299-302

Smith BE, Lang G. 1974. Mössbauer spectroscopy of the nitrogenase proteins from *Klebsiella pneumoniae*. *Biochem. J.* 137:169-80

Spiro TG, ed. 1985. *Molybdenum Enzymes*, New York: John Wiley & Sons. 611 pp

Stacey G, Burris RH, Evans HJ, eds. 1992. *Biological Nitrogen Fixation*, New York: Chapman and Hall. 943 pp.

Stephens PJ. 1985. The structures of the iron-molybdenum and the iron proteins of the nitrogenase enzyme. See Spiro, 1985, pp. 117-160

Stiefel EI, Coucouvanis D, Newton WE, eds. 1993. *Molybdenum Enzymes, Cofactors and Model Systems.* Washington DC: Am. Chem. Soc. 387 pp.

Strandberg GW, Wilson PW. 1968. Formation of the nitrogen-fixing enzyme system in *Azotobacter vinelandii*. *Can. J. Microbiol.* 14:25-31

Story RM, Steitz TA. 1992. Structure of the recA protein-ADP complex. *Nature* 355:374-76

Surerus KK, Hendrich MP, Christie PD, Rottgardt D, Orme-Johnson WH, Münck E. 1992. Mössbauer and integer-spin EPR of the oxidized P-clusters of nitrogenase: P^{ox} is a non-kramers system with a nearly degenerate ground doublet. *J. Am. Chem. Soc.* 114:8579-90

Thomann H, Bernardo M, Newton WE, Dean DR. 1991. N coordination of the FeMo cofactor requires His-195 of the MoFe protein α subunit and is essential for biological nitrogen fixation. *Proc. Natl. Acad. Sci. USA* 88:6620-23

Thomann H, Morgan TV, Jin H, Burgmayer SJN, Bare RE, Stiefel EI. 1987. Protein nitrogen coordination to the FeMo center of nitrogenase from *Clostridium pasteurianum*. *J. Am. Chem. Soc.* 109:7913-14

Thöny B, Kaluza K, Hennecke H. 1985. Structural and functional homology between the α and β subunits of the nitrogenase MoFe protein as revealed by sequencing the Rhizobium japonicum nifK gene. *Molec. Gen. Genet.* 198:441-48

Thorneley RNF. 1975. Nitrogenase of *Klebsiella pneumoniae*: A stopped-flow study of magnesium-adenosine triphosphate-induced electron transfer between the component proteins. *Biochem. J.* 145:391-96

Thorneley RNF, Ashby GA, Fisher K, Lowe DJ. 1993. Electron-transfer reactions associated with nitrogenase from Klebsiella pneumoniae. See Stiefel *et al.*, 1993, pp. 290-302

Thorneley RNF, Ashby G, Howarth JV, Millar NC, Gutfreund H. 1989. A transient-

kinetic study of the nitrogenase of *Klebsiella pneumoniae* by stopped-flow calorimetry. *Biochem. J.* 264:657-61

Thorneley RNF, Ashby GA, Julius C, Hunter JL, Webb MR. 1991. Nitrogenase of *Klebsiella pneumoniae*: Reversibility of the reductant-independent MgATP-cleavage reaction is shown by MgADP-catalysed phosphate/water oxygen exchange. *Biochem. J.* 277:735-41

Thorneley RNF, Deistung J. 1988. Electron-transfer studies involving flavodoxin and a natural redox partner, the iron protein of nitrogenase: Conformational constraints on protein-protein interactions and the kinetics of electron transfer with the protein complex. *Biochem. J.* 253:587-95

Thorneley RNF, Lowe DJ. 1983. Nitrogenase of *Klebsiella pneumoniae*: Kinetics of the dissociation of oxidized iron protein from molybdenum-iron protein: Identification of the rate-limiting step for substrate reduction. *Biochem. J.* 215:393-403

Thorneley RNF, Lowe DJ. 1984a. The mechanism of *Klebsiella pneumoniae* nitrogenase action: Pre-steady-state kinetics of an enzyme-bound intermediate in N_2 reduction and NH_3 formation. *Biochem. J.* 224:887-94

Thorneley RNF, Lowe DJ. 1984b. The mechanism of *Klebsiella pneumoniae* nitrogenase action: Simulation of the dependence of H_2-evolution rate on component-protein concentration and ratio and sodium dithionite concentration. *Biochem. J.* 224:903-09

Thorneley RNF, Lowe DJ. 1985. Kinetics and mechanism of the nitrogenase enzyme system.See Spiro, 1985, pp. 222-284

Tong L, de Vos AM, Milburn MV, Kim S-H. 1991. Crystal structures at 2.2 Å resolution

of the catalytic domains of normal *ras* protein and an oncogenic mutant complexed with GDP. *J. Mol. Biol.* 217:503-16

Vieira J, Messing J. 1987. Production of single-stranded plasmid DNA. *Methods in Enzymol.* 153:3-11

Walker GA, Mortenson LE. 1974. Effect of magnesium adenosine 5'-triphosphate on the accessibility of the iron of clostridial azoferredoxin, a component of nitrogenase. *Biochemistry* 13:2382-88

Watt GD, Bulen WA, Burns A, Hadfield KL. 1975. Stoichiometry, ATP/2e values, and energy requirements for reactions catalyzed by nitrogenase from *Azotobacter vinelandii*. *Biochemistry* 14:4266-72

Watt GD, Burns A. 1977. Kinetics of dithionite ion utilization and ATP hydrolysis for reactions catalyzed by the nitrogenase complex from *Azotobacter vinelandii*. *Biochemistry* 16:264-70

Watt GD, Wang Z-C, Knotts RR.1986. Redox reactions of and nucletide binding to the iron protein of *Azotobacter vinelandii*. *Biochemistry* 25:8156-62

Wherland S, Burgess BK, Stiefel EI, Newton WE. 1981. Nitrogenase reactivity: Effects of component ratio on electron flow and distribution during nitrogen fixation. *Biochemistry* 20:5132-40

Willing AH, Georgiadis MM, Rees DC, Howard JB. 1989. Cross-linking of Nitrogenase Components. *J. Biol. Chem.* 264:8499-8503

Willing A, Howard JB. 1990. Cross-linking site in *Azotobacter vinelandii* complex. *J.*

Biol. Chem. 265:6596-99

Wolle D, Dean DR, Howard JB. 1992a. Nucleotide iron-sulfur cluster signal transduction in the nitrogenase iron-protein: The role of Asp^{125}. *Science* 258:992-95

Wolle D, Kim C-H, Dean DR, Howard JB. 1992b. Ionic interactions in the nitrogenase complex: Properties of Fe-protein containing substitutions for Arg-100. *J. Biol. Chem.* 267:3667-73

Yates MG. 1992. The enzymology of molybdenum-dependent nitrogen fixation. See Stacey *et al.*, 1993, pp. 685-735

Zumft WG, Mortenson LE, Palmer G. 1974. Electron-paramagnetic-resonance studies on nitrogenase. *Eur. J. Biochem.* 46:525-35

VITA

John W. Peters Jr. was born on June 29, 1965 in White Pine, Michigan as the only son of John Peters and Lois Whyte Peters. He spent his childhood in Missouri, New Mexico, and Oklahoma. After attending Oklahoma State University for three years, he transferred to the University of Oklahoma and received a Bachelor of Science degree in Microbiology in 1989. He began graduate school at Virginia Tech in the summer of 1989 at the Anaerobe Lab. John married Martha Cabell in August, 1990. After completing his Ph.D. at Virginia Tech, he will continue research on nitrogenase at Cal Tech in Pasadena, CA in the laboratory of Professor Douglas C. Rees.

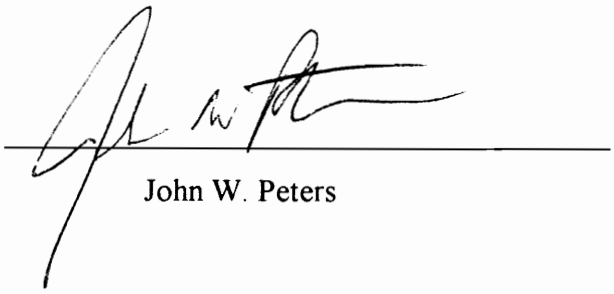

John W. Peters